

Technical Evaluation Motor No. 10 (TEM-10) Final Test Report

August 1993

Prepared for

National Aeronautics and Space Administration
George C. Marshall Space Flight Center
Marshall Space Flight Center, Alabama 35812

Contract No. NAS8-38100
DR No. 5-3
WBS No. 4Q601-20-10
ECS No. SS1031

Thiokol CORPORATION
SPACE OPERATIONS

P.O. Box 707, Brigham City, UT 84302-0707 (801) 863-3511

Prepared by Space Publications
Publications No. 940151

N94-14907

Unclas

G3/20 0189633

(NASA-CR-193846) TECHNICAL
EVALUATION MOTOR NO. 10 (TEM-10)
Final Report (Thiokol Corp.)
130 p

100

1
2
3
4
5
6
7
8
9
10
11
12
13
14
15
16
17
18
19
20
21
22
23
24
25
26
27
28
29
30
31
32
33
34
35
36
37
38
39
40
41
42
43
44
45
46
47
48
49
50
51
52
53
54
55
56
57
58
59
60
61
62
63
64
65
66
67
68
69
70
71
72
73
74
75
76
77
78
79
80
81
82
83
84
85
86
87
88
89
90
91
92
93
94
95
96
97
98
99
100


THE FOLLOWING PAGES WERE INTENTIONALLY
LEFT BLANK

PER S. SNIDER

i, IV, VI, XII, 2, 4, 8, 12, 14, A-2, B-2, C-2

**Technical Evaluation Motor No. 10 (TEM-10)
Final Test Report**

Prepared by:

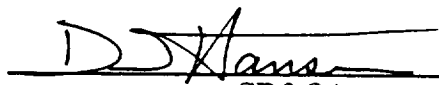

Systems Planning and Interfaces


Approved by:


Project Engineer


Design Engineer


Program Manager


SR&QA 8-19-93


Data Management/Release
ECS No. SS1031

MAJOR CONTRIBUTORS

| | |
|------------------------------------|--------------|
| Project Engineer | S. Pottorff |
| Instrumentation | D. South |
| Case/Leak Check/Seals | A. Carlisle |
| Insulation | B. Lesko |
| Nozzle | M. Clark |
| Igniter | M. Tobias |
| Ballistics/Mass Properties | A. Drendel |
| Aero/Thermal | E. Mathias |
| Structural Analysis | P. Simpson |
| Postfire Hardware Evaluation | J. Furgeson |
| Photo Instrumentation | C. Larsen |
| Integration | J. Wilkenson |

PRECEDING PAGE BLANK NOT FILMED

EX-10

10

INTENTIONALLY MEANS



ABSTRACT

Technical Evaluation Motor No. 10 (TEM-10) was static fired on 27 April 1993 at the Thiokol Corporation full-scale motor static test bay, T-24.

This final test report documents the procedures, performance, and results of the static test firing of TEM-10. All observations, discussions, conclusions, and recommendations contained in this report are final.

Included is a presentation and discussion of TEM-10 performance, anomalies, and test results in concurrence with the objectives outlined in CTP-0110, Revision D, Space Shuttle Technical Evaluation Motor No. 10 (TEM-10) Static Fire Test Plan.

PRECEDING PAGE BLANK NOT FILMED

CONTENTS

| Section | | Page |
|---------|--|------|
| 1 | INTRODUCTION | 1 |
| 2 | TEST OBJECTIVES | 3 |
| | 2.1 PASS/FAIL CRITERIA | 3 |
| 3 | EXECUTIVE SUMMARY | 5 |
| | 3.1 SUMMARY | 5 |
| | 3.2 CONCLUSIONS | 5 |
| | 3.3 RECOMMENDATIONS | 7 |
| 4 | INSTRUMENTATION | 9 |
| | 4.1 INTRODUCTION | 9 |
| | 4.2 OBJECTIVES/CONCLUSIONS | 9 |
| | 4.3 RECOMMENDATIONS | 10 |
| | 4.4 RESULTS/DISCUSSION | 10 |
| | 4.4.1 Acceleration | 10 |
| | 4.4.2 Pressure | 10 |
| | 4.4.3 Thrust | 10 |
| | 4.4.4 Calorimeter and Radiometer | 11 |
| | 4.4.5 Strain Measurement | 11 |
| | 4.4.6 Temperature Measurement | 11 |
| | 4.4.7 Sound Pressure | 11 |
| | 4.4.8 Real Time Radiography | 11 |
| 5 | PHOTOGRAPHY | 13 |
| | 5.1 STILL PHOTOGRAPHY | 13 |
| | 5.2 MOTION PICTURES | 13 |
| 6 | TEST DESCRIPTION AND RESULTS | 17 |
| | 6.1 TEST ARTICLE DESCRIPTION | 17 |
| | 6.2 TEST ARRANGEMENT AND FACILITIES | 18 |
| | 6.3 CASE AND CASE SEALS PERFORMANCE | 18 |
| | 6.3.1 Introduction | 18 |
| | 6.3.2 Objectives/Conclusions | 21 |
| | 6.3.3 Recommendations | 21 |
| | 6.3.4 Results/Discussion | 21 |
| | 6.4 CASE INTERNAL INSULATION PERFORMANCE | 23 |
| | 6.4.1 Introduction | 23 |
| | 6.4.2 Objectives/Conclusions | 24 |
| | 6.4.3 Recommendations | 24 |
| | 6.4.4 Results/Discussion | 24 |
| | 6.5 LEAK CHECK PERFORMANCE | 27 |
| | 6.5.1 Introduction | 27 |
| | 6.5.2 Objectives/Conclusions | 28 |
| | 6.5.3 Recommendations | 28 |
| | 6.5.4 Results/Discussion | 28 |
| | 6.6 NOZZLE PERFORMANCE | 29 |
| | 6.6.1 Introduction | 29 |
| | 6.6.2 Objectives/Conclusions | 30 |
| | 6.6.3 Recommendations | 30 |
| | 6.6.4 Results/Discussion | 30 |

CONTENTS (cont)

| <i>Section</i> | | <i>Page</i> |
|-----------------|---|-------------|
| 6.7 | IGNITION SYSTEM PERFORMANCE | 41 |
| 6.7.1 | Introduction | 41 |
| 6.7.2 | Objectives/Conclusions | 43 |
| 6.7.3 | Recommendations | 44 |
| 6.7.4 | Results/Discussion | 44 |
| 6.8 | JOINT PROTECTION SYSTEMS | 46 |
| 6.8.1 | Introduction | 46 |
| 6.8.2 | Objectives/Conclusions | 46 |
| 6.8.3 | Recommendations | 46 |
| 6.8.4 | Results/Discussion | 46 |
| 6.9 | BALLISTICS/MASS PROPERTIES PERFORMANCE | 47 |
| 6.9.1 | Introduction | 47 |
| 6.9.2 | Objectives/Conclusions | 47 |
| 6.9.3 | Recommendations | 47 |
| 6.9.4 | Results/Discussion | 47 |
| 6.10 | PRESSURE PERTURBATION SUMMARY | 62 |
| 6.10.1 | Introduction | 62 |
| 6.10.2 | Objectives/Conclusions | 62 |
| 6.10.3 | Recommendations | 62 |
| 6.10.4 | Results/Discussion | 62 |
| 6.11 | STATIC TEST SUPPORT EQUIPMENT | 91 |
| 6.11.1 | Introduction | 91 |
| 6.11.2 | Objectives/Conclusions | 91 |
| 6.11.3 | Recommendations | 91 |
| 6.11.4 | Results/Discussion | 91 |
| 7 | APPLICABLE DOCUMENTS | 95 |
| | | |
| <i>Appendix</i> | | |
| A | TEM-10 Drawing Tree | A-1 |
| B | Summary of Measured Ballistic and Nozzle Performance Data | B-1 |
| C | TEM-10 Timeline of Events | C-1 |

FIGURES

| <i>Figure</i> | | <i>Page</i> |
|---------------|--|-------------|
| 5-1 | T-24 Photography Coverage--TEM-10 | 15 |
| 6-1 | TEM-10 Static Test Arrangement | 17 |
| 6-2 | TEM-10 Field Joint Configuration | 19 |
| 6-3 | TEM-10 (HPM modified) Nozzle-to-Case Joint Configuration | 20 |
| 6-4 | TEM-10 Nozzle Strain Gage Locations | 34 |
| 6-5 | Nozzle Fixed Housing Hoop Strain Versus Predictions | 35 |
| 6-6 | Nozzle Fixed Housing Meridional Strain Versus Predictions | 35 |
| 6-7 | Nozzle Fixed Housing Hoop Strain Postburn Observations (120 sec-8 hr) | 36 |
| 6-8 | Nozzle Fixed Housing Hoop Strain Postburn Observations (120 sec-2 hr) | 36 |
| 6-9 | Nozzle Fixed Housing Meridional Strain Postburn Observations (120 sec-8 hr) | 37 |
| 6-10 | Nozzle Fixed Housing Meridional Strain Post Burn Observations (120 sec-2 hr) | 37 |
| 6-11 | TEM Nozzle Internal Joints | 38 |
| 6-12 | Baseline Redesign Igniter | 42 |
| 6-13 | Pressure-Sensitive Adhesive Application Location | 42 |
| 6-14 | Predicted and Measured Pressure at 69°F | 49 |
| 6-15 | Reconstructed Vacuum Thrust at 69°F | 49 |
| 6-16 | Reconstructed and Measured Pressure at 69°F | 50 |
| 6-17 | Reconstructed and Measured Vacuum Thrust at 69°F | 50 |
| 6-18 | Comparison of Vacuum Thrust to Head-End Pressure Ratio Versus Time for TEMs | 51 |
| 6-19 | Measured Head-End Pressure Transients | 53 |
| 6-20 | Comparison of Igniter Performance with Limits at 80°F | 55 |
| 6-21 | Igniter Pressure Versus Head-End and Nozzle Stagnation Pressure .. | 57 |
| 6-22 | Measured Head-End and Nozzle Stagnation Pressure Time Histories .. | 57 |
| 6-23 | PNCAC002 Waterfall Plot | 58 |
| 6-24 | Maximum Oscillation Amplitudes--PNCAC002 1-L Acoustic Mode ... | 58 |
| 6-25 | Maximum Oscillation Amplitudes--PNCAC002 2-L Acoustic Mode ... | 59 |
| 6-26 | Reconstructed Thrust Compared to CEI Limits | 62 |
| 6-27 | Calorimeter/Radiometer Location | 64 |
| 6-28 | Calorimeter/Radiometer Data Versus Time (0-160 sec) | 64 |
| 6-29 | Calorimeter/Radiometer Data Versus Time (50-100 sec) | 65 |
| 6-30 | Calorimeter Versus Motor Pressure | 65 |
| 6-31 | Calorimeter Data Minus Predicted Versus Time (0-160 sec) | 66 |
| 6-32 | Calorimeter Data Minus Predicted Versus Time (50-100 sec) | 66 |
| 6-33 | Calorimeter Data Minus Predicted Versus Time (70-80 sec) | 67 |
| 6-34 | Calorimeter Data Minus Predicted Versus Time (100-110 sec) | 67 |
| 6-35 | Nozzle Fixed Housing Hoop Strain Versus Chamber Pressure at 72-76 sec (80 deg) | 68 |
| 6-36 | Nozzle Fixed Housing Hoop Strain Versus Chamber Pressure at 72-76 sec (170 deg) | 68 |
| 6-37 | Nozzle Fixed Housing Hoop Strain Versus Chamber Pressure at 72-76 sec (260 deg) | 69 |

FIGURES (cont)

| Figure | | Page |
|--------|--|------|
| 6-38 | Nozzle Fixed Housing Hoop Strain Versus Chamber Pressure at 72-76 sec (350 deg) | 69 |
| 6-39 | Nozzle Fixed Housing Meridional Strain Versus Chamber Pressure at 72-76 sec (80 deg) | 70 |
| 6-40 | Nozzle Fixed Housing Meridional Strain Versus Chamber Pressure at 72-76 sec (170 deg) | 70 |
| 6-41 | Nozzle Fixed Housing Meridional Strain Versus Chamber Pressure at 72-76 sec (260 deg) | 71 |
| 6-42 | Nozzle Fixed Housing Meridional Strain Versus Chamber Pressure at 72-76 sec (350 deg) | 71 |
| 6-43 | Nozzle Fixed Housing Hoop Strain Versus Chamber Pressure at 102-110 sec (80 deg) | 72 |
| 6-44 | Nozzle Fixed Housing Hoop Strain Versus Chamber Pressure at 102-110 sec (170 deg) | 72 |
| 6-45 | Nozzle Fixed Housing Hoop Strain Versus Chamber Pressure at 102-110 sec (260 deg) | 73 |
| 6-46 | Nozzle Fixed Housing Hoop Strain Versus Chamber Pressure at 102-110 sec (350 deg) | 73 |
| 6-47 | Nozzle Fixed Housing Meridional Strain Versus Chamber Pressure at 102-110 sec (80 deg) | 74 |
| 6-48 | Nozzle Fixed Housing Meridional Strain Versus Chamber Pressure at 102-110 sec (170 deg) | 74 |
| 6-49 | Nozzle Fixed Housing Meridional Strain Versus Chamber Pressure at 102-110 sec (260 deg) | 75 |
| 6-50 | Nozzle Fixed Housing Meridional Strain Versus Chamber Pressure at 102-110 sec (350 deg) | 75 |
| 6-51 | Case Accelerometer Versus Pressure (typical) | 77 |
| 6-52 | Nozzle Accelerometer Versus Pressure (typical) | 77 |
| 6-53 | Nozzle Accelerometer Waterfall Plot | 78 |
| 6-54 | Nozzle Accelerometer Compared With Motor Pressure (50-60 sec) | 78 |
| 6-55 | Nozzle Accelerometer Compared With Motor Pressure (60-70 sec) | 79 |
| 6-56 | Nozzle Accelerometer Compared With Motor Pressure (70-80 sec) | 79 |
| 6-57 | Nozzle Accelerometer Compared With Motor Pressure (80-90 sec) | 80 |
| 6-58 | Nozzle Accelerometer Compared With Motor Pressure (90-100 sec) | 80 |
| 6-59 | Nozzle Accelerometer Compared With Motor Pressure (100-110 sec) | 81 |

FIGURES (cont)

| <i>Figure</i> | | <i>Page</i> |
|---------------|--|-------------|
| 6-60 | Nozzle Accelerometer Compared With Motor Pressure (110-120 sec) | 81 |
| 6-61 | RTR Locations | 83 |
| 6-62 | Forward Field Joint | 83 |
| 6-63 | Aft Dome Factory Joint | 84 |
| 6-64 | Lower View RTR Data Plotted With Calorimeter Data (20-120 sec) .. | 84 |
| 6-65 | Upper View RTR Data Plotted With Calorimeter Data (20-120 sec) .. | 85 |
| 6-66 | Upper and Lower RTR Data Plotted With Calorimeter Data (70-80 sec) | 85 |
| 6-67 | Upper and Lower RTR Data Plotted With Calorimeter Data (104-114 sec) | 86 |
| 6-68 | Upper RTR Data Plotted With Calorimeter Data (70-80 sec) | 86 |
| 6-69 | Upper RTR Data Plotted With Calorimeter Data (104-114 sec) | 87 |
| 6-70 | Lower RTR Waterfall Plot | 87 |
| 6-71 | Upper RTR Waterfall Plot | 88 |
| 6-72 | Calorimeter/Radiometer Waterfall Plot | 88 |
| 6-73 | Motor Pressure Waterfall Plot | 89 |
| 6-74 | Upper RTR Slag Movement Activity | 89 |
| 6-75 | Lower RTR Slag Movement Activity | 90 |
| 6-76 | RTR Slag Movement Data (60-100 sec) | 90 |
| 6-77 | RTR Slag Movement Data (100-120 sec) | 91 |
| 6-78 | Maximum Case Temperature Versus Time | 92 |
| 6-79 | Maximum Case Temperatures Versus Slag Weight | 93 |

TABLES

| <i>Table</i> | | <i>Page</i> |
|--------------|---|-------------|
| 5-1 | Photography and Video Coverage | 13 |
| 5-2 | Photography and Video Sequencing | 14 |
| 6-1 | TEM-10 Segment History | 17 |
| 6-2 | TEM-10 Seal Leak Testing | 28 |
| 6-3 | TEM-10 Case Field Joint Leak Test Results | 28 |
| 6-4 | TEM-10 Igniter and S&A Leak Test Results | 29 |
| 6-5 | TEM-10 Nozzle-to-Case Leak Test Results | 29 |
| 6-6 | Nozzle Strain Gage Summary--Fixed Housing (station 1867.0) | 34 |
| 6-7 | Burn Rate Data Comparison Subscale to Full-scale at 62 psia, 60°F .. | 52 |
| 6-8 | Historical 3/5 Point Average Maximum Thrust and Pressure Rise Rate Data | 54 |
| 6-9 | Measured SRM Ignition Performance Data at 73°F | 55 |
| 6-10 | Maximum Pressure Oscillation Amplitude Comparison | 60 |
| 6-11 | TEM-10 Nozzle Component Postfire Heat Soak Data | 93 |

ACRONYMS

| | | | |
|-----------------|--|---------|---|
| B-B | barrier-booster | NDE | nondestructive evaluation |
| BTU | British thermal unit | No | north |
| CCP | carbon-cloth phenolic | OBR | outer boot ring |
| CEI | contract end item | OD | outside diameter |
| CF/EPDM | carbon-fiber-filled ethylene-propylene-diene monomer | OPT | operational pressure transducer |
| CO ₂ | carbon dioxide | PBAN | polybutadiene acrylic acid acrylonitrile terpolymer |
| CP | circular perforated | PFAR | postfire anomaly record |
| CTPB | carboxyl-terminated polybutadiene | PFOR | postfire observation record |
| CV | coefficient of variation | PLI | preload indicating |
| Doc | documentary | PMBT | propellant mean bulk temperature |
| DM | development motor | PSA | pressure-sensitive adhesive |
| ET | external tank | psi | pounds per square inch |
| ETM | engineering test motor | psia | pounds per square inch absolute |
| °F | degrees Fahrenheit | psig | pounds per square inch gage |
| FPS | frames per second | PVM | production verification motor |
| FSM | flight support motor | QM | qualification motor |
| ft ² | square feet | R | required |
| FWC | filament wound case | RSRM | redesigned solid rocket motor |
| FWD/Fwd | forward | RTD | resistance temperature detector |
| GCP | glass-cloth phenolic | RTR | real-time radiography |
| HPM | high-performance motor | RTV | room-temperature vulcanized rubber |
| hr | hour | S&A | safe and arming (device) |
| HS | high speed | SBRE | surface burn rate error |
| Hz | hertz | sccs | standard cubic centimeters per second |
| ID | inside diameter | SCP | silica-cloth phenolic |
| in. | inch | SEC/sec | second |
| IPT | igniter pressure transducer | SII | SRM ignition initiator |
| IR | infrared | S/N | serial number |
| KSC | Kennedy Space Center | So | south |
| lb | pound | SPS | samples per second |
| lbf | pound force | SRM | solid rocket motor |
| lbm | pound mass | Sta | station |
| LSC | linear shaped charge | STS | Space Transportation System |
| μ | micro | TEM | technical evaluation motor |
| M | mandatory | TVC | thrust vector control |
| min | minute | V | volt |
| MSEC/ms | millisecond | VAC | volts alternating current |
| MSFC | Marshall Space Flight Center | VDC | volts direct current |
| MST | mountain standard time | Vid | video |
| N/A | not applicable | 1-L | first longitudinal |
| NASA | National Aeronautics and Space Administration | 2-L | second longitudinal |
| NBR | nitrile butadiene rubber | | |

1 / INTRODUCTION

Technical Evaluation Motor No. 10 (TEM-10) was successfully static tested at 1349 hours on 27 April 1993 at the Thiokol Corporation full-scale motor static test bay, T-24. The ambient temperature at the time of the test was 56°F and the propellant mean bulk temperature (PMBT) was 69°F. Ballistics performance values were within the specified requirements.

TEM-10 was a full-scale, full-duration static test firing of a high-performance motor (HPM) configuration solid rocket motor (SRM). TEM-10 was the fourth TEM on which all segments were more than five years old.

The primary purpose of TEM static tests is to recover SRM case and nozzle hardware for use in the RSRM flight program; however, TEM static tests also provide opportunities to evaluate or certify various design, process, and supplier issues for the RSRM flight program.

This was the third full-scale static test motor to successfully use a redesigned baseline igniter and the first full-scale static test motor to use real-time radiography (RTR).

Instrumentation measurements consisted of head-end chamber and igniter pressure; case, forward, and aft domes and nozzle acceleration; case, forward, and aft domes and nozzle strain; safe and arming (S&A) device temperature; free air temperature; test stand water deluge pressure; case temperature for deluge control and indirect propellant bulk measurement; joint temperatures; and timing. Calorimeter and radiometer data were also collected.

TEM-10 postfire inspection procedures followed TWR-62073 and TWR-63821.

2

2 / TEST OBJECTIVES

The TEM-10 test objectives of CTP-0110, Revision D, were derived from the objectives of System Test Summary Sheet, TGX-21.9, to satisfy the requirements of contract end item (CEI) specification CPW1-3600A, dated 3 August 1987.

Qualification objectives of this test were:

- a. Certify baseline redesign igniter outer J-joint insulation performance with two-sided pressure-sensitive adhesive (PSA).
- b. Certify the unibody SRM standard initiator (SII) seal interface for use in the RSRM ignition system (CPW1-3600A paragraphs 3.2.1.2, 3.2.1.2.4.a, 3.2.1.2.4.b, 3.2.1.2.4.c, 3.2.1.5.a).

Other test objectives included:

- c. Recover igniter, case, and nozzle hardware for RSRM flight and static test motors.
- d. Measure motor head-end chamber pressure oscillations.
- e. Obtain plume particulate data.
- f. Obtain RTR, acceleration, infrared (IR) plume, sound pressure, and strain data in support of the RSRM-29 pressure anomaly investigation.

2.1 PASS/FAIL CRITERIA

- a. The baseline redesign igniter outer J-joint with two-sided PSA shall perform as good as or better than the baseline redesign igniter outer J-joint with one-sided PSA.

Flag Criteria*: There shall be no visible evidence of combustion gas downstream of the forward contact point of the outer joint J-leg insulation.

- b. The unibody SII seals shall reveal no evidence of blowby, erosion, or hot gas leakage; shall accommodate structural deflections and operate in the static test thermal environment (natural or induced).

* Flag criteria is defined as a condition which, if violated, will result in an anomaly investigation. Based upon the information gained by the investigation, Marshall Space Flight Center (MSFC) and Thiokol will determine whether or not the certification test objective was met.

PRECEDING PAGE BLANK NOT FILMED

1978 INTERNATIONALLY BLANK

3 / EXECUTIVE SUMMARY

3.1 SUMMARY

TEM-10 was static test fired in T-24 at 1349 hours on 27 April 1993. All systems functioned normally. The motor performed well with no apparent anomalies.

Inspection and instrumentation data indicated that the TEM-10 static test firing was successful overall. Data were gathered at instrumented locations during pretest, test, and post-test operations.

All comments presented here are based on final data and external observations. An assessment of the test data and physical inspection information gathered from the test and during disassembly are included.

An external walk-around inspection was conducted. No case hot spots were observed. No debris was noted. The external condition of the nozzle appeared nominal. The external condition of the heaters appeared normal.

The TEM-10 ballistic performance was within specification limits and compared well with previous TEM performance and HPM historical data. The more than seven-year storage of loaded case segments did not affect motor performance.

The baseline redesign igniter performance was nominal. S&A safe-to-arm cycle time was 0.6 sec, which is less than the required 2.0 sec and within historical database performance.

Nozzle erosion was typical. The aft exit cone carbon-cloth phenolic (CCP) liner showed no shallow wash areas and no surface ply lifting. The interior of the aft exit cone was in very good condition with smooth erosion and typical circumferential delaminations.

The nose cap, forward nose ring, and aft inlet ring shifted from the nose inlet housing and dropped into the motor. This is an HPM nose inlet assembly. The loss or shifting of the nose inlet phenolics was observed on 13 nozzles during the SRM/HPM program.

All test objectives for TEM-10 were met except one. No data were obtained for the plume particulate study. The success rate for TEM-10 data collection was 99 percent.

3.2 CONCLUSIONS

The following conclusions are listed as each specifically relates to the test objectives and applicable CEI specification (CPW1-3600A) paragraphs. Additional information about each conclusion can be found in the appendices of this report.

PRECEDING PAGE BLANK NOT FILMED

| <u>Objective</u> | <u>CEI Paragraphs</u> | <u>Conclusions</u> |
|--|--|--|
| A. Certify baseline redesign igniter outer J-joint insulation performance with two- sided PSA. | None. | <i>Certified.</i> Both igniter J-joints performed as expected with two-sided PSA. Adequate thermal protection was provided to the metal hardware. There was no visible evidence that combustion gas penetrated either J-joint, and none reached the seals. PSA did not move from the allowable application zone. The two-sided PSA performed as good or better than one-sided PSA. |
| B. Certify the unibody SII seal interface for use in the RSRM ignition system. | 3.2.1.2, 3.2.1.2.4.a, 3.2.1.2.4.b, 3.2.1.2.4.c, 3.2.1.5.a. | <i>Certified.</i> The unibody SIIs performed nominally. No anomalous conditions were observed. |
| C. Recover igniter, case, and nozzle hardware for RSRM flight and static test motors. | None. | <i>Recovered.</i> No hardware was lost as a result of the full-scale static test. |
| D. Measure motor head-end chamber pressure oscillations. | None. | <i>Measured.</i> Motor head-end chamber pressure oscillations were measured. Motor dynamic performance appears nominal and no anomalous behavior was noted. Designated pressure oscillation data channel failed to acquire data because of incorrect circuit in ground data collection system. |
| E. Obtain plume particulate data. | None. | <i>Not obtained.</i> The NASA-provided control box relay switches became disconnected due to ground vibrations during motor firing. |
| F. Obtain RTR, acceleration, IR plume, sound pressure, and strain data in support of RSRM-29 pressure anomaly investigation. | None. | <i>Obtained.</i> RTR, acceleration, IR plume, sound pressure, and strain data were successfully collected. |

3.3 RECOMMENDATIONS

Pass/fail criteria were met for all certification issues. Demonstration/evaluation objectives were satisfied except for Objective E. Data were successfully obtained except for those specific instruments identified in Section 4.

The following features have successfully satisfied the qualification objectives of this test and should be considered for use on flight motors:

- a. Unibody SIIs
- b. Two-sided PSA

Plume particulate data could be obtained by hardening the NASA-provided control box (reference Objective E).

The TEM-10 motor pressure perturbation was benign compared to the pressure perturbations recorded on flight motors. Thiokol recommends gathering additional data on the pressure perturbation study. Future static tests should have more comprehensive coverage of accelerometers through the length of the nozzle and include girth gage measurements on case and nozzle.

RECEIVED
JAN 10 1964
U.S. AIR FORCE

4 / INSTRUMENTATION

4.1 INTRODUCTION

The basic TEM-10 instrumentation measurements consisted of: motor thrust measurements head-end chamber pressure, motor pressure oscillation, igniter chamber pressure, nozzle fixed housing temperature and strain, case temperature for deluge control, aft segment case accelerometers, case temperature for indirect propellant bulk temperature measurement, test stand water deluge pressure, field joint temperature, nozzle-to-case joint temperature, igniter and S&A flange temperatures, and timing.

Fifty data channels were added to the released instrumentation drawing to gather data in support of the chamber pressure perturbation study. These added data channels were sound pressure, force measurement on fixed links, accelerometers and strain gages down the length of the motor case, and accelerometers on the nozzle forward and aft exit cones.

A duplicate set of strain gages were installed with the resistance temperature detector (RTD) on each quadrant of the nozzle fixed housing. One set of strain gages was sampled at 2,000 samples per second and the other set was sampled at 32 samples per second. The 32 sample per second (SPS) strain gage set was used to gather postfire heat soak data on the fixed housing.

The nozzle-to-case joint temperature was ensured to be above 75°F by monitoring measurements and from RTDs on the nozzle-to-case joint heater.

Thermocouples were installed on the forward and aft case segments at 90-deg location intervals. These data were recorded at a slow sample rate from time of motor assembly to T-0. This mode of measurement provides data used in the PMBT prediction.

The baseline igniter was instrumented with RTDs on the S&A flange to monitor a test temperature of 68-125°F. The requirement was met.

4.2 OBJECTIVES/CONCLUSIONS

The objectives and corresponding conclusions from Section 2 regarding instrumentation performance were:

| OBJECTIVES | CONCLUSIONS |
|--|---|
| D. Measure motor head-end chamber pressure oscillations. | Pressure oscillation data channel failed to acquire data because of incorrect circuit in the ground data collection system. However, PNCAC0C1, which is a split signal from the operational pressure transducer (OPT) performed nominally. Data were collected from PNCAC0C1. |

F. Obtain RTR, acceleration, IR plume, sound pressure, and strain data in support of the RSRM-29 pressure, anomaly investigation.

All sound pressure data and strain data were successful. One acceleration data channel was intermittent (AANAV011). All other accelerometer data channels were satisfactory. RTR data were obtained for the forward field joint and aft dome factory joint regions. One IR camera was lost pretest.

4.3 RECOMMENDATIONS

Continue instrumentation of case and nozzle as modified on TEM-10 to gather additional data on pressure perturbation study. Add a more comprehensive coverage of accelerometers through the length of the nozzle and include strain gage measurements on case and nozzle.

4.4 RESULTS/DISCUSSION

Generally, the instrumentation performed satisfactorily. Two data channels of the 143 total data channels were lost resulting in a data collection success rate of 99 percent.

4.4.1 Acceleration

Three accelerometers were installed on the aft center segment to gather standard dynamic vibration data in the three motor axis. These data channels were all nominal. Analysis of the data is included in TWR-63827.

In support of pressure perturbation study, four triaxial accelerometers were installed midway on the case segments and one each uniaxial accelerometer on the forward and aft domes. The following accelerometers were installed on the nozzle; one triaxial on the aft exit cone, six uniaxial on aft exit cone, and six uniaxial on the forward exit cone. The intent of these measurements was to track any disturbance progressing within the motor. One of these accelerometers (AANAV011) was intermittent during the motor firing.

4.4.2 Pressure

The igniter and chamber pressures were nominal. Pressure oscillation measurements were also recorded.

The three chamber pressures and the igniter pressure measurements were nominal. An additional dedicated OPT was installed at the 100-deg port on the forward dome closure to measure chamber pressure oscillation. This dedicated pressure oscillation transducer performed nominally, but the ground signal processing circuit failed. A signal split off the OPT was used to measure chamber pressure oscillation. Data were nominal.

4.4.3 Thrust

All test stand thrust measurements were nominal.

4.4.4 Calorimeter and Radiometer

One calorimeter (CNPAX001) and radiometer (UMPAX028) were positioned on the test stand under the nozzle with a view angle midway between the end of the nozzle and the test stand floor. These measurements were successful. These gages were considered experimental facility instrumentation and are not on the instrumentation drawing.

4.4.5 Strain Measurement

The biaxial strain gages on the nozzle fixed housing performed nominally and correlated to prior measurements on the nozzle components. Postfire data were collected on the fixed housing for eight hours to evaluate heat soak effects.

The added biaxial strain gages at the midpoint of each case segment for pressure perturbation study and the strain gages added at the midpoints of the forward and aft domes all performed nominal.

Strain gages were installed on the thrust adapter struts on four quadrants to collect measured strain in correlation to thrust. These gages performed well and should add to possible data extrapolation for secondary measurement of thrust.

4.4.6 Temperature Measurement

All four RTDs on the nozzle fixed housing performed nominally and postfire heat soak data were collected.

The 22 slag thermocouples on the case (used to control case deluge) performed nominally.

The ambient temperature was 56°F and the PMBT was 69°F at T-0. The data collected from the eight thermocouples on the forward and aft motor segments to predict PMBT performed nominally and operated from motor assembly throughout motor firing.

All field joint, nozzle-to-case joint, igniter, and S&A flange RTD operations were nominal.

4.4.7 Sound Pressure

One sound pressure measurement was taken on top of the motor at the miniskirt. This measurement was requested in support of the pressure perturbation study. The measurement was satisfactory.

4.4.8 Real-Time Radiography

The RTR systems were evaluated for potential detrimental effects on the instrumentation and data acquisition systems. Both analyses and pretest demonstrations were performed and no problems were found. These systems were provided by outside contractors (Arnold Engineering Development Center and High Energy Systems Company for the forward joint and Naval Weapons Center on the aft stiffener cylinder) and useful data were obtained. Section 6.10 discusses the results of the RTR systems.

SECRET

5 / PHOTOGRAPHY

Photographic coverage was required to document the test, test configuration, instrumentation, and any anomalous conditions which may have occurred. The TEM-10 photographs and video tapes are available from the Thiokol Corporation Photographic Services Department.

5.1 STILL PHOTOGRAPHY

Still color photographs of the test configuration were taken before, during, and after the test. Photographs were taken of joints each 45 deg minimum and at anomalous conditions.

5.2 MOTION PICTURES

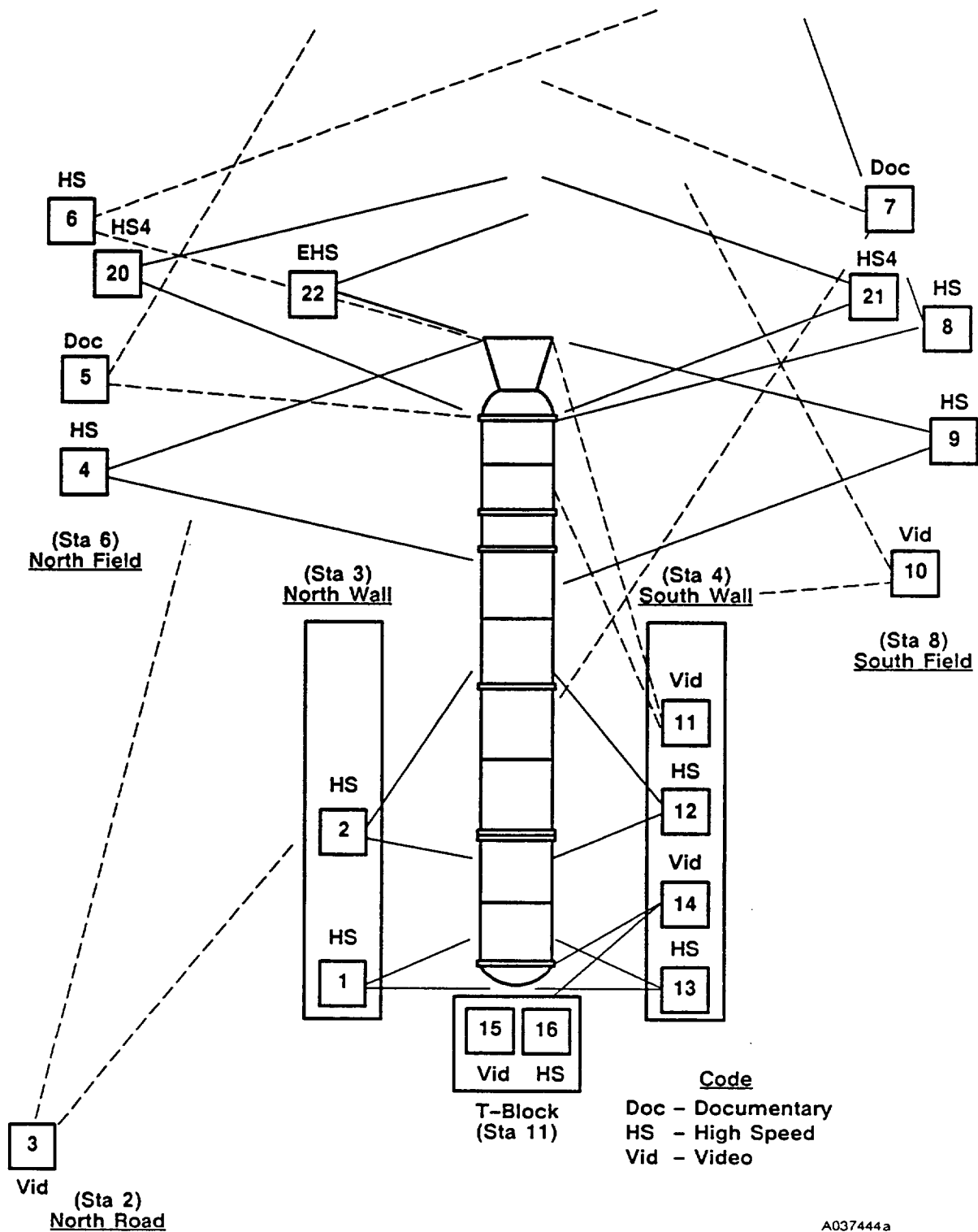
Color motion pictures of the test were taken with 10 high-speed cameras, two real-time documentary cameras, and five video cameras. Documentary motion pictures are recorded on roll 8709, high-speed motion pictures on roll 8708, and videotape on T0347. Cameras are listed in Tables 5-1 and 5-2. The camera setup is shown in Figure 5-1.

Table 5-1. Photography and Video Coverage

| Camera | Station | Location | Type | Coverage |
|---|---------|--------------|------|---|
| 1 | 3 | North wall | HS | Igniter port |
| 2 | 3 | North wall | HS | Center forward and center joints |
| 3 | 2 | North road | Vid | Overall motor and plume |
| 4 | 6 | North field | HS | Center aft and nozzle-to-case joints |
| 5 | 6 | North field | Doc | Aft case, nozzle, and plume |
| 6 | 6 | North field | HS | Nozzle, 200-ft plume |
| 7 | 9 | South field | Doc | Overall motor and plume |
| 8 | 8 | South field | HS | Nozzle, 200-ft plume |
| 9 | 8 | South field | HS | Aft center and nozzle-to-case joints |
| 10 | 8 | South field | Vid | Aft case, nozzle, plume, deluge |
| 11 | 4 | South wall | Vid | Aft joint nozzle and plume |
| 12 | 4 | South wall | HS | Forward center and center joints |
| 13 | 4 | South wall | HS | Igniter port |
| 14 | 4 | South wall | Vid | Igniter and CO ₂ quench system |
| 15 | 11 | Thrust block | Vid | Top of case, nozzle, and plume |
| 16 | 11 | Thrust block | HS | Top of case, nozzle, and plume |
| 20 | 6 | North field | HS4 | Nozzle and plume, medium shot |
| 21 | 8 | South field | HS4 | Nozzle and plume, medium shot |
| 22 | 6 | North field | EHS | Nozzle and plume, closeup |
| CODE: EHS - 1 each, 3,000 FPS HS4 - 2 each, 400 FPS HS - 9 each, 300 FPS Doc - 2 each, 24 FPS Video - 5 each, real-time | | | | |

Table 5-2. Photography and Video Sequencing

| Camera | Controller | Station | Location | Start Time | Stop Time | Priority* |
|-------------------------------|------------|---------|-------------------------|------------|-----------|-----------|
| 1 | 5 | 3 | North of bay | T-5 sec | T+150 sec | M |
| 2 | 6 | 3 | North of bay | T-5 sec | T+150 sec | M |
| 3 | N/A | 2 | Northwest of bay | Manual | Manual | R |
| 4 | 9 | 6 | North of nozzle | T-5 sec | T+150 sec | M |
| 5 | 10 | 6 | North of nozzle | T-15 sec | T+180 sec | R |
| 6 | 11 | 6 | North of nozzle | T-5 sec | T+150 sec | M |
| 7 | 15 | 9 | South and aft of nozzle | T-15 sec | T+180 sec | M |
| 8 | 16 | 8 | South of nozzle | T-5 sec | T+150 sec | M |
| 9 | 16 | 8 | South of nozzle | T-5 sec | T+150 sec | M |
| 10 | N/A | 8 | South of nozzle | Manual | Manual | R |
| 11 | N/A | 4 | South wall | Manual | Manual | R |
| 12 | 7 | 4 | South wall | T-5 sec | T+150 sec | M |
| 13 | 8 | 4 | South wall | T-5 sec | T+150 sec | M |
| 14 | N/A | 4 | South wall | Manual | Manual | R |
| 15 | N/A | 11 | Top of thrust block | Manual | Manual | R |
| 16 | 20 | 11 | Top of thrust block | T-5 sec | T+150 sec | M |
| 20 | 11 | 6 | North of nozzle | T-5 sec | T+150 sec | M |
| 21 | 16 | 8 | South of nozzle | T-5 sec | T+150 sec | M |
| 22 | 12 | 6 | North of nozzle | T+60 sec | T+75 sec | M |
| * M = mandatory, R = required | | | | | | |



A037444a

Figure 5-1. T-24 Photography Coverage--TEM-10

1998

6 / TEST DESCRIPTION AND RESULTS

6.1 TEST ARTICLE DESCRIPTION

The TEM-10 test article was assembled in accordance with Drawing 1U77609. The motor was instrumented to provide data to satisfy the test objectives. An overall view of the static test arrangement is shown in Figure 6-1. A TEM-10 drawing tree is included in Appendix A.

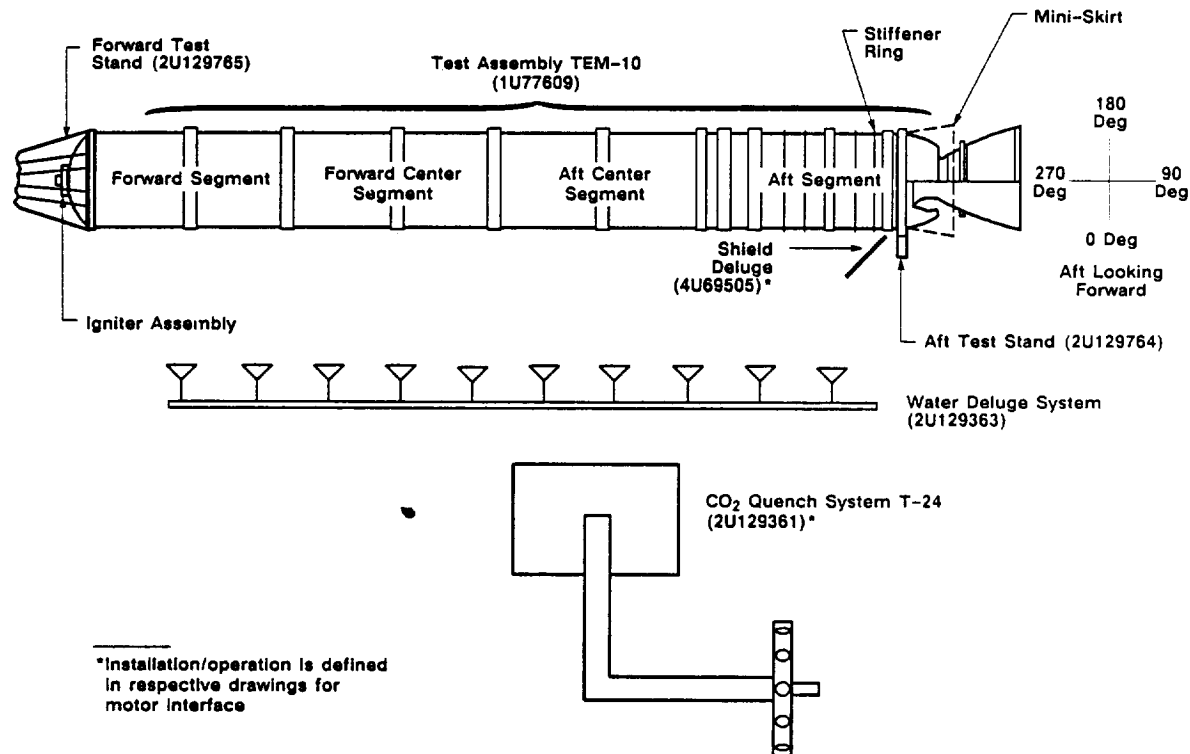


Figure 6-1. TEM-10 Static Test Arrangement

TEM-10 consisted of HPM-configuration motor segments which were fabricated and loaded with propellant more than seven years before the static test fire on 27 April 1993. A listing of each segment, segment flight identification, cast date, and storage and transportation history is shown in Table 6-1.

Table 6-1. TEM-10 Segment History

| TEM-10 Segment | Forward | Forward Center | Aft Center | Aft |
|---------------------------------------|-----------|----------------|------------|-----------|
| Flight Identification | SRM-26B | SRM-25A | SRM-29B* | SRM-27A |
| Casting Date | 26 Jul 85 | 28 Jun 85 | 23 Oct 85 | 19 Aug 85 |
| Shipped to Kennedy Space Center (KSC) | 31 Oct 85 | 9 Oct 85 | 6 Nov 85 | 24 Nov 85 |
| Arrived at KSC | 11 Nov 85 | 18 Oct 85 | 14 Nov 85 | 2 Dec 85 |
| Shipped to Thiokol | 21 Nov 89 | 24 Apr 90 | 18 Jan 89 | 27 Aug 87 |
| Arrived at Thiokol | 28 Nov 89 | 5 May 90 | 25 Jan 89 | 8 Sep 87 |
| *Reassigned to SRM-26B | | | | |

The high-performance SRM static test motor consisted of insulated, lined, segmented rocket motor cases loaded with solid propellant; a redesigned baseline ignition system complete with electro-mechanical S&A device, unibody initiators and loaded igniter; and movable nozzle with flexible bearing and exit cone. For this test, the nozzle was held rigid using fixed links with no thrust vector control (TVC).

The assembled static test motor was approximately 116 feet in length and 12 feet in diameter. The test item configuration was controlled by the released engineering drawings (reference TEM-10 drawing tree) and CTP-0110, Revision D. Deviations to this configuration were processed through the normal configuration control system and approved by the project engineer, program manager, and NASA and are included in this final test report.

Postfire hardware evaluation of TEM-10 was accomplished in accordance with TWR-60273 and TWR-63821. Observations were recorded on the postfire observation records (PFOR). Any anomalous condition which was a limits violation or a first-time occurrence was documented on a postflight anomaly report (PFAR).

6.2 TEST ARRANGEMENT AND FACILITIES

The TEM-10 static test arrangement (Figure 6-1) was assembled in accordance with Drawing 2U65151. T-24 was equipped with a water deluge system and a carbon dioxide (CO₂) quench. A fixed link support assembly (Drawing 7U76924) was installed in place of the aft skirt. This ring provided mounting provisions for the fixed links (Drawing 2U132116) which were used in place of TVC actuators.

6.3 CASE AND CASE SEALS PERFORMANCE

6.3.1 Introduction

The case consisted of 11 individual weld-free segments: the forward dome, six cylinder segments, the external tank (ET) attach segment, two stiffener segments and the aft dome. The 11 segments were preassembled into four subassemblies to facilitate propellant casting.

The four loaded assemblies were the forward segment assembly (Drawing 1U77555), the forward center segment assembly (Drawing 1U50543), the aft center segment assembly (Drawing 1U50543), and the aft segment assembly (Drawing 1U77613). These segments were joined by means of tang and clevis field joints, which in turn, were held in place by pins.

The TEM-10 forward center cylinder (1U50717, S/N 0000077) had a discrepant outer clevis leg. The clevis was bent outward, with the bend centered at the 310-deg location. Pin holes at the 92-, 292-, 310-, and 328-deg locations were also damaged. Nondestructive evaluation (NDE) of the discrepant region revealed no cracks.

The forward segment and forward center segment were mated using custom fitted, custom tapered shims (Drawing 7U77681) at the 308-, 310-, and 312-deg locations. A

nonload bearing nylon pin (Drawing 7U77684) was installed at the 310 degree location. This ensured that the load was redistributed to the undamaged adjacent holes. Positive margins of safety were maintained at the 92-, 292-, 310-, and 328-deg locations. Primary and secondary O-rings (1U75150-11, S/N 0000785, and 1U75150-11, S/N 0000795, respectively) were preassigned to increase squeeze in this joint.

Stiffener rings (Drawing 1U52501) were installed on the forward stub of the forward stiffener cylinder. An outer ligament crack existed at 322-deg on the forward stub.

The nozzle-to-case joint was formed by bolting the nozzle fixed housing into the aft dome with 100 axial bolts (Drawing 1U76034). The field joints had a standard HPM insulation configuration as shown in Figure 6-2. The nozzle-to-case joint had the standard HPM nozzle joint insulation configuration as shown in Figure 6-3. Nozzle Joint No. 1 (forward/aft exit cone) was configured with a special O-ring

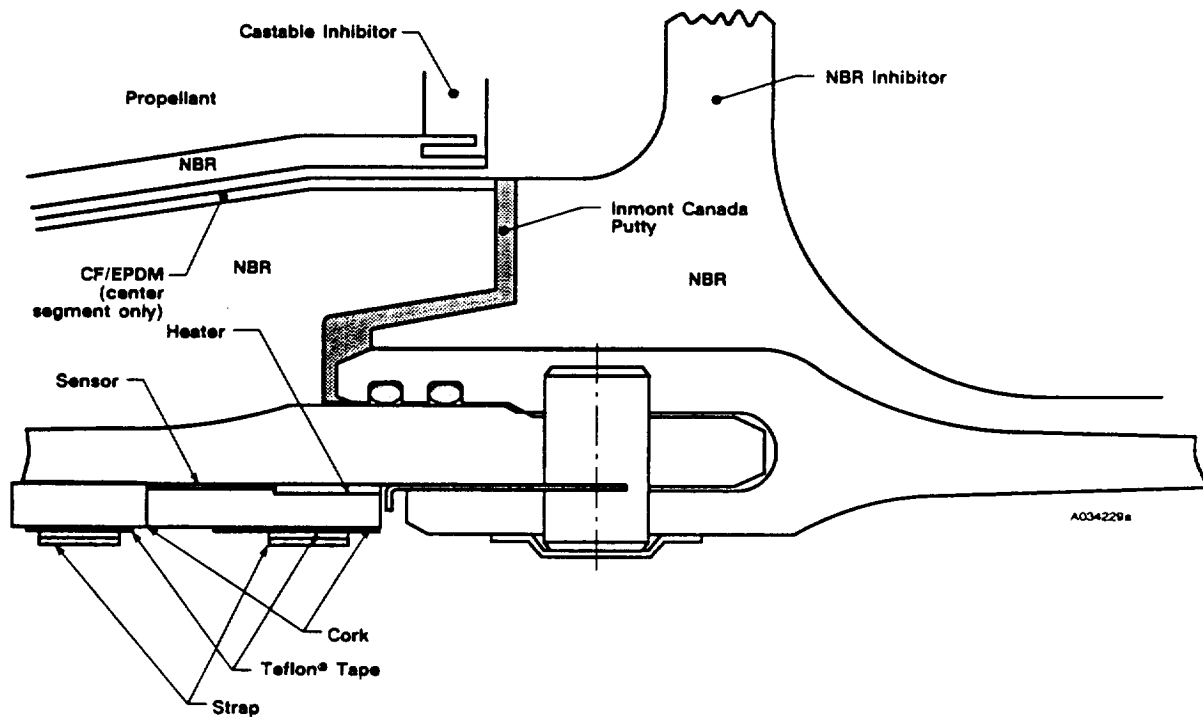


Figure 6-2. TEM-10 Field Joint Configuration

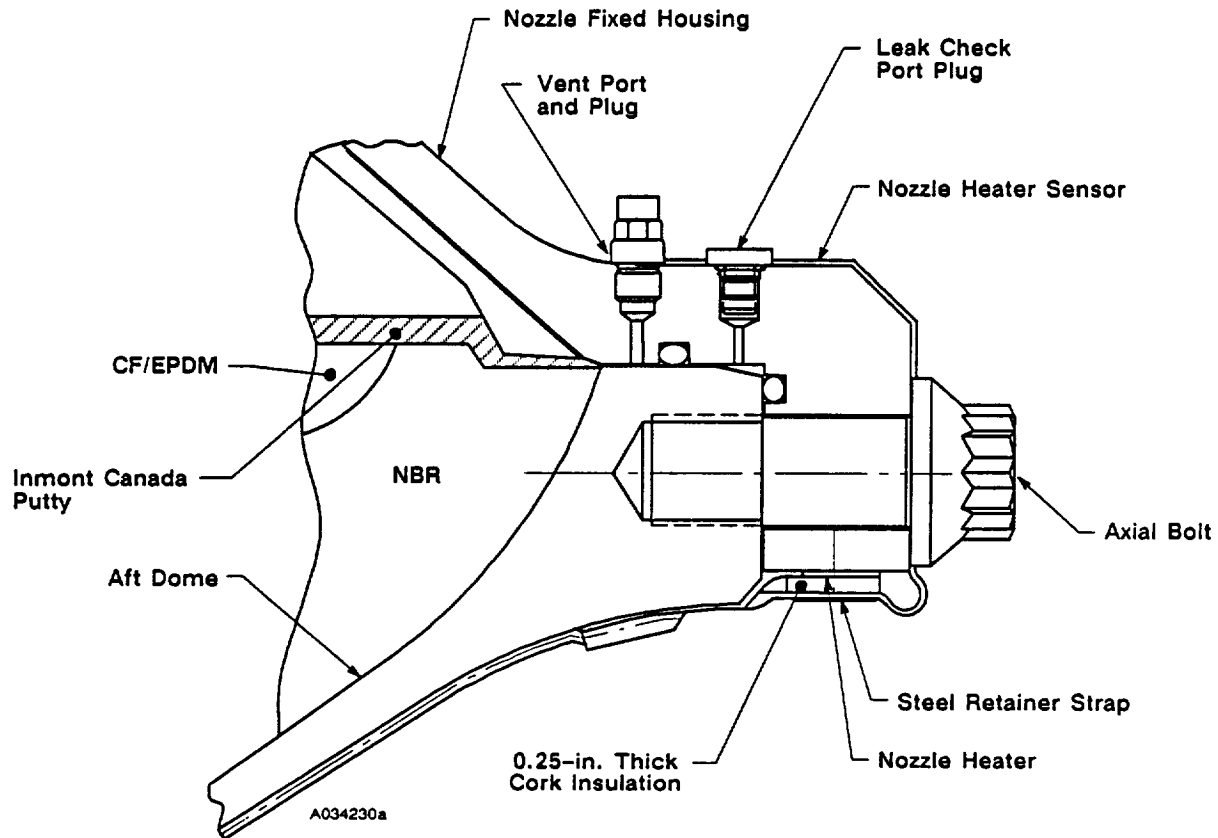


Figure 6-3. TEM-10 (HPM Modified) Nozzle-to-Case Joint Configuration

The assembly and joint configuration was as follows:

- a. Forward segment and forward center segment were mated to form the forward field joint. The forward center segment and aft center segment were mated to form the center field joint. The aft center segment and aft segment were mated to form the aft field joint. The field joints (with the exception of the forward-to-center-forward segment joint mentioned above) which connect these segments were configured with:
 - Tang and clevis with long pins (Drawing 1U51055), custom fitted shims (Drawing 1U51899), and hat band pin retainers (Drawing 1U82840).
 - Standard HPM insulation configuration with putty joint filler (STW4-3266) as shown in Figure 6-2.
 - Primary and secondary O-rings are fluorocarbon (1U75801-02)
 - Leak check port plugs (Drawing 1U100269)
 - Improved field joint heater (Drawing 1U77252)
 - Baseline TEM joint protection system (JPS) (Drawing 7U77607)

- b. The nozzle-to-case joint was configured with:
 - Primary (larger diameter RSRM) and secondary O-ring seals are fluorocarbon (1U75801-15 and 1U75801-16, respectively)
 - Standard HPM nozzle joint insulation configuration with putty joint filler (STW4-3266) as shown in Figure 6-3
 - RSRM configuration ultrasonic preload axial bolts installed in accordance with Drawing 1U77613
 - MS16142 vent ports at 15, 105, 195, and 285 deg in the fixed housing (1U50088-08) upstream of the primary O-ring
 - Baseline TEM JPS (Drawing 7U77607) with nozzle-to-case joint heater (Drawing 7U77254)
 - Adjustable vent port plugs (Drawing 1U76425 and 1U50159)
 - Leak check port plug (Drawing 1U100269)
- c. Factory joints were configured with the following:
 - HPM tang and clevis hardware design
 - Insulation overlaid and cured over interior of the joint
- d. Igniter to forward dome joint was configured with:
 - Primary and secondary seals of the outer gasket (Drawing 1U77463) are fluorocarbon
 - Redesigned J-joint insulation on outer and inner joints
 - Two-sided PSA (STW5-3479) applied to inner and outer joints
 - Thicker igniter adapter (Drawing 1U77452) with new inner (Drawing 1U77358) and outer (Drawing 1U77460) joint attach bolts
 - Baseline TEM JPS (Drawing 7U77607) with igniter-to-case joint heater (Drawing 1U77253)

Corrosion protection consisted of full external paint and a film of grease applied as specified in Drawing 1U77611 and STW7-3688 (including O-rings, sealing surfaces, and pin holes).

6.3.2 Objectives/Conclusions

The TEM-10 case and seals performed nominally.

6.3.3 Recommendations

None.

6.3.4 Results/Discussion

This section documents the condition of the forward, center, and aft field joints, the nozzle-to-case joint, and related special issues. The motor joints were nominal.

6.3.4.1 Forward Field Joint. The TEM-10 forward field joint was disassembled on 11 May 1993. No anomalous conditions were observed on the forward field joint. Zinc chromate putty was in contact with the primary O-ring full circumference. Typical pin hole slivers were seen on the clevis side at the 56-, 68-, 72-, 88-, 198-, 200-, 208-, 292-, and 336-deg locations and on the tang side at the 300-deg location.

6.3.4.2 Center Field Joint. The TEM-10 center field joint was disassembled on 11 May 1993. The center field joint was in nominal condition. Zinc chromate putty was observed up to the primary O-ring full circumference. Typical pin hole slivers were seen on the clevis side at the 80-, 90-, 136-, 154-, 176-, 204-, 206-, 208-, 212-, 214-, 222-, 316-, 318-, 328- and 342-deg locations. The center field joint leak check port through-hole was plugged with grease. PFAR TEM10-01 was written against this observation.

6.3.4.3 Aft Field Joint. The TEM-10 aft field joint was disassembled on 10 May 1993. The aft field joint was in nominal condition. Zinc chromate putty was observed in contact with the primary O-ring intermittently full circumference. Typical pin hole slivers were seen at the 70-deg (clevis side), 86-deg (tang side), and 90-deg (clevis side) locations.

6.3.4.4 Nozzle-to-Case Joint. The TEM-10 nozzle-to-case joint was disassembled on 13 May 1993. Scratches were observed on the aft dome boss primary seal surface and lead-in ramp intermittently from the 216- to 333-deg location. It appeared as if soot or slag or both were dragged across the putty and then across the seal surface and lead-in ramp causing the scratches. A preliminary PFAR was written against this observation. No other anomalous conditions were observed. Zinc chromate putty was observed up to the primary O-ring full circumference.

6.3.4.5 Results of Special Issues (TWR-63821, para. 3.2). The following items were designated Special Issues unique to TEM-10 case and case seals to be evaluated in conjunction with the standard postfire evaluation. This section lists the conditions as written in TWR-63821, Revision A, and the resulting evaluations:

3.2.1 Case

- 1) Condition: The forward field joint outer clevis leg had a discernable outward bend between the 308- and 312-deg locations. The clevis gap measured 0.049 in. over allowed refurbishment criteria (worst case at 310 deg). A non-load bearing pin (nylon) was used at the 310-deg location. Specialized tapered pin retainers (shims) were installed to fill the gap between outer clevis leg and tang at the 308- to 312-deg pin holes.

Results: No anomalous conditions were observed on the forward field joint. The nylon pin and specialized tapered shims appeared to perform nominally.

- 2) Condition: The 322-deg pin hole on the forward stiffener cylinder forward flange had an outboard crack.

Results: Following stiffener ring removal no new cracks were discernable, there were no signs that the old crack had changed, and there were no visible signs of inboard cracks in this region.

3.2.3 Joints

- 1) Condition: The forward field joint outer clevis leg had a discernable outward bend between 308 to 312 deg. The clevis gap measures 0.049 in. over allowed refurbishment criteria (worst case at 310 deg).

Results: No anomalous conditions were observed due to the bent clevis.

6.4 CASE INTERNAL INSULATION PERFORMANCE

The internal insulation system included case acreage insulation, joint insulation, and propellant stress relief flaps. The insulation material used for these components was an asbestos/silica-filled acrylonitrile butadiene rubber (NBR) (STW4-2621). Carbon-fiber-filled ethylene-propylene-diene monomer (CF/EPDM) (STW4-2868) was bonded to the NBR in a sandwich-type construction under the propellant stress relief flaps in both center segments. CF/EPDM was also used in sandwich construction in the aft dome. The CF/EPDM was installed to reduce the erosion of the insulator near the submerged nozzle in the aft dome and under the stress relief flaps in the center segments.

The liner material specified in STW5-3224 was an asbestos-filled carboxyl-terminated polybutadiene (CTPB) polymer which bonded the propellant to the internal insulation in the SRM. The forward-facing full web inhibitors were made of NBR. They were located on the forward end of the center and aft segments. The aft facing partial web castable inhibitors were made of a material (STW5-3223) similar in type (CTPB polymer) to the liner. They were HPM configuration and were located on the aft end of the forward and center segments.

Field joints and nozzle-to-case joint were standard HPM configuration. Field joint putty was tamped following assembly to repair defects and reduce the potential for blow holes.

6.4.1 Introduction

The four TEM-10 segments had been insulated and cast with propellant more than seven years before the TEM-10 static test.

6.4.1.1 Field Joint Assembly. The case insulation of the three HPM-configuration field joints consisted of asbestos/silica-filled NBR. Prior to mating, the joints were inspected per STW7-2831, Revision NC, the flight motor insulation criteria for the HPM joints. Putty was applied to the clevis joints per STW7-3746, and the joints were mated. After mating, each joint was inspected from the bore for discontinuities and the putty was tamped.

6.4.1.1.1 Prefire Inspection/Joint Putty Tamping. A prefire bore inspection was performed to assess the putty flow/layup of each field joint. The inspection occurred after the chocks were removed and the final leak check had been performed. This did not include the nozzle-to-case joint, which was inaccessible during this operation. The putty in the field joints was inspected for grease, discontinuities, bubbles, blow holes, etc. Due to the test delay, the joints were inspected three different times. All tamping and inspections are documented in TWR-64992.

All volcanoes, bubbles, and possible bubbles were tamped closed with a putty tamping tool. No grease contamination was found in any of the joint putty and the field joint putty condition was nominal. The overall prefire insulation condition of TEM-10 was similar to previous TEMs.

6.4.1.2 Nozzle-to-Case Joint Assembly. The putty layup for the nozzle-to-case joint was performed to the dimensions of STW7-3745, as were previous TEMs. The TEM-10 nozzle was mated to the aft segment with no apparent anomalies. Because of inaccessibility, the nozzle-to-case joint was not inspected nor tamped as were the field joints.

Similar to TEM-5, TEM-6, TEM-7, TEM-8, and TEM-9 the nozzle-to-case joint incorporated four vent ports in the fixed housing. The vent ports were left open during assembly to exhaust entrapped air from within the joint. This concept was intended to reduce the potential for O-ring damage from gas flow through-holes in the putty.

6.4.2 Objectives/Conclusions

The case internal insulation performed as expected; no anomalous conditions were present. The performance in all three field joints and the nozzle-to-case joint was excellent; no gas penetration to the seals was observed. The joints functioned within the HPM experience.

6.4.3 Recommendations

None.

6.4.4 Results/Discussion

This section documents the results of: the postfire internal insulation inspection; the condition of the aft, center, forward, and nozzle-to-case joints insulation and the igniter insulation; and special issues.

6.4.4.1 Postfire Internal Insulation Inspection. An internal walk-through inspection was performed on 10 May 1993. The internal acreage insulation appeared to be in normal condition during the internal walk-through inspection. Full flap with approximately 10-15 in. of castable inhibitor remained on the forward segment over the majority of the circumference.

The slag pool extended the full length of the aft segment and 37 in. into the aft center segment. The size of the slag pool appeared larger than that typical of previous static test TEMs.

6.4.4.2 Aft Field Joint Insulation. The aft field joint was disassembled and inspected on 10 May 1993. The joint insulation and putty were in excellent condition, showing normal heat effects, charring, and erosion. No gas penetration into the joint was identified. The putty exhibited a constant olive green color with normal tack. The putty failure at disassembly was estimated at 5 percent adhesive to the NBR insulation and 95 percent cohesive failure.

No clevis or tang edge separations greater than 0.25 in. were detected. The aft center segment stress relief flap and the aft segment NBR inhibitor were in normal condition. The flap was eroded back to the bulb full circumference. No tears were present on either the flap or NBR inhibitor.

6.4.4.3 Center Field Joint Insulation. The center field joint was disassembled and inspected on 11 May 1993. The joint insulation and putty were in good condition, showing normal heat effects, charring, and erosion. No gas penetration into the joint was identified. Several areas of deeper heat effects reaching 0.70 in. maximum into the putty were seen intermittently over the full circumference. The putty exhibited a constant olive green color with normal tack. The putty failure at disassembly was estimated at 20 percent adhesive to the NBR insulation and 80 percent cohesive.

No clevis or tang edge separations greater than 0.25 in. deep were detected. The forward center stress relief flap and aft center NBR inhibitor were in normal condition. The flap was eroded approximately three-quarters back to the flap bulb full circumference. The NBR inhibitor showed normal erosion with no tears present.

6.4.4.4 Forward Field Joint Insulation. The forward field joint was disassembled and inspected on 11 May 1993. The joint insulation and putty were in normal condition, showing normal heat effects, charring, and erosion. No gas penetration in the joint was identified. Several areas of deeper heat effects reaching 0.40 in. maximum in the putty were seen intermittent from the 200-300 deg location. The putty exhibited a constant olive green color and normal tack. The putty failure at disassembly was estimated at 5 percent adhesive to the NBR insulation and 95 percent cohesive. No tang or clevis edge separations greater than 0.25 in. deep were detected.

The forward segment stress relief flap showed normal erosion. The full flap remained for the full circumference with virgin NBR and FEP film under the flap. The castable inhibitor also remained intact and attached to the split flap for the majority of the circumference.

Approximately 10 to 15 in. in height of castable inhibitor remained from the 190-360-142 deg location. From the 142-190 deg location only a stub of castable inhibitor remained attached to the flap. The forward center segment NBR inhibitor was also in normal condition. Approximately 25 to 28 in. radially of NBR inhibitor remained.

6.4.4.5 Nozzle-to-Case Joint Insulation. The nozzle-to-case joint was disassembled and inspected on 13 May 1993. The joint insulation and putty were in normal condition, showing normal heat effects and sooting on the forward edge of the bondline. There was no evidence of gas penetration into the joint insulation bondline (putty). The putty exhibited a consistent olive green color with normal tack. The putty failure at disassembly was estimated 5 percent adhesive and 95 percent cohesive. No voids in the putty were observed. Three small aft dome edge unbonds were detected with the largest located at the 265-deg location and measuring 0.12 in. deep by 0.34 in. circumferential.

6.4.4.6 Igniter Outer Joint and Chamber Insulation. See Section 6.7, Ignition System Performance.

6.4.4.7 Igniter Inner Joint and Adapter Insulation. See Section 6.7, Ignition System Performance.

6.4.4.8 Results of Special Issues (TWR-63821, para. 3.1.2, 3.1.3). The following items were designated special issues unique to the TEM-10 internal insulation to be evaluated in conjunction with the standard postfire evaluation. This section lists the condition as written in TWR-63821, Revision A, and the resulting evaluation.

3.1.2 Internal Insulation

3.1.2.1

Condition: TEM-10 forward segment was built with a long inner split flap leg similar to the TEM-08 forward segment. The TEM-10 inner split flap leg may also be contaminated with propellant and experience similar erosion as TEM-08 on the case wall insulation and NBR inhibitor.

Results: No evidence of abnormal erosion to the flap, case wall insulation, or NBR inhibitor was seen. The forward segment stress relief flap showed normal erosion. The full flap remained for the full circumference with virgin NBR and FEP film under the flap. The castable inhibitor also remained intact and attached to the split flap for the majority of the circumference. Approximately 10 to 15 in. in height of castable inhibitor remained from the 190-360-142 deg location. From the 142-190 deg location only a stub of castable inhibitor remained attached to the flap. The forward center segment NBR inhibitor was also in normal condition. Approximately 25-28 in. radially of NBR inhibitor remained.

3.1.2.2

Condition: Internal insulation aging and surveillance study analysis was performed on TEM-9. More data are needed from the TEM-10 aft segment for analysis.

Results: After a final analysis of the data obtained from TEM-9 was performed, it was concluded that no additional internal case insulation data was required from the TEM-10 aft segment. Action order 4C2-1241 was released which deleted the TEM-10 data collection requirement.

3.1.2.3

Condition: TEM-10 case field joints are insulated with putty that have been tamped three times because of the extended assembly time in the horizontal position.

Results: No abnormal conditions due to the repeated putty tamping were evident. All field joints were in good condition with no blowholes through the putty. The forward segment flap and castable inhibitor was in good condition as explained in condition 3.1.2.2.

3.1.3 Igniter Insulation

3.1.3.1

Condition: The baseline redesigned igniter was used in TEM-10. The baseline redesigned igniter includes J-leg insulation for the inner and outer igniter joints. The outer J-leg insulation incorporates two-sided PSA.

Results: Both igniter J-joints performed as expected with two-sided PSA. Adequate thermal protection was provided to the metal hardware. There was no visible evidence that combustion gas penetrated either J-joint, and none reached the seals. The PSA did not move from the allowable application zone. There was no PSA on the primary seal of the outer gasket. The two-sided PSA performed as good or better than one-sided PSA. See PFOR A-5 for detailed PSA failure mode information.

3.1.3.2

Condition: The redesigned igniter adapter used in TEM-10 had insulation line profiles that were out of tolerance. This condition may result in slightly more J-leg engagement with the igniter chamber (inner joint).

Results: The inner J-joint insulation was in excellent condition and performed as expected. No gas penetrated into the J-joint. The PSA was in good condition with a 0.250 to 0.350 J-leg contact zone evident full circumference. The line profile out of tolerance condition appears to have had no negative effect on the J-leg performance.

6.5 LEAK CHECK PERFORMANCE

6.5.1 Introduction

After each pressure vessel joint is assembled, a leak test is performed to determine the integrity of the seals. The leak tests usually consist of a joint volume determination and a pressure decay test. The volume and pressure information is combined with temperature and time data collected during the test and used in the calculation of a leak rate, which is expressed in terms of standard cubic centimeters per second (sccs). Each leak test has a maximum leak rate allowed.

Some specifications require only a maximum pressure decay over time. This method has been determined as sufficient based on the small, constant volumes, and the equivalent leak rates, which are conservative when using all worst-case variables.

Table 6-2 comprises a list of all joints tested for TEM-10, the leak test specification, and the equipment used to test the joints. The leak tests will be discussed in detail in Section 6.5.4. The case factory joints were tested after the original assembly. This report does not discuss the results of the case factory joint tests. The nozzle internal joints (Joints 1 through 5) contained components of HPM configuration. HPM internal nozzle joints are not leak tested and contain no leak test port.

Table 6-2. TEM-10 Seal Leak Testing

| Joint | Specification | Equipment |
|---------------------------|---------------|-----------|
| Case Field Joints | STW7-3682 | 8U75902 |
| Nozzle-to-Case Joint | STW7-3682 | 2U129714 |
| Ignition System | | |
| Inner Gasket | STW7-3894 | 2U129714 |
| Outer Gasket | STW7-3894 | 2U129714 |
| Special Bolt Installation | STW7-3894 | 2U129714 |
| S&A Joint | STW7-3895 | 8U76500 |
| Transducer Assembly | STW7-2853 | 2U65686 |
| Barrier-Booster/SII | STW7-3896 | 2U65848 |

6.5.2 Objectives/Conclusions

Leak tests were performed to verify that the joints were properly assembled and the O-rings would perform properly. As discussed in the following section, it is concluded the seals were acceptable for the TEM-10 joints. No further conclusions were reached.

6.5.3 Recommendations

None.

6.5.4 Results/Discussion

The case field joint leak test results are shown in Table 6-3. The TEM field joints were tested at lower pressures (185 psig) than RSRM field joints (1,000 psig) because of their configuration. These joints were tested with and without the assembly stands (chocks) in place. All results were within the limits.

Table 6-3. TEM-10 Case Field Joint Leak Test Results

| Pressure (psig) | Maximum Leak Rate (scgs) | Actual Leak Rates (scgs), Prechock/Postchock | | |
|-----------------|--------------------------|--|---------------|---------------|
| | | Forward | Center | Aft |
| 185 | 0.072 | 0.0128/0.0129 | 0.0136/0.0135 | 0.0164/0.0124 |
| 30 | 0.0082 | 0.0010/-0.0004 | 0.0005/0.0004 | 0.0004/0.0000 |

The field joint tests were performed with a variation of the 8U75902 ground support equipment leak test system. For testing of the TEMs, the equipment was modified to include a pressure relief valve to preclude the possibility of over-pressurizing the joint.

The ignition system leak test results are shown in Table 6-4. The tests were performed with the leak test equipment shown in Table 6-2. The equipment was identical to that used to test the equivalent RSRM joints. All results were within the limits.

Table 6-4. TEM-10 Igniter and S&A Leak Test Results

| Joint Seal | Allowable Leak Rate (sccs), HI/LO* | Actual Leak Rate (sccs), HI/LO* |
|---|---------------------------------------|------------------------------------|
| Inner | 0.10/0.0082 | 0.0038/-0.0001 |
| Outer | 0.10/0.0082 | 0.0039/-0.0001 |
| Transducer Installation | 0.10/0.0082 | 0.0015/-0.0005 |
| OPT** | 10 psi, 10 min/1 psi, 10 min | 3.0/0.0 2.0/0.0 3.0/0.0 |
| Barrier-Booster | 1 psi/10 min | 0.2/10 min |
| SII (198 degrees) | 1 psi/10 min | 0.6/10 min |
| SII (18 degrees) | 1 psi/10 min | 0.0/10 min |
| S&A | 0.10/0.0082 | 0.0089/-0.0001 |
| * HI = 1000 psig, LO = 30 psig | | |
| ** OPTs tested at 1024 psig and 30 psig, leak rate units are psi/10 minutes | | |

Table 6-5 lists the results of the TEM-10 nozzle-to-case joint leak test. This joint was tested at a maximum pressure of 185 psig. This differs from the RSRM nozzle-to-case joint leak tests which are performed at 920 psig. The TEM-10 nozzle-to-case leak test was performed after the first torque sequence, when the axial bolts are torqued to 25 ft-lb. This procedure prevented the occurrence of a metal-to-metal seal between the fixed housing and the aft dome when the axial bolts were fully torqued. All results were within the limits.

Table 6-5. TEM-10 Nozzle-to-Case Leak Test Results

| Pressure (psig) | Allowable Leak Rate (sccs) | Actual Leak Rate (sccs) |
|--------------------|-------------------------------|----------------------------|
| 185 | 0.0720 | 0.0054 |
| 30 | 0.0082 | 0.0030 |

The 2U129714 equipment was used to test the TEM-10 nozzle-to-case joint. This is the new equipment used to test all RSRM nozzle-to-case joints starting with 360L006A.

TEM-10 contained the HPM configuration nozzle which has no leak test ports for the nozzle internal joints. No leak tests were performed on the nozzle internal joints.

6.6 NOZZLE PERFORMANCE

6.6.1 Introduction

The nozzle assembly (1U77584-02) was a partially submerged convergent/divergent movable design with an aft pivot point flexible bearing (Drawing 1U52840).

Four MS16142 vent ports were machined into the nozzle fixed housing (1U50088-08) forward of the primary O-ring to facilitate venting of the cavity between the joint putty and the primary O-ring when assembling the nozzle to the case.

The nozzle-to-case joint was assembled in the large motor casting pits with RSRM axial bolts with preload measuring capability. The assembly preload was a nominal 120,000 lb.

The snubbers had been removed from the forward exit cone assembly (Drawing 1U50532) for this test.

The linear shaped charge (LSC) had been removed from the aft exit cone assembly (Drawing 1U76778) for this test.

A fixed link support assembly (Drawing 7U76924) was installed in place of the aft skirt. This ring provided mounting provisions for the fixed links (Drawing 2U132116) which was used in place of TVC actuators.

6.6.2 Objectives/Conclusions

The TEM-10 nozzle performed nominally within HPM experience. The objectives and corresponding conclusions from Section 2 regarding nozzle performance were:

| Objective | Conclusion |
|---|--|
| C. Recover igniter, case, and nozzle hardware for RSRM flight and static test motors. | Recovered. Nozzle hardware is available for refurbishment. |

6.6.3 Recommendations

None.

6.6.4 Results/Discussion

Overall, the postburn condition of the nozzle liners was nominal. Typical erosion patterns were observed on the liners. The postburn mean throat diameter was 56.156 inches. This is within the historical database of the RSRM/HPM throat diameters. The throat erosion rate was 9.37 mils/sec.

The nose inlet phenolics were found in the bottom of the aft segment. This condition is discussed in Section 6.6.4.1.

All postfire flow gaps between phenolic components were uniform around the circumference and measured gap widths were within the historical database.

6.6.4.1 Nozzle Subassemblies.

6.6.4.1.1 Aft Exit Cone. The liner showed dimpled erosion on the forward 12.0 in. and smooth erosion on the remainder of the liner. No surface ply lifting or wash areas were observed. Intermittent ply separations were observed.

The postburn exit plane diameters (measured at T-24 prior to aft exit cone removal) were:

| Degrees | Diameter |
|------------|----------|
| 0-to-180 | 149.393 |
| 45-to-225 | 149.293 |
| 90-to-270 | 149.252 |
| 135-to-315 | 149.620 |

This is a HPM configured aft exit cone and char and erosion assessment will not impact the RSRM program.

The phenolic-to-metal housing bondline was in typical condition upon phenolic dissection. The mode of separation was 86 percent metal to adhesive and 4 percent within glass-cloth phenolic (GCP). Numerous large (2.0 in. diameter) voids were present throughout the bondline.

6.6.4.1.2 Forward Exit Cone. The forward exit cone liner erosion was smooth on the forward 11.5 in. and dimpled over the remaining length and circumference.

6.6.4.1.3 Throat/Throat Inlet Rings. The erosion of the throat and throat inlet rings was smooth with the typical rippled erosion pattern occurring on the aft 6.5 in. of the throat ring. The postfire throat diameters were as follows:

| Degrees | Diameter |
|------------|----------|
| 0-to-180 | 56.025 |
| 45-to-225 | 56.220 |
| 90-to-270 | 56.184 |
| 135-to-315 | 56.196 |

The postburn mean throat diameter was 56.156 inches. This yields an erosion rate of 9.37 mils/sec based on an action time of 122.5 sec. This is within the historical database of RSRM/HPM throat diameters.

6.6.4.1.4 Nose Inlet Assembly. The nose cap, forward nose ring, and aft inlet ring shifted from the nose inlet housing and dropped into the motor. A preliminary PFAR was written due to this condition. This is an HPM nose inlet assembly. The loss or shifting of the nose inlet phenolics was observed on 13 nozzles during the SRM/HPM program. The nose cap and forward nose ring shifted on the TEM-06 and TEM-9 nozzles.

An internal aft segment inspection of the nose inlet phenolics was performed. The phenolic had separated approximately 99 percent metal-to-adhesive. Slag was observed on the aft end of the nose cap phenolics. After the nozzle was demated from the aft segment, slag was observed on the forward end of the cowl phenolics. Heat-affected cowl silica-cloth phenolics (SCP) were observed at the slag deposit locations. A preliminary PFAR was written due to this condition. All bondline surfaces were sharp with no sign of erosion.

The RTR did not detect the phenolics laying in motor during motor operation or directly after tail-off. The RTR was run approximately 24 hours after the test firing and the phenolics were observed in the motor. Most likely, the phenolics shifted forward at motor tail-off allowing slag to enter between the nose inlet and cowl. The phenolics fell off at a later time after firing.

This is an SRM/HPM-related condition and will have no impact on the RSRM program. RSRM design changes have been implemented since this nose inlet assembly was manufactured.

The nose cap showed smooth erosion with no wash erosion. The aft 2.0 in. had typical intermittent postburn popped plies. One post burn wedgeout was present on the aft end.

6.6.4.1.5 Cowl Ring (-50 deg ply angle). The cowl ring erosion was smooth. Seven of the 36 cowl vent holes remained partially open. The largest remaining open cowl vent hole was located at 120 deg and measured 0.125 in. at both locations. The cowl/outer boot ring (OBR) bondline was intact with a flow surface gap of 0.25 in. and showed no evidence of flow or erosion.

The cowl phenolic-to-metal housing bondline was in good condition. The mode of separation was 98 percent adhesive to SCP and 2 percent within SCP. A few small (0.10 in. diameter) voids were found throughout the bondline. The char and erosion performance margins of safety were all positive.

6.6.4.1.6 OBR/Flex Boot. The OBR had smooth erosion and no wash areas. Intermittent popped plies were observed but no wedgeouts were present. Typical cooldown ply separations and intermittent slag deposits were observed. Intermittent wedgeouts were present on the structural support ring aft tip. The char and erosion performance margins of safety were all positive.

6.6.4.1.7 Fixed Housing. The fixed housing erosion was smooth. No popped plies or wedgeouts were found. Intermittent slag deposits were observed.

An NDE ultrasonic inspection was completed on the fixed housing assembly. Unbonds, circumferential bands, were observed during the inspection. This is similar to past static test fixed housing assemblies (FSM-02 and FSM-03). This assembly was partially ultrasonic inspected before firing and no unbonds were found.

The phenolic-to-metal bondline failure mode upon disassembly/removal of the phenolic assembly was 100 percent metal-to-adhesive. Circumferential bands of stains were found on the bare metal housing. These were similar in size and shape showing some correlation to the ultrasonic indications found prior to phenolic removal. The acceptable condition is 80 percent metal-to-adhesive separation. A preliminary PFAR was written due to this condition.

General Strain Data Observations for TEM-10 Nozzle. The TEM-10 nozzle fixed housing was instrumented with eight biaxial strain gages at motor station 1867.0 (Figure 6-4). These were the only strain gages mounted on the nozzle. Table 6-6 summarizes the nozzle strain gage instrumentation.

Gages at the 81-, 171-, 261-, and 351-deg locations ran at 31.25 SPS, while the gages at the 80-, 170-, 260-, and 350-deg locations ran at 2,000 SPS. The gages ran at 31.25 SPS were intended to monitor the fixed housing steel to GCP bondline subsequent to burn, during motor cooldown.

Figure 6-5 shows the measured hoop strain for all eight hoop strain gages plotted against the predicted strains for motor location 1867.0. The predictions are taken from an RSRM finite element model and have been adjusted to account for the HPM fixed housing which is slightly thinner in the conical region. The predictions are given at 10, 20, 50, 80 and 110 sec during motor operation. The measured strain data have been filtered to eliminate noise. The trend of the strain matches the predictions; however, the measured data are larger in magnitude than the predictions by approximately 150 μ strain. The measured strain magnitudes are typical of past observations.

Figure 6-6 shows the measured meridional strain versus predicted values at station location 1867.0. The predicted strains (given at 10, 20, 50, 80 and 110 sec during motor operation) match the measured strains very well. The predictions are taken from a RSRM finite element model, no adjustments to the meridional strain predictions were made since the thinner HPM housing should not significantly affect the meridional strain response. The meridional strains are typical of past observations on static tests.

Postfire Observation of the Nozzle Housing-to-GCP Insulation Bondline. Eight gages run at 31.25 SPS were used on the TEM-10 nozzle fixed housing to monitor the metal housing-to-GCP insulation bondline during motor cooldown. The gages were run from -20 sec to approximately 8 hr after burn. Figures 6-7 and 6-8 show the hoop strain from 120 sec to approximately 8 hr and 2 hr after burn, respectively. Figures 6-9 and 6-10 show the meridional strain for the same times. Both the hoop and meridional strain gages at 351 deg shows an event occurring approximately 37 minutes after pressure tail-off. It is possible that this event is the result of bondline failure in that quadrant of the nozzle fixed housing. Ultrasonics of the TEM-10 fixed housing prior to disassembly showed large areas of unbond. During phenolic removal the phenolics separated easily from the metal housing with total EA 913 adhesive to metal failure.

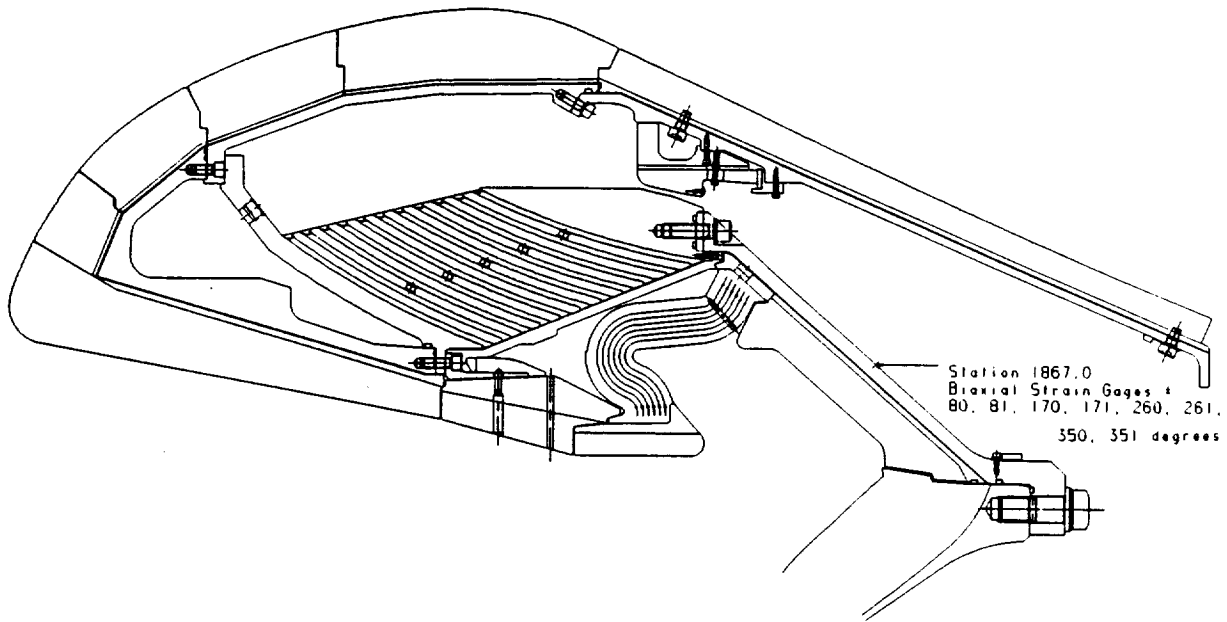


Figure 6-4. TEM-10 Nozzle Strain Gage Locations

Table 6-6. Nozzle Strain Gage Summary--Fixed Housing (station 1867.0)

| TEM-10 Static Test Nozzle Strain Gage Summary | | | | |
|--|---------------|--------------------------|-----------------|-------------|
| Location | Motor Station | Circumferential Location | Gage Identifier | Strain Type |
| Fixed Housing | 1867.0 | 80 | SHNAR018 | Hoop |
| Fixed Housing | 1867.0 | 170 | SHNAR021 | Hoop |
| Fixed Housing | 1867.0 | 260 | SHNAR024 | Hoop |
| Fixed Housing | 1867.0 | 350 | SHNAR027 | Hoop |
| Fixed Housing | 1867.0 | 81 | SHNAR189 | Hoop |
| Fixed Housing | 1867.0 | 171 | SHNAR190 | Hoop |
| Fixed Housing | 1867.0 | 261 | SHNAR191 | Hoop |
| Fixed Housing | 1867.0 | 351 | SHNAR192 | Hoop |
| Fixed Housing | 1867.0 | 80 | SMNAR043 | Meridional |
| Fixed Housing | 1867.0 | 170 | SMNAR045 | Meridional |
| Fixed Housing | 1867.0 | 260 | SMNAR044 | Meridional |
| Fixed Housing | 1867.0 | 350 | SMNAR046 | Meridional |
| Fixed Housing | 1867.0 | 81 | SMNAR064 | Meridional |
| Fixed Housing | 1867.0 | 171 | SMNAR065 | Meridional |
| Fixed Housing | 1867.0 | 261 | SMNAR066 | Meridional |
| Fixed Housing | 1867.0 | 351 | SMNAR067 | Meridional |

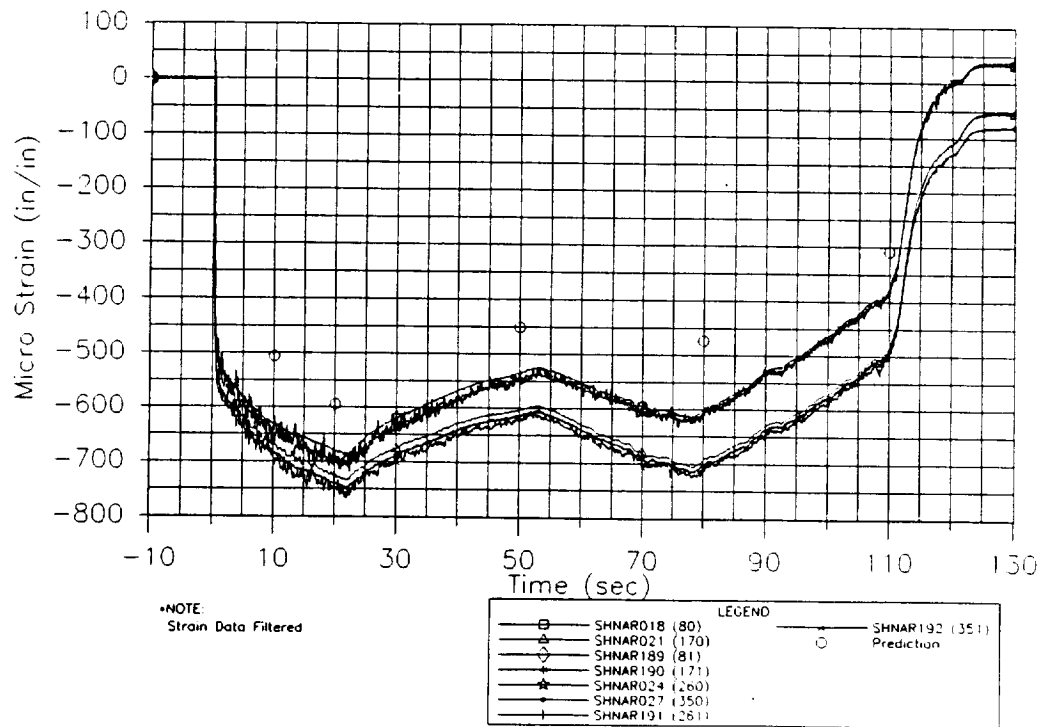


Figure 6-5. Nozzle Fixed Housing Hoop Strain Versus Predictions

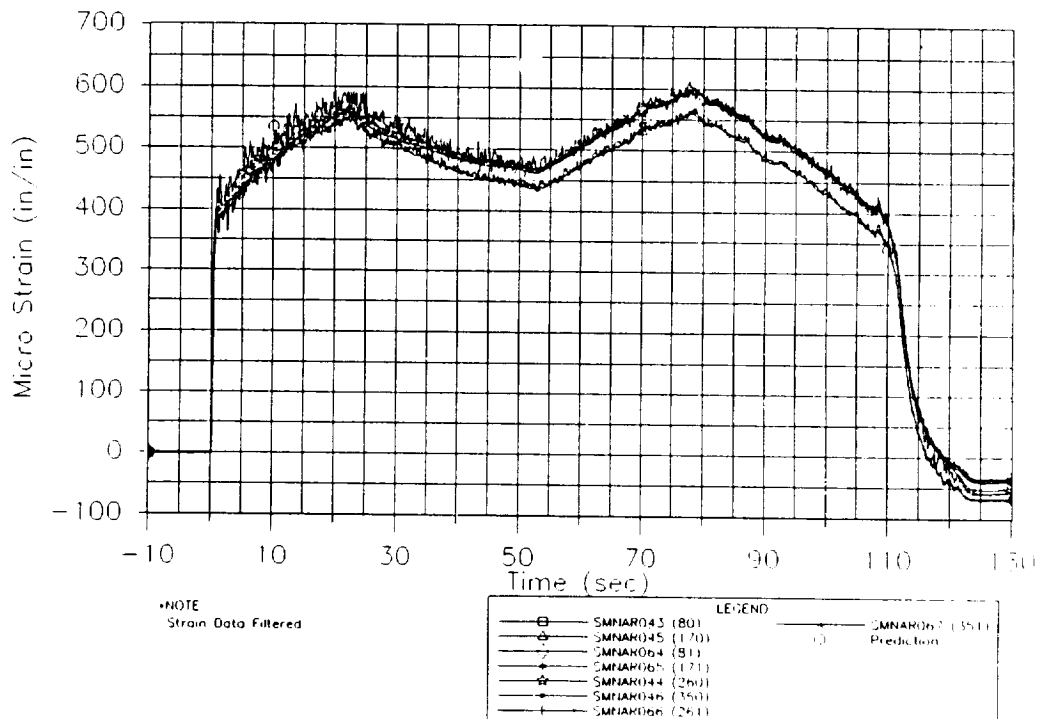


Figure 6-6. Nozzle Fixed Housing Meridional Strain Versus Predictions

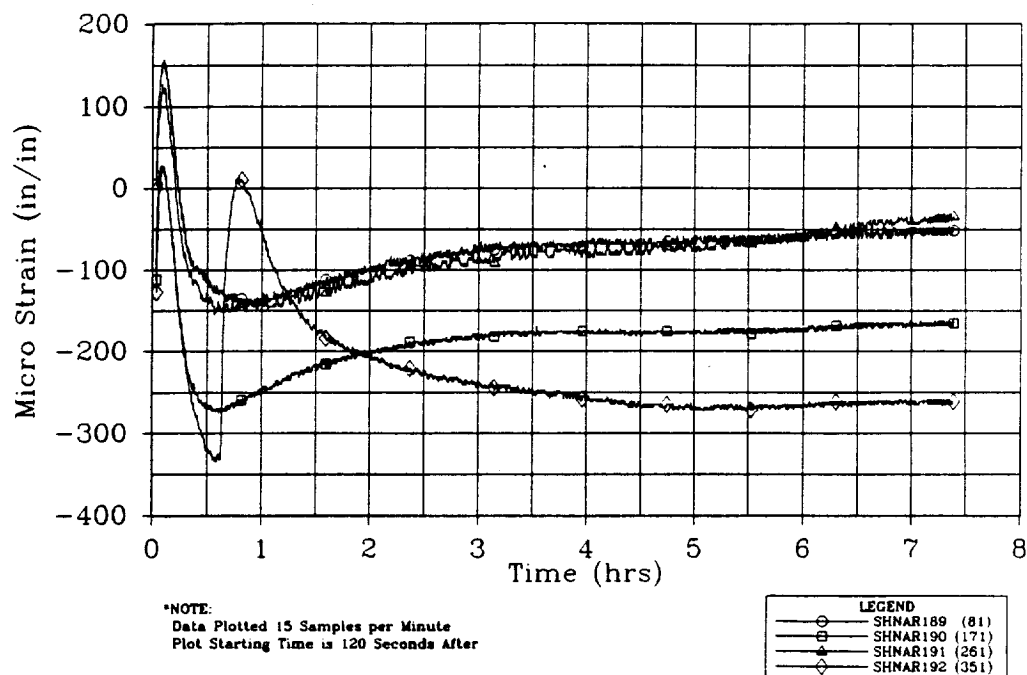


Figure 6-7. Nozzle Fixed Housing Hoop Strain Postburn Observations (120 sec-8 hr)

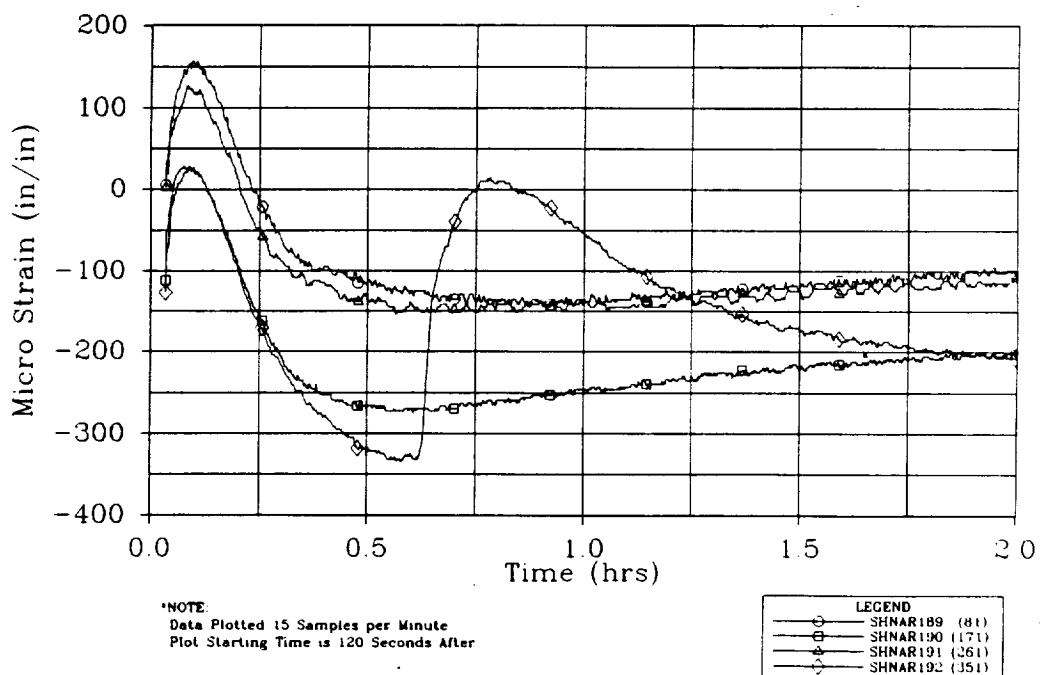


Figure 6-8. Nozzle Fixed Housing Hoop Strain Postburn Observations (120 sec-2 hr)

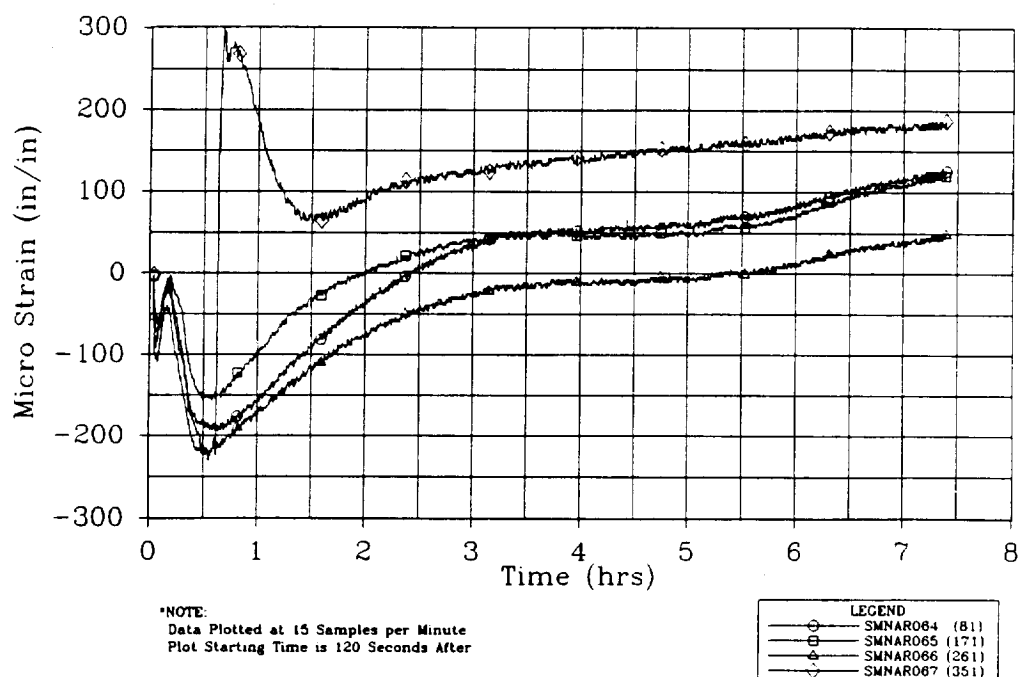


Figure 6-9. Nozzle Fixed Housing Meridional Strain Postburn Observations (120 sec-8 hr)

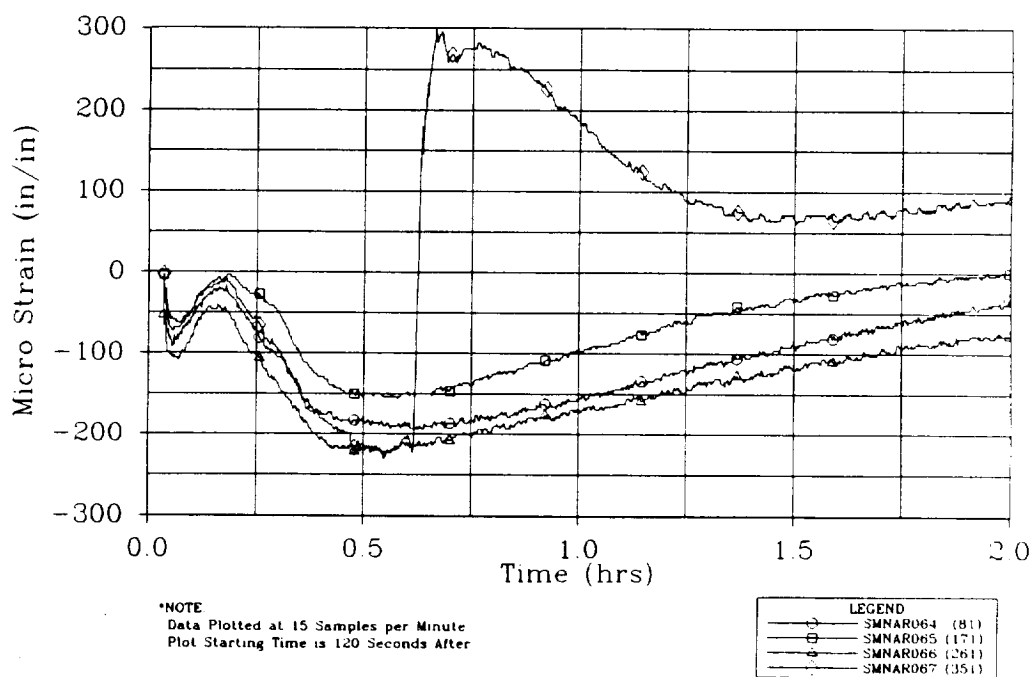


Figure 6-10. Nozzle Fixed Housing Meridional Strain Postburn Observations (120 sec-2 hr)

6.6.4.1.8 Flex Bearing Protector (Extended Belly Band). The bearing protector was lightly coated with soot. Erosion occurred on the belly band in-line with the cowl vent holes. No burn-through was observed. The erosion was deeper at the 330-0-120 deg location with the greatest erosion of 0.193 in. at the 40 deg location.

6.6.4.1.9 Flex Bearing. The flex bearing performance during test was acceptable. This nozzle was not vectored.

6.6.4.2 Nozzle-to-Case and Internal Joints. A discussion of observations made after each nozzle joint disassembly follows. Figure 6-11 shows the joint configurations and designations.

6.6.4.2.1 Joint 1--Forward Exit Cone-to-Aft Exit Cone Joint. The aft exit cone-to-forward exit cone joint was disassembled on 6 May 1993. The room-temperature vulcanized rubber (RTV) reached the primary O-ring intermittently around the circumference. No RTV was observed past the primary O-ring. No gas paths or soot was found in the RTV.

Postburn cohesive separations in the aft exit cone polysulfide occurred intermittently around the circumference. A separation within the aft exit cone GCP with a maximum radial width of 0.125 in. was observed at the 165-to-175 deg location.

A metal-to-adhesive separation was observed around the full circumference of the forward exit cone with a 0.06-in. maximum radial width.

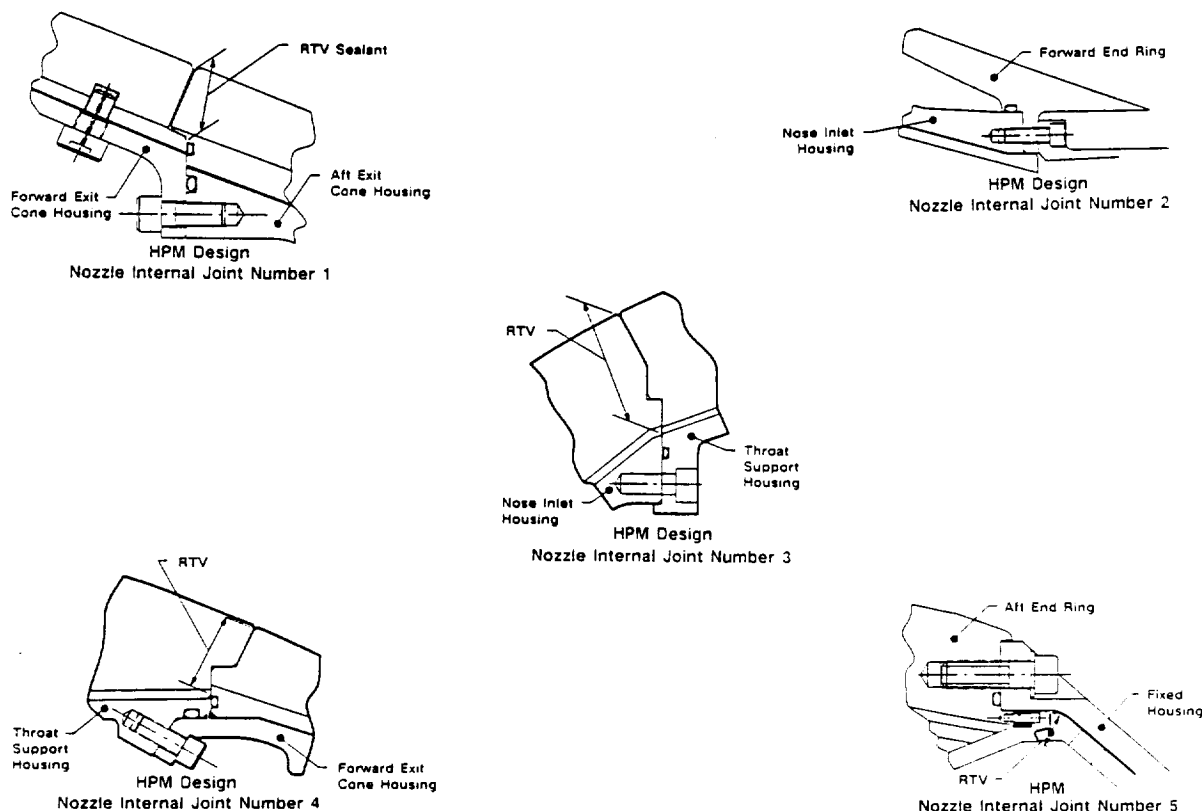


Figure 6-11. TEM Nozzle Internal Joints

6.6.4.2.2 Joint 2--Forward End Ring-to-Nose Inlet Housing (backfilled). The nose inlet-to-flex bearing-to-cowl was disassembled on 17 May 1993. This nozzle incorporated the improved bonding process for the cowl insulation. This included the backfilling of RTV in this joint after assembly rather than buttering the joint surfaces with RTV prior to joint assembly. The RTV backfill was excellent and reached below the char line the full circumference. The RTV extended on to the nose inlet housing a maximum of 0.40 in. at the 106-to-156 deg location. An encapsulated void in the RTV was observed at 179 deg and measured 0.80 in. radial by 0.50 in. circumference. There was no gas paths found in the joint.

Slag deposits were observed on both the nose cap aft end and the cowl forward end. Heat-affected SCP was observed in some of the areas of slag deposits. A preliminary PFAR was written on this condition. There was a light coat of soot on the RTV and metal surfaces. These conditions are the result of the loss of the nose inlet phenolics that was discussed in Section 6.6.4.1.

Light-to-medium corrosion was observed on the forward end ring flange outside diameter (OD) forward tip at the 108-to-120 deg location.

The cowl assembly showed no phenolic separations.

6.6.4.2.3 Joint 3--Nose Inlet Housing-to-Throat Support Housing. The nose inlet-to-throat was disassembled on 17 May 1993. The buttered RTV reached below the char line and to the O-ring around the full circumference. Two encapsulated voids in the RTV were observed at the 72 and 280 deg locations. The largest void measured 0.90 in. radial by 0.20 in. circumference. A terminated gas path was found in the RTV at the 318 deg location.

Soot was present in the O-ring groove at 260 deg. There was a light coat of soot on the RTV surfaces. These conditions are the result of the loss of the nose inlet phenolics that was discussed in Section 6.6.4.1.

Medium corrosion was observed in the primary O-ring groove at the 255-to-272 deg location on inboard side wall and at the 255-to-265 deg location on the bottom.

Two metal-to-adhesive separations were observed at the 0-to-340 and 345-to-355 deg locations of the throat with a 0.01 in. maximum radial width. Two adhesive-to-GCP separations were observed at 340-to-345 and 355-to-360 deg of the throat with a 0.01 in. maximum radial width.

6.6.4.2.4 Joint 4--Throat to Forward Exit Cone. The throat-to-forward exit cone was disassembled on 17 May 1993. The buttered RTV reached below the char line and past the primary O-ring around the full circumference. A preliminary PFAR was written for this condition. The RTV reached the secondary O-ring intermittently at the 212-to-275 deg location. No gas paths were found in the RTV.

No corrosion or edge separations observed. Grease coverage was nominal.

6.6.4.2.5 Joint 5--Fixed Housing-to-Aft End Ring. The aft end ring-to-fixed housing was disassembled on 17 May 1993. The buttered RTV coverage was nominal. The RTV did not reach the O-ring. A terminated gas path with soot was found in the RTV at 70 deg. Several other terminated gas paths without soot were observed. The gas paths are caused by voids in the RTV that are open to the boot cavity.

No corrosion or edge separations observed. Grease coverage was nominal.

The cowl insulation segments were removed after Joint 5 was demated. The segments separated 50 percent metal-to-adhesive and 50 percent adhesive-to-segment. Intermittent voids were observed on the bondline.

6.6.4.2.6 Nozzle-to-Case Joint. The joint performance was nominal. No bondline separations were observed on the aft end of the fixed housing. The joint region was examined for signs of heat effects and foreign material with none found.

6.6.4.3 Results of Special Issues (TWR-63821, Revision A, para. 3.2.3). The following items were designated special issues unique to TEM-10 nozzle to be evaluated in conjunction with the standard postfire evaluation. This section lists the conditions as written in TWR-63821, Revision A, and the resulting evaluations:

3.3 Nozzle

3.3.1

Condition: The TEM-10 HPM nozzle Joint 2 was found to have a small full radial length void at 280 deg during radiographic inspection. The void was repaired.

Results: No anomalous conditions were found. A void was found at 179 deg located adjacent to the cowl housing measuring 0.50 in. circumferentially by 0.25 in. radially. No gas paths were present.

3.3.2

Condition: During postfire evaluation an unbond was observed on the FSM-3 fixed housing. The TEM-10 fixed housing will be instrumented for gathering strain data.

Results: Ultrasonic inspection detected large circumferential bands of unbonds. Upon removal of the phenolics, the bondline failure mode was 100 percent metal to adhesive. Stains were found on the housing that correlated to the ultrasonic indications.

3.3.3

Condition: The FSM-03 nozzle bearing protector exhibited burn through erosion in three places. The FSM-3 nozzle was vectored whereas the TEM-10 will not be vectored.

Results: The bearing protector erosion was nominal with no burn through. Erosion depth was typical.

3.3.4

Condition: The TEM-10 HPM aft exit cone assembly was modified to include a polysulfide groove in the phenolic material similar to the RSRM design.

Results: The polysulfide groove performed as expected. No anomalous conditions were found.

3.3.5

Condition: An oversize O-ring was installed in the forward exit cone-to-aft exit cone (Joint 1) primary O-ring groove.

Results: No anomalous conditions were observed as a result of the oversized O-ring. The joint was in typical condition.

3.3.6

Condition: Nozzle Design is developing an understanding of adhesive application process and fill around the forward and aft exit cone shear pins. The shrinkage of phenolics with age is being studied.

Results: No misalignment between the housing threaded holes and the phenolic holes was observed visually on the forward exit cone shear pins. Breakaway torque was obtained on the aft exit cone shear pins. The adhesive appeared to be in typical condition and No hole misalignment was observed.

3.3.7

Condition: RTV backfill injection air pressure was 76 psi instead of the required pressure of 95 psi for Joint 1.

Results: The RTV backfill was in typical condition. No anomalous conditions were found.

6.7 IGNITION SYSTEM PERFORMANCE

6.7.1 Introduction

The TEM-10 ignition system (Figure 6-12) was a test configuration redesigned igniter assembly (1U77636-04). The igniter had a steel chamber with a single nozzle and external and internal NBR (STW4-2621) insulation. The igniter chamber contained case bonded TP-H1178 (STW5-2833) solid propellant with a 40-point star grain.

The baseline design static test igniter insulated adapter assembly (1U77453-03) with a CO₂ quench port was installed into the igniter assembly. The igniter adapter was attached to igniter chamber and forward dome via ultrasonic multiphase alloy bolts 1U77358-02 and 1U77460-01, respectively.

The igniter outer joint was assembled with a new two-sided PSA application. PSA was applied to the NBR and steel surface of the forward dome and to the outer J-joint NBR on the igniter chamber. The NBR was hand sanded to blend mold lines. PSA was applied between points D and H per STW7-9008 as shown in Figure 6-13.

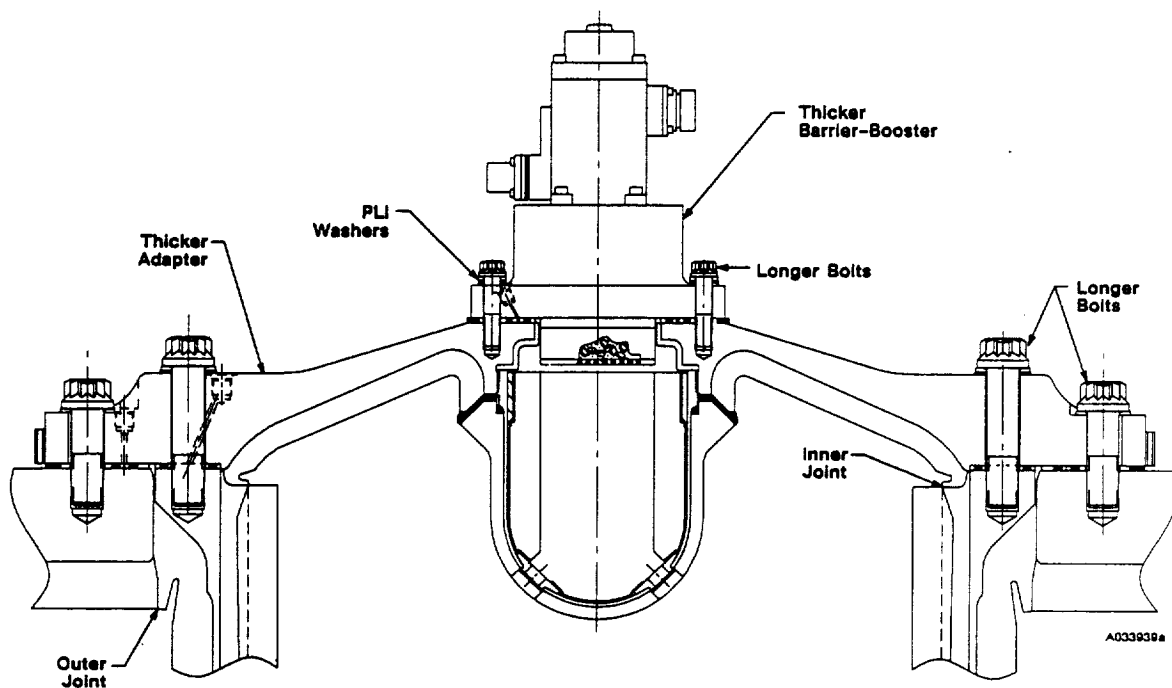


Figure 6-12. Baseline Redesign Igniter

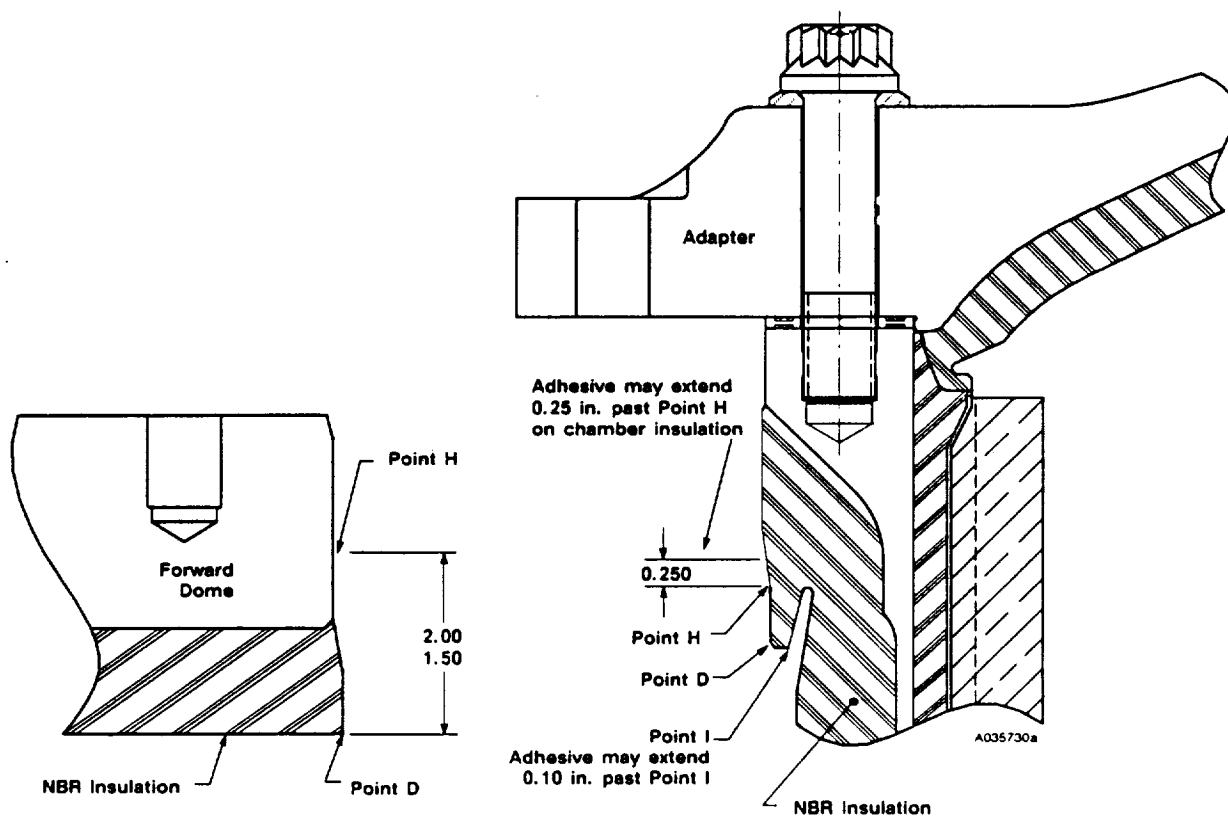


Figure 6-13. Pressure-Sensitive Adhesive Application Location

Two flight OPTs (Drawing 1U50188) and two static test pressure transducers (Drawing 7U76902) were installed in the igniter adapter at the time the igniter is installed into the forward segment. One OPT was dedicated to measuring chamber pressure oscillation. An additional static test pressure transducer (Drawing 7U76902) was installed into the igniter adapter to measure igniter chamber pressure. The OPTs and the two static test pressure transducers were installed with special bolts (Drawing 1U77356).

A redesigned S&A device (1U77387) which incorporates unibody SIIs and stainless steel ball bearings was attached to the igniter by 10 1U77359-01 bolts. All 10 bolts were installed with preload indicating (PLI) washers (1U77472-01).

A thermal blanket was wrapped and tightly sealed around the forward thrust adapter to simulate the thermal protection provided to the igniter and S&A by flight configuration.

The TEM-10 igniter insulation was the baseline redesigned configuration consisting of the inner and outer J-joint insulation as assembled per STW7-3884.

The SII arming cable was connected to the igniter initiator using the prototype or the 2U132880 SII arming cable installation/ removal kit.

6.7.2 Objectives/Conclusions

The objectives and conclusions from Section 2 are:

| Objectives | Conclusions |
|---|--|
| A. Certify baseline redesign igniter outer J-joint insulation performance with two-sided PSA. | <i>Certified.</i> Both igniter J-joints performed as expected with two-sided PSA. Adequate thermal protection was provided to the metal hardware. There was no visible evidence that combustion gas penetrated either J-joint, and none reached the seals. The PSA did not move from the allowable application zone. The two-sided PSA performed as good or better than one-sided PSA. |
| B. Certify the unibody SII seal interface for use in the RSRM ignition system (CPW1-3600A para. 3.2.1.2, 3.2.2.4.a, 3.2.1.2.4.b, 3.2.1.2.4.c, 3.2.1.5.a). | <i>Certified.</i> The unibody SIIs performed nominally. No anomalous conditions were observed. |

6.7.3 Recommendations

Two-sided PSA is recommended for flight. The unibody SIIs are recommended for use on flight motors.

6.7.4 Results/Discussion

This section documents the S&A cycle times, the S&A condition at removal, the S&A condition at disassembly, the igniter special bolts condition, the igniter pressure transducer (IPT) and OPTs conditions, the igniter outer joint and chamber insulation condition, the igniter inner joint and adapter insulation condition, and the results of the special issues.

6.7.4.1 S&A Cycle Times. S&A cycle time (0.6 sec) was within the engineering requirements of 2.0 sec or less at 24 VDC.

6.7.4.2 S&A Device Removal. The TEM-10 S&A device was removed from the igniter adapter 30 April 1993. No anomalous conditions were observed. Soot was observed on the S&A gasket forward face at the 216-deg location but did not reach the primary seal cushion.

6.7.4.3 S&A Disassembly. The TEM-10 S&A device was disassembled 18 May 1993. No anomalous conditions were observed. The unibody SIIs performed nominally.

6.7.4.4 Igniter Special Bolts. A radial scratch was observed on the 180 degrees special bolt-to-OPT secondary seal surface. A preliminary PFAR was written against this observation. No other anomalous condition was observed.

6.7.4.5 Igniter Pressure Transducer

No anomalous condition was observed on the 115-deg location IPT.

6.7.4.6 Igniter Operational Pressure Transducers and Static Test Transducers. No anomalous conditions were observed on the OPTs or Taber pressure transducers.

6.7.4.7 Igniter Outer Joint and Chamber Insulation. The TEM-10 igniter outer joint was disassembled 17 May 1993. No anomalous conditions were observed. Molykote was observed around every bolt hole on the forward dome. Molykote was observed around eight bolt holes on the outer gasket retainer aft face. No soot was observed past the outer J-joint. No outer gasket damage was noted. No leak check plug, O-ring, or port seal surface damage was observed.

The outer J-joint insulation was in good condition and performed as expected. There was no evidence that combustion gas penetrated beyond the J-joint thermal barrier. The PSA was in good condition with J-leg contact evident full circumference. The band of thermal barrier contact was typically 1.50 to 1.70 inches. The J-joint exhibited a distinct char layer and heat-affected zone which was typically 0.150 to 0.200 in. for the entire circumference.

The J-leg insulation mold lines were in good condition with no gas paths at the mold lines. This indicates the prefire mold line blending was successful. Mold line separations were observed in the char layer and heat-affected region as expected.

The pressurization slot was open with slight char swelling and loose soot in the slot. The OPT through-holes were determined to be unobstructed. Loose soot was found in the OPT through-holes. Light probing loosened all soot. No edge separations were found. The igniter chamber internal acreage insulation was in good condition.

6.7.4.8 Igniter Inner Joint and Adapter Insulation. The TEM-10 igniter inner joint was disassembled 20 May 1993. The igniter inner joint experienced no soot or gas penetration past the inner joint insulation J-joint. A small white fiber was observed on the inner gasket, forward face, outer primary seal at 150 deg. A preliminary PFAR was written against this observation.

Two small scratches/dings were observed on the 310-deg bolt hole spot face packing with retainer seal surface. PFAR TEM10-02 was written against this observation. No other anomalous conditions were observed. Typical disassembly damage was observed on 18 of 36 inner joint packing with retainer elastomer elements.

The inner J-joint insulation was in excellent condition and performed as expected. No gas penetrated into the J-joint. The PSA was in good condition with a 0.250- to 0.350-in. J-leg contact zone evident full circumference. The J-joint exhibited a distinct char layer and heat-affected zone which was typically 0.050 to 0.200 in. for most of the circumference. Slightly less charring and heat effects were observed at the 0-deg location due to less heat soak from the quench system.

The pressurization slot was open and unobstructed full circumference. No edge separations were found. The igniter adapter acreage insulation was in good condition.

6.7.4.9 Results of Special Issues (TWR-63821, Revision A, para. 3.2.2 and 3.2.3). The following items were designated special issues unique to TEM-10 igniter seals and joints to be evaluated in conjunction with the standard postfire evaluation. This section lists the conditions as written in TWR-63821, Revision A, and the resulting evaluations:

3.2.2 Seals

- 1) Condition: TEM-9 igniter inner joint had disassembly damage to the seals on the packing with retainer at six bolt hole locations (60, 90, 170, 200, and 260 deg).

Results: 18 of 36 inner joint packing with retainers had disassembly damage.

3.2.3 Joints

- 1) Condition: TEM-10 S&A device used the redesigned barrier-booster (B-B) assembly to eliminate interference between the S&A gasket and B-B housing.

Results: No anomalous condition observed with this assembly.

- 2) Condition: TEM-10 B-B uses unibody SIIs.

Results: No anomalous conditions observed associated with the unibody SIIs.

- 3) Condition: TEM-10 igniter had two Taber 206 pressure transducers. The installation tool will stay on the motor during the static test firing.
Results: No anomalous condition observed associated with the installation tool remaining on the Taber gages during motor firing.
- 4) Condition: The baseline redesigned igniter will be used in TEM-10. The redesigned igniter included J-leg insulation for the outer Joint.
Results: No soot or heat affects were evident downstream of the J-leg.

6.8 JOINT PROTECTION SYSTEMS

6.8.1 Introduction

Improved field joint heaters (Drawing 1U77252), igniter-to-case joint heater (Drawing 1U77253), and nozzle-to-case joint heater (Drawing 7U77254) were installed as shown in Drawing 7U77607. These heaters consisted of redundant, chemically etched, foil circuits which are superimposed upon one another and laminated in polyamide plastic sheets. The underside Kapton surface of the field joint heaters and the nozzle-to-case joint heater was coated with a pressure-sensitive adhesive. This adhesive provided bonding to the case during assembly. The lead wires extend from the heaters and were terminated in electrical connectors.

Field joint heater closeouts (Drawing 7U77607, static test only) consisted of cork strips retained with Kevlar straps as used on previous TEM static test motors. The external joint temperatures were measured by sensor assemblies mounted adjacent to the heater. Each assembly contained two RTD sensors. New sensor cables (Drawings 7U77349-14 or 1U77075-01 and 7U77349-16 or 1U77075-02) were used on this motor. These cables incorporated positive locking in the back shell and compliance to NHB 5300.43G during their building.

RSRM JPS power cables were installed to provide 208 VAC to the RSRM field joint and igniter-to-case joint heaters.

6.8.2 Objectives/Conclusions

There were no objectives from Section 2 concerning the JPSs.

6.8.3 Recommendations

None.

6.8.4 Results/Discussion

The field joint protection system (FJPS) (static test configuration) performed nominally and maintained the joint temperatures within the required temperature range at the time of motor ignition.

Post-test inspection was conducted with the FJPS still on the motor. The FJPS performed nominally with no evidence of damage observed.

6.9 BALLISTICS/MASS PROPERTIES PERFORMANCE

6.9.1 Introduction

The SRM propellant, TP-H1148 (STW5-3343), was a composite-type solid propellant, formulated of polybutadiene acrylic acid acrylonitrile terpolymer binder (PBAN), epoxy curing agent, ammonium perchlorate oxidizer, and aluminum powder fuel. A small amount of burning rate catalyst (iron oxide) was added to achieve the desired propellant burn rate.

The propellant grain design consisted of an 11-point star with a smooth bore to fin cavity transition region that tapered into a circular perforated (CP) configuration in the forward segment (Drawing 1U52565). The two center segments (Drawing 1U52566) were double-tapered CP configurations and the aft segment (Drawing 1U52568) was a triple-tapered CP configuration with a cutout for the partially submerged nozzle.

6.9.2 Objectives/Conclusions

The objectives and corresponding conclusions from Section 2 regarding ballistics/mass properties were:

| Objectives | Conclusions |
|--|---|
| D. Measure motor head-end chamber pressure oscillations. | Motor head-end chamber pressure oscillations were measured. The motor dynamic performance appears to be nominal and no anomalous behavior was noted. |
| F. Obtain RTR, acceleration, IR plume, sound pressure, and strain data in support of the RSRM-29 pressure anomaly investigation. | <i>All data were obtained.</i> The largest pressure blip in the 62 to 75 sec time period using the Thiokol routine which was recommended by MSFC was 6.6 psi at 71 sec. Work is continuing on pressure perturbations. |

6.9.3 Recommendations

The TEM-10 ballistic performance was within expected limits. The TEM-10 ballistic performance compared well with previous TEM performance and HPM historical data. All ballistic test objectives were met.

The TEM-10 motor exhibited chamber pressure oscillations similar to previously tested space shuttle HPMs. The first-longitudinal (1-L) mode oscillations were typical for an HPM. In general, HPM 1-L mode amplitudes are lower than those for RSRMs.

6.9.4 Results/Discussion

TEM-10 performance was within HPM specification limits and compared well with predicted performance. The predicted burn rate for TEM-10 was 0.368 ips at 625 psia and 60°F, the target burn rate was 0.368 ips, and the delivered burn rate was 0.368 ips.

Appendix B is a summary of the measured ballistic and nozzle performance data. Figure 6-14 is a comparison of measured and predicted pressure-time histories and Figure 6-15 is a comparison of measured and predicted vacuum thrust-time histories. The measured and predicted performance compare well.

Figures 6-16 and 6-17 contain plots of the analytical reconstruction of the TEM-10 performance. The analytical model calculated the motor burn rate and surface burn rate error (SBRE) factor. The calculated burn rate of 0.3681 ips at 625 psia and 60°F was the same as the predicted value of 0.3681.

TEM performance typically differs from HPM nominal performance since the segments do not come from the same propellant evaluations. The TEM-10 motor is no exception as all four segments have different propellant evaluations (and thus a high potential of burn rate difference between segments). The delivered performance differs from the predicted performance even though the average burn rate is the same as predicted because of the burn rate mismatch between segments. Nonetheless, the TEM-10 performance was nominal and all performance parameters were within HPM specification limits.

A comparison of the thrust-to-head-end chamber pressure ratios for TEM-1 through TEM-10 (excluding TEM-3, -5, -7, -8, and -9 since there was no measured thrust on these motors) is shown in Figure 6-18. The traces are similar and within the variation of HPM thrust-to-head-end pressure ratios.

The motor average subscale burn rates, full-scale motor burn rates (determined from post-test curve matching) and resulting scale factors for SRM-15 to SRM-24, used to predict the TEM-10 burn rate are listed in Table 6-7. The full-scale motor burn rates were determined from post-test curve matching in which the analytical model was forced to match the measured motor performance. The mean scale factor was 1.0175 with a sigma 0.00440 and a CV of 0.432 percent.

A plot of the measured data comparing the ignition transients of the TEM static tests is shown in Figure 6-19. The TEM-10 transient was similar to previously measured motor ignition performance. The TEM-10 maximum pressure rise rate was 74.83 psi/10 ms. The historical three-point average pressure rise rate is 90.70 psi/10 ms with a variation of 6.96 psi/10 ms. The TEM-10 ignition interval was 0.2355 sec which compares well with the population average of 0.2314 sec. A summary table showing the historical pressure rise rates, thrust rise rates, and ignition intervals is shown in Table 6-8. A summary of the TEM-10 ignition events is shown in Table 6-9.

The TEM-10 igniter was the baseline redesigned igniter for RSRM flight. The igniter was cast from propellant batch number H280002 using TP-H1178 propellant. The delivered maximum mass flow rate was 358.4 lbm/sec at 74°F for the TEM-10 igniter. The TEM-10 igniter performance characteristics were within the expected ranges. Comparison of the TEM-10 igniter performance at 80°F with the igniter limits at 80°F is shown in Figure 6-20. The TEM-10 is within the limits at 80°F.

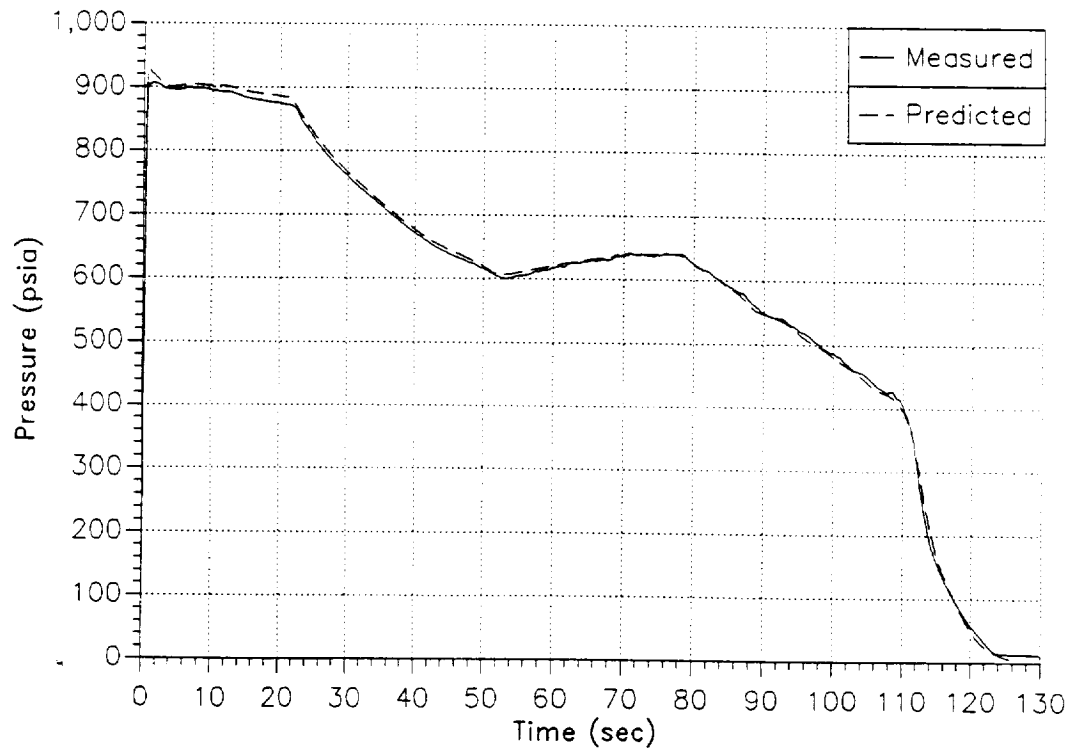


Figure 6-14. Predicted and Measured Pressure at 69°F

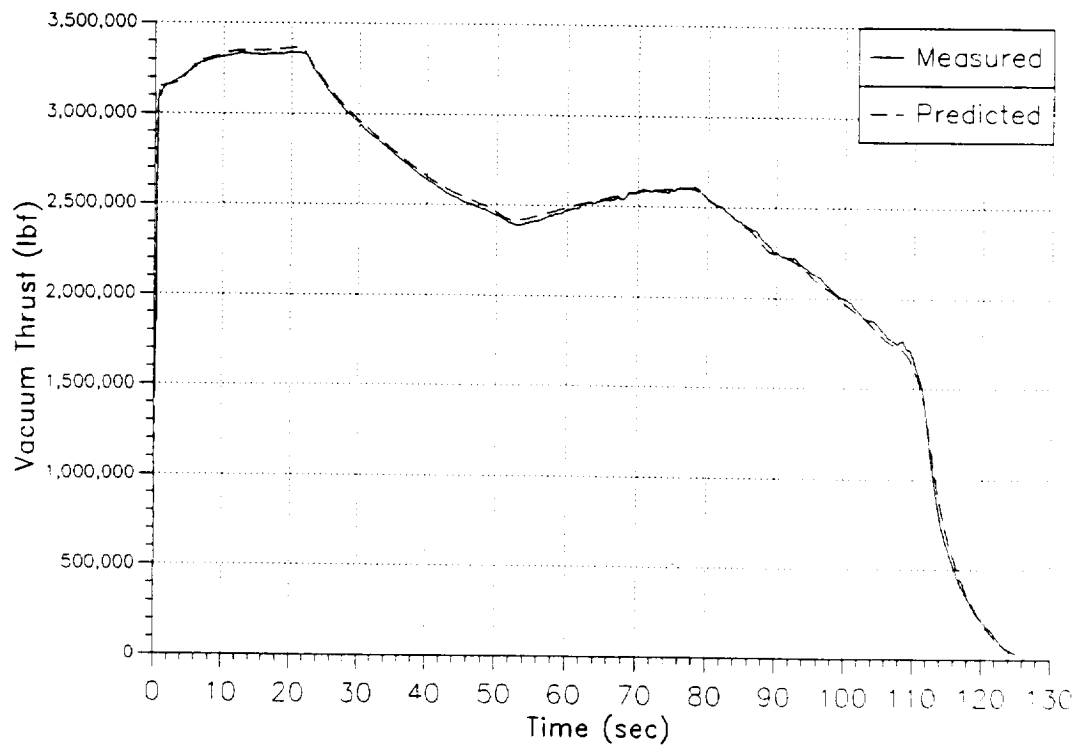


Figure 6-15. Predicted and Measured Vacuum Thrust at 69°F

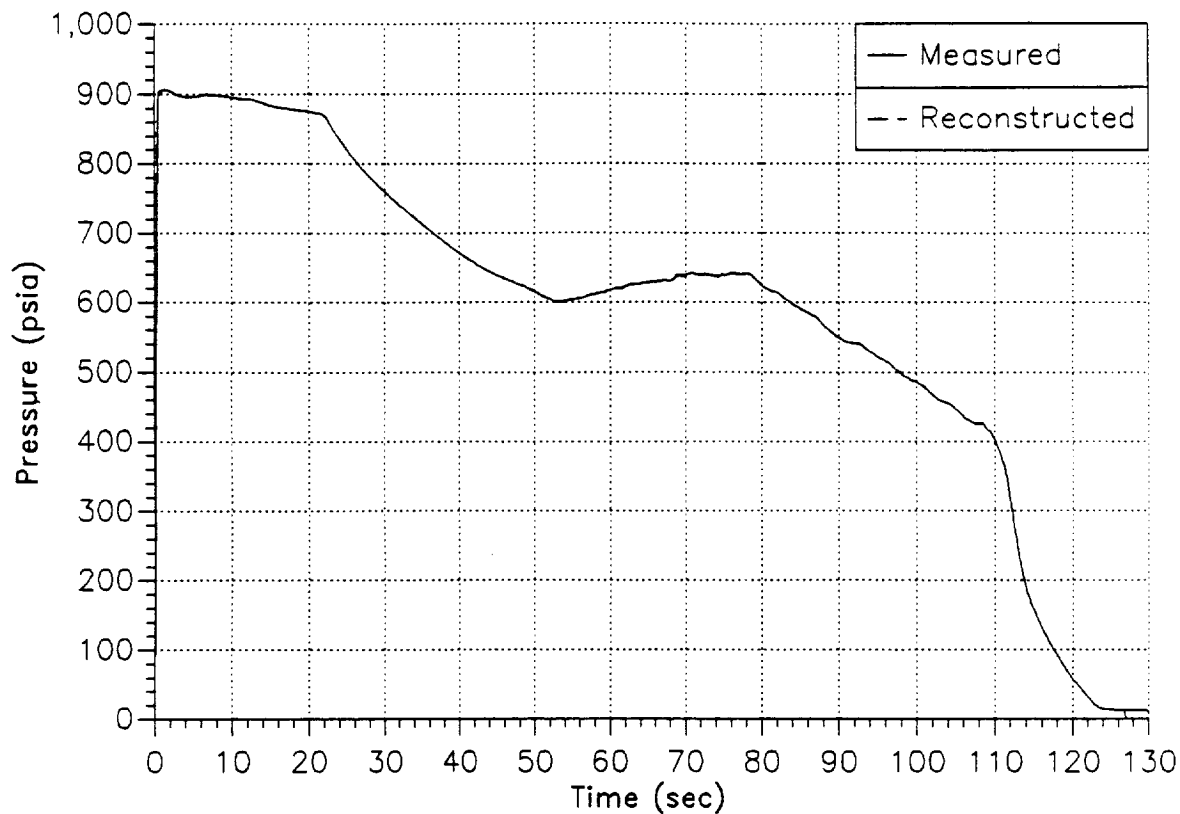


Figure 6-16. Reconstructed and Measured Pressure at 69°

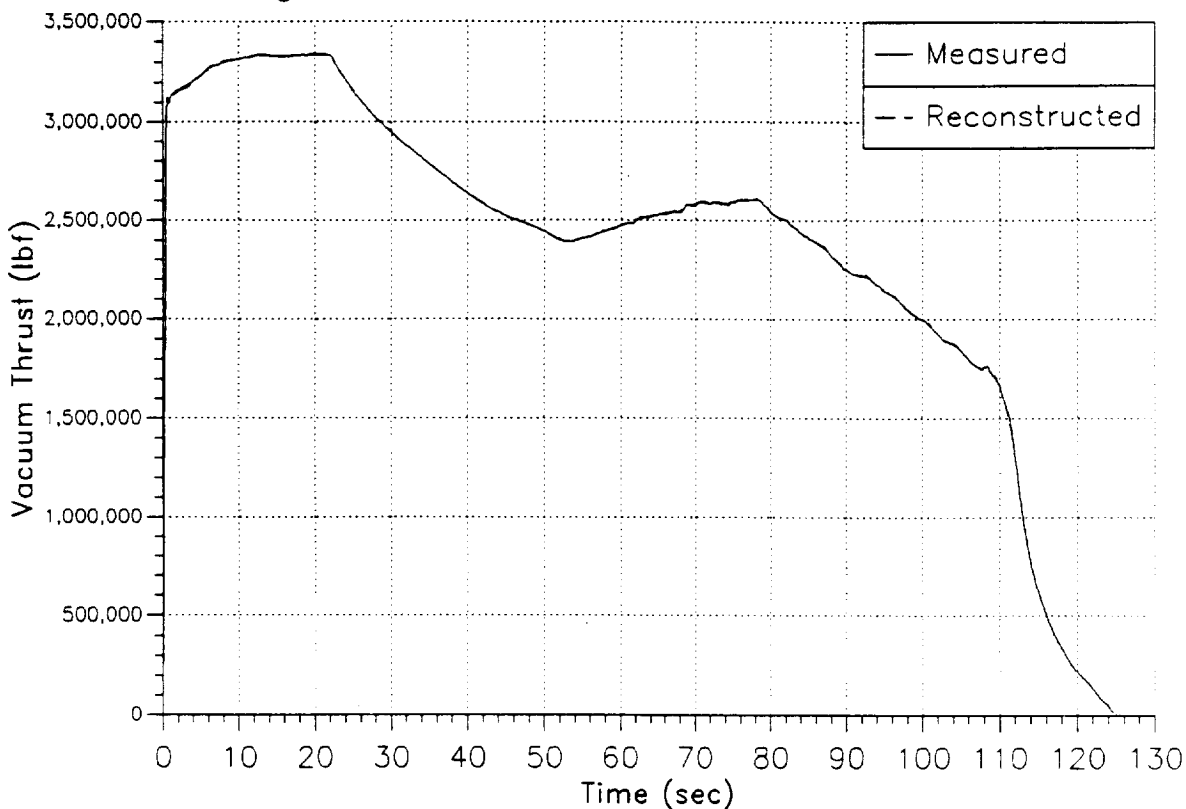


Figure 6-17. Reconstructed and Measured Vacuum Thrust at 69°

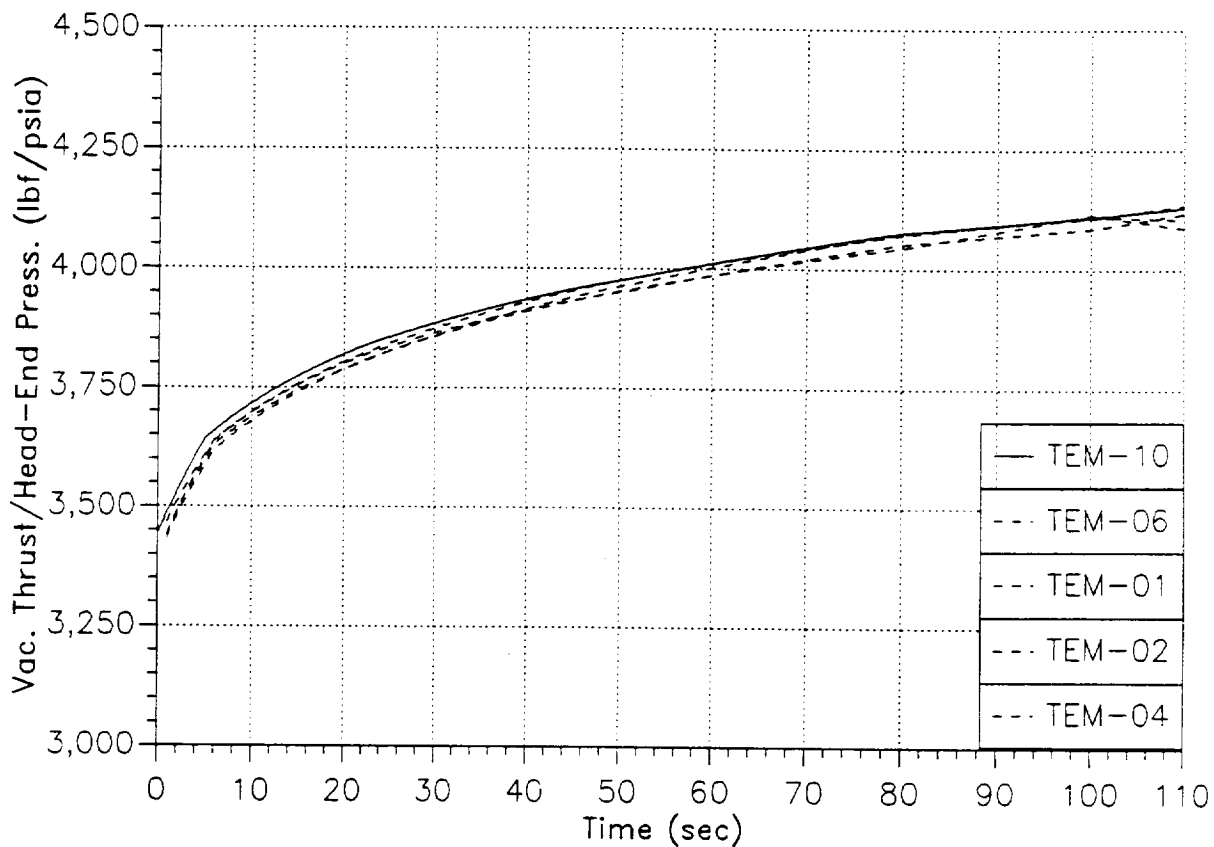


Figure 6-18. Comparison of Vacuum Thrust to Head-End Pressure Ratio Versus Time for TEMs

Table 6-7. Burn Rate Data Comparison Subscale to Full-scale at 62 psia, 60°F

| Motor | Burn Rate | | | | Scale Factor 5-in. CP Standard |
|---|---------------|----------------------|------------------|------------------|--------------------------------------|
| | SRM Target | 5-in. CP Standard | SRM Predicted | SRM Delivered | |
| SRM-15A | 0.368 | 0.366 | 0.370 | 0.3701 | 1.0112 |
| SRM-15B | 0.368 | 0.366 | 0.370 | 0.3709 | 1.0134 |
| SRM-16A | 0.368 | 0.365 | 0.369 | 0.3684 | 1.0093 |
| SRM-16B | 0.368 | 0.365 | 0.369 | 0.3688 | 1.1040 |
| SRM-17A | 0.368 | 0.363 | 0.367 | 0.3680 | 1.0138 |
| SRM-17B | 0.368 | 0.362 | 0.366 | 0.3694 | 1.0204 |
| SRM-18A | 0.368 | 0.362 | 0.367 | 0.3693 | 1.0202 |
| SRM-18B | 0.368 | 0.363 | 0.368 | 0.3690 | 1.0165 |
| SRM-19A | 0.368 | 0.364 | 0.369 | 0.3703 | 1.0173 |
| SRM-19B | 0.368 | 0.364 | 0.369 | 0.3704 | 1.0176 |
| SRM-20A | 0.368 | 0.368 | 0.373 | 0.3742 | 1.0168 |
| SRM-20B | 0.368 | 0.366 | 0.371 | 0.3744 | 1.0230 |
| SRM-21A | 0.368 | 0.367 | 0.370 | 0.3737 | 1.0183 |
| SRM-21B | 0.368 | 0.365 | 0.368 | 0.3744 | 1.0258 |
| SRM-22A | 0.368 | 0.362 | 0.365 | 0.3675 | 1.0152 |
| SRM-22B | 0.368 | 0.362 | 0.365 | 0.3697 | 1.0213 |
| SRM-23A | 0.368 | 0.364 | 0.367 | 0.3713 | 1.0201 |
| SRM-23B | 0.368 | 0.364 | 0.367 | 0.3721 | 1.0223 |
| SRM-24A | 0.368 | 0.360 | 0.365 | 0.3678 | 1.0217 |
| SRM-24B | 0.368 | 0.361 | 0.366 | 0.3674 | 1.0177 |
| Average Scale Factor = 1.0175, Sigma = 0.00440, %CV = 0.432 | | | | | |
| ETM-1 | 0.368 | 0.365 | 0.372 | 0.3681 | 1.0085 |
| DM-8 | 0.368 | 0.360 | 0.366 | 0.3677 | 1.0214 |
| DM-9 | 0.368 | 0.362 | 0.368 | 0.3691 | 1.0196 |
| QM-6 | 0.368 | 0.360 | 0.366 | 0.3665 | 1.0181 |
| QM-7 | 0.368 | 0.358 | 0.364 | 0.3657 | 1.0215 |
| PVM-1 | 0.368 | 0.360 | 0.366 | 0.3677 | 1.0214 |
| TEM-1 | 0.368 | 0.362 | 0.368 | 0.3659 | 1.0116 |
| TEM-2 | 0.368 | 0.362 | 0.368 | 0.3664 | 1.0122 |
| TEM-3 | 0.368 | 0.362 | 0.368 | 0.3672 | 1.0155 |
| TEM-4 | 0.368 | 0.362 | 0.369 | 0.3681 | 1.0160 |
| TEM-5 | 0.368 | 0.362 | 0.368 | 0.3654 | 1.0105 |
| TEM-6 | 0.368 | 0.361 | 0.367 | 0.3667 | 1.0166 |
| FSM-1 | 0.368 | 0.364 | 0.370 | 0.3701 | 1.0165 |
| TEM-7 | 0.368 | 0.363 | 0.370 | 0.3709 | 1.0208 |
| TEM-8 | 0.368 | 0.363 | 0.370 | 0.3662 | 1.0077 |
| TEM-9 | 0.368 | 0.364 | 0.370 | 0.3696 | 1.0159 |
| FSM-2 | 0.368 | 0.360 | 0.366 | 0.3652 | 1.0144 |
| FSM-3 | 0.368 | 0.361 | 0.367 | 0.3667 | 1.0152 |
| TEM-10 | 0.368 | 0.362 | 0.368 | 0.3681 | 1.0174 |

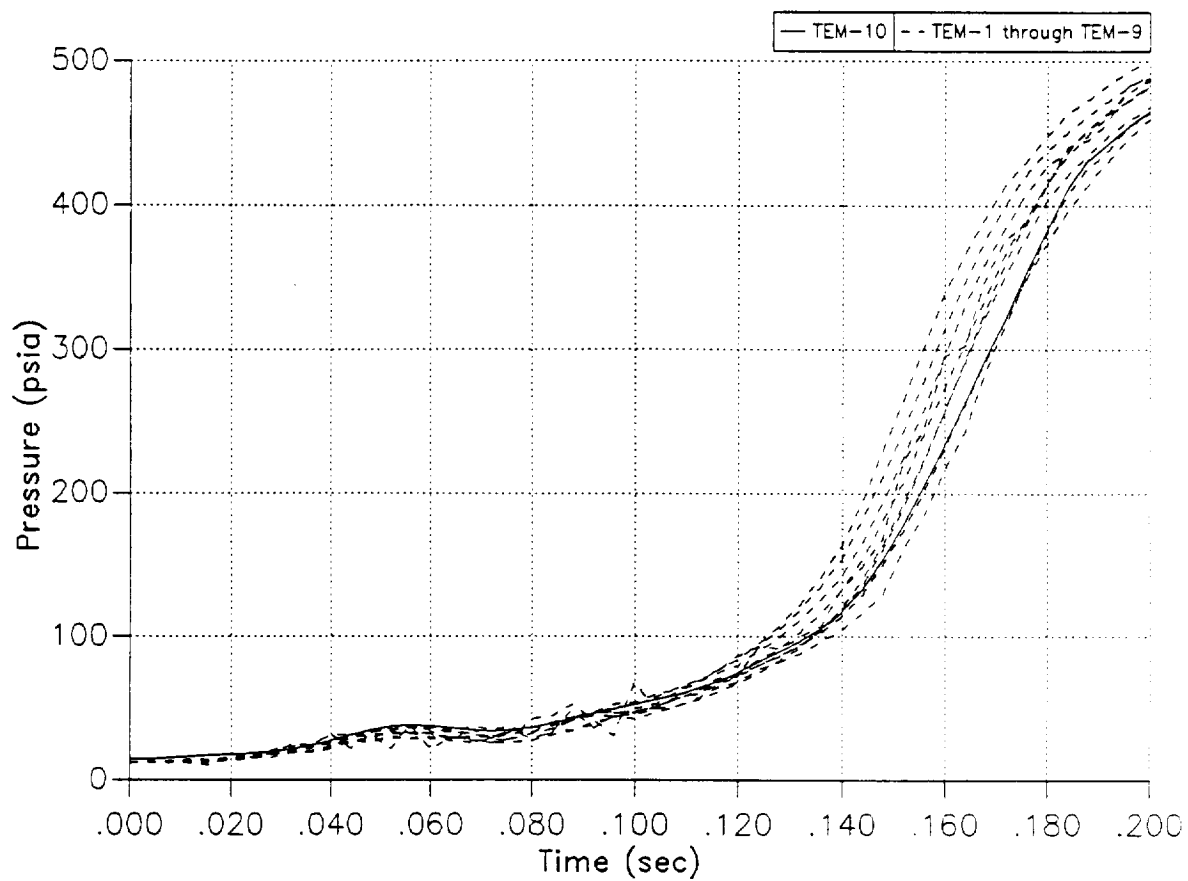


Figure 6-19. Measured Head-End Pressure Transients

Table 6-8. Historical 3/5 Point Average Maximum Thrust and Pressure Rise Rate Data

| Motor | Occurrence Time (sec) | Maximum PDOT (psi/10 ms) | Occurrence Time (sec) | Max TDOT (lbf/10 ms) | Ignition Interval (sec) |
|--|-----------------------|--------------------------|-----------------------|----------------------|-------------------------|
| Static Test | | | | | |
| DM-2 | 0.1480 | 85.30 | 0.1480 | 245,380 | 0.2330 |
| QM-1 | 0.1560 | 86.38 | 0.1560 | 246,128 | 0.2362 |
| QM-2 | 0.1640 | 93.58 | 0.1720 | 234,950 | 0.2391 |
| QM-3 | 0.1560 | 94.45 | 0.1520 | 245,615 | 0.2287 |
| QM-4 | 0.1505 | 91.96 | 0.1545 | 216,048 | 0.2192 |
| ETM-1A | 0.1520 | 86.72 | 0.1560 | 230,023 | 0.2279 |
| TEM-1 | 0.1520 | 85.13 | 0.1520 | 238,583 | 0.2255 |
| TEM-2 | 0.1520 | 94.40 | 0.1520 | 288,772 | 0.2280 |
| TEM-3 | 0.1520 | 88.51 | 0.1520 | 227,835 | 0.2272 |
| TEM-4 | 0.1480 | 81.52 | 0.1520 | 279,764 | 0.2283 |
| TEM-5 | 0.1560 | 87.12 | 0.1560 | 221,094 | 0.2299 |
| TEM-6 | 0.1600 | 84.49 | 0.1520 | 273,946 | 0.2342 |
| TEM-7 | 0.1600 | 80.62 | 0.1600 | 201,047 | 0.2359 |
| TEM-8 | 0.1440 | 100.47 | 0.1480 | 236,046 | 0.2234 |
| TEM-9 | 0.1680 | 93.36 | 0.1640 | 230,839 | 0.2365 |
| DM-8 | 0.1680 | 77.00 | 0.1760 | 257,272 | 0.2424 |
| DM-9 | 0.1640 | 81.00 | 0.1720 | 275,525 | 0.2436 |
| QM-6 | 0.1480 | 87.40 | 0.1520 | 211,476 | 0.2321 |
| QM-7 | 0.1480 | 99.60 | 0.1480 | 239,502 | 0.2230 |
| PVM-1 | 0.1520 | 92.80 | 0.1520 | 294,664 | 0.2338 |
| QM-8 | 0.1720 | 72.30 | 0.1720 | 198,337 | 0.2517 |
| FSM-1 | 0.1520 | 97.06 | 0.1440 | 250,453 | 0.2278 |
| FSM-2 | 0.1520 | 95.69 | 0.1520 | 267,614 | 0.2330 |
| FSM-3 | 0.1520 | 89.77 | 0.14802 | 82,826 | 0.2269 |
| Flight Motors | | | | | |
| SRM-1A | 0.1530 | 88.45 | 0.1530 | 221,534 | 0.2358 |
| SRM-1B | 0.1500 | 92.49 | 0.1530 | 228,886 | 0.2345 |
| SRM-2A | 0.1530 | 91.64 | 0.1530 | 228,790 | 0.2332 |
| SRM-2B | 0.1660 | 91.17 | 0.1660 | 234,434 | 0.2327 |
| SRM-3A | 0.1500 | 91.05 | 0.1500 | 225,414 | 0.2289 |
| SRM-3B | 0.1500 | 90.58 | 0.1530 | 228,445 | 0.2251 |
| SRM-5A | 0.1530 | 96.06 | 0.1530 | 237,676 | 0.2342 |
| SRM-5B | 0.1660 | 85.27 | 0.1660 | 220,103 | 0.2362 |
| SRM-6A | 0.1530 | 93.64 | 0.1530 | 234,797 | 0.2328 |
| SRM-6B | 0.1470 | 89.10 | 0.1500 | 220,255 | 0.2315 |
| SRM-7A | 0.1500 | 100.90 | 0.1530 | 251,265 | 0.2263 |
| SRM-7B | 0.1500 | 100.31 | 0.1500 | 247,054 | 0.2257 |
| SRM-8A | 0.1530 | 107.36 | 0.1530 | 267,644 | 0.2204 |
| SRM-8B | 0.1500 | 91.97 | 0.1530 | 234,784 | 0.2178 |
| SRM-9A | 0.1530 | 93.23 | 0.1530 | 234,022 | 0.2287 |
| SRM-10A | 0.1530 | 93.82 | 0.1530 | 232,302 | 0.2360 |
| SRM-10B | 0.1500 | 85.41 | 0.1530 | 212,298 | 0.2328 |
| SRM-13B | 0.1410 | 99.84 | 0.1440 | 214,245 | 0.2098 |
| RSRM-1A | 0.1571 | 99.81 | 0.1562 | 245,741 | 0.2254 |
| RSRM-1B | 0.1666 | 80.98 | 0.1719 | 218,388 | 0.2374 |
| RSRM-2A | 0.1554 | 88.49 | 0.1562 | 223,579 | 0.2361 |
| RSRM-2B | 0.1491 | 100.81 | 0.1500 | 244,314 | 0.2322 |
| RSRM-3A | 0.1600 | 83.69 | 0.1594 | 207,924 | 0.2439 |
| RSRM-3B | 0.1579 | 91.01 | 0.1562 | 223,483 | 0.2442 |
| Number | | 48 | 48 | | 48 |
| Average | | 90.70 | 238,148 | | 0.2314 |
| Standard Deviation | | 6.96 | 22,617 | | 0.0075 |
| % CV | | 7.67 | 9.50 | | 3.23 |
| TEM-10 | 0.1440 | 74.83 | 0.1480 | 219,496 | 0.2355 |
| Flight and static test motors fired in T-97 used thrust overpressure ratio from static test motors that had measured thrust. Thrust overpressure ratio was calculated from DM-2, -8, -9; QM-1 to -4, -6; ETM-1A; PVM-1; FSM-1; TEM-1, -4, -6 | | | | | |

Table 6-9. Measured SRM Ignition Performance Data at 73°F

| Parameter | TEM-10 | Specification Requirement |
|---|-----------|---------------------------|
| Maximum Igniter Mass Flow Rate (lbm/sec) | 358.4 | N/A |
| Ignition Transient (sec) (0 to 563.5 psia) | 0.2355 | 0.170 - 0.340 |
| Maximum Pressure Rise Rate (psi/10 ms) | 74.83 | 109 |
| Pressure Level at Start of Maximum Rise Rate (psia) | 120 | N/A |
| Time Span of Maximum Pressure Rise (ms) | 144 - 154 | N/A |
| Equilibrium Pressure 0.6 sec (ignition end) (psia) | 904 | N/A |
| Time to First Ignition (sec) (begin pressure rise) | 0.028 | N/A |

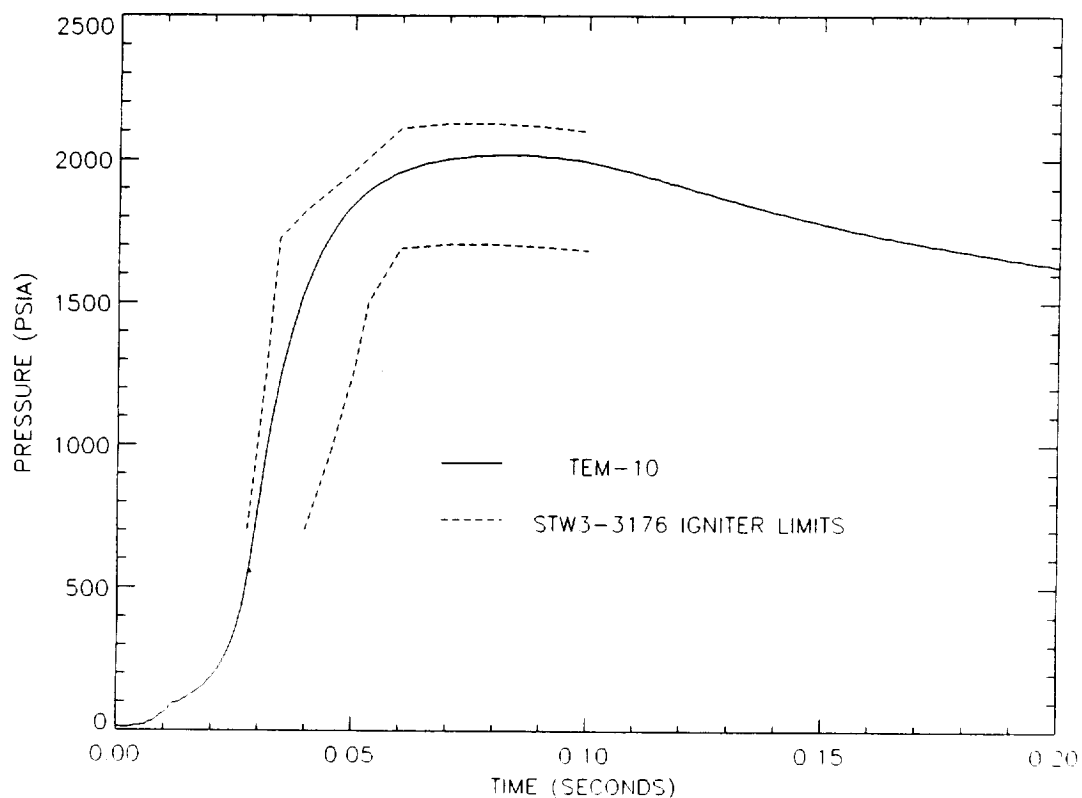


Figure 6-20. Comparison of Igniter Performance with Limits at 80°F

A comparison of the igniter pressure versus motor head-end and nozzle stagnation pressure for the first 1.4 sec of motor operation is shown in Figure 6-21. The slight mismatch between igniter and head-end chamber pressure values from 0.6 to 1.4 sec is within allowed transducer error. A plot of head-end and nozzle stagnation pressure for the full duration of the static test is shown on Figure 6-22. These curves are characteristic of the ratio of the head-end to nozzle stagnation pressures from previous SRM static test motors.

TEM-10 was instrumented with four pressure transducers for head-end pressure measurement (PNCAC001-PNCAC003 and PNCAC016) and 1 gage for igniter pressure measurement (PNCAC005). The signal from the head-end OPT data channel (PNCAC001) was split to provide both A-C coupled data (for chamber pressure oscillation data) and mean pressure. Gage PNCAC016 was also to be dedicated to chamber pressure oscillation measurement but was not obtained on this test. In addition, the mean pressure data channels are used to calculate dynamic pressure and to verify the accuracy of the A-C coupled data.

Data acquired from gage PNCAC002 are displayed in a waterfall plot format in Figure 6-23. The 1-L and second longitudinal (2-L) acoustic modes can be observed at about 15 and 30 Hz, respectively. This waterfall plot is fairly typical of HPM designs. The magnitudes on this static test were typical for an HPM. In general, HPM 1-L mode amplitudes are lower than those for RSRMs.

Figures 6-24 and 6-25 describe the running, instantaneous, peak-to-peak oscillation amplitudes of the 1-L and 2-L acoustic modes, respectively, for the TEM-10 motor head-end pressure. This type of analysis is more representative of instantaneous oscillations than are the time averaged oscillations presented in a waterfall plot.

When using waterfall plots to compare static test motor oscillation amplitudes, it is important to remember that this format uses an averaging method of analysis. This presents no difficulty for steady-state signals but has an attenuating effect on transient signals. Since most of the data obtained from an SRM are transient, any oscillation magnitudes referred to as maxima are, in fact, not true but averaged values over a given time slice. These numbers are, nonetheless, very useful for comparison. Table 6-10 shows such a comparison for recent static test motors and the flight motors. This table contains the most recent data. DM-6 and DM-7 were filament wound case (FWC) motors.

A comparison of TEM-10 thrust data at 60°F and a burn rate of 0.368 ips at 625 psia and 60°F with the CEI specification CPW1-3300, dated 15 January 1986, thrust-time limits at 0.368 ips is shown on Figure 6-26. The TEM-10 performance was within average population limits. Note that the limits are for the average of the historical SRM population not an individual motor. The historical motor population is well within the limits. None of the individual motor performance tolerances and limit parameters were exceeded. The TEM-10 ignition performance satisfied the ignition interval and the maximum pressure rise rate requirements as shown in Table 6-9.

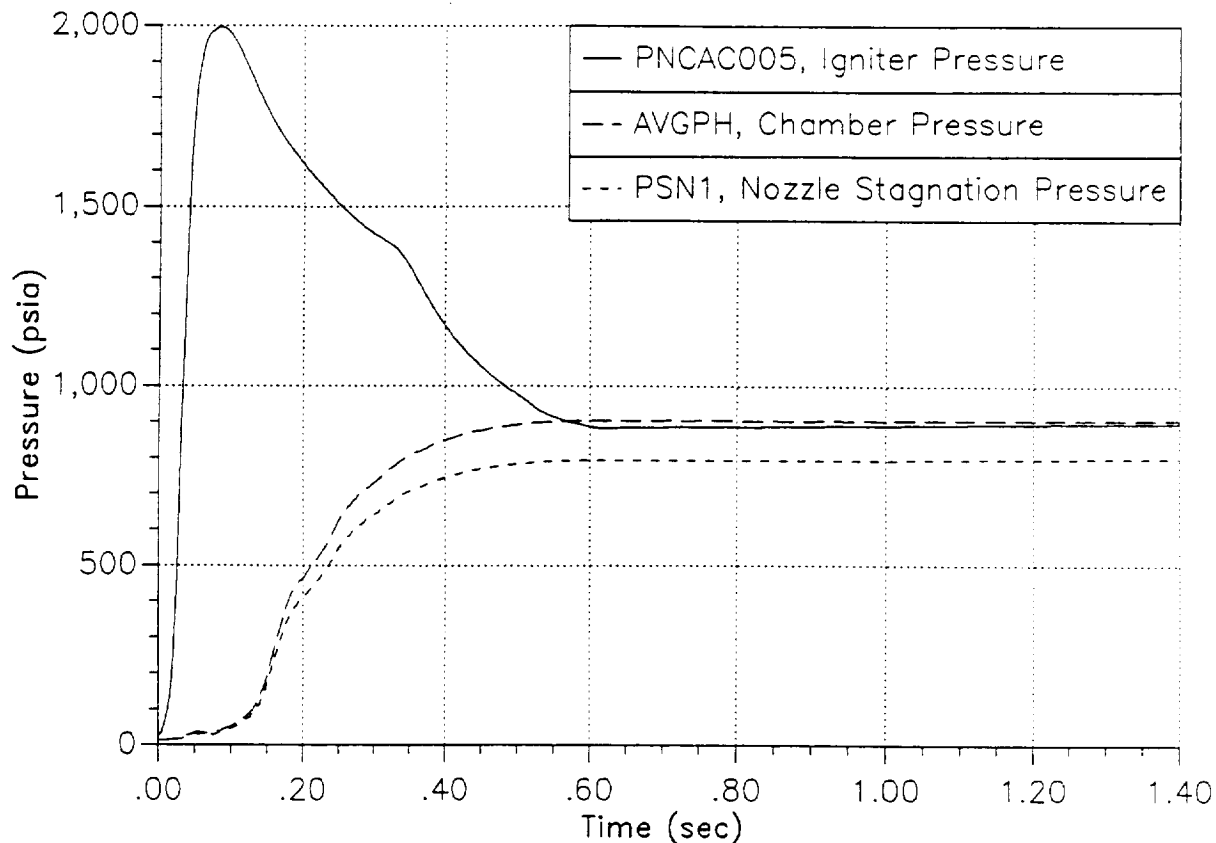


Figure 6-21. Igniter Pressure Versus Head-End and Nozzle Stagnation Pressure

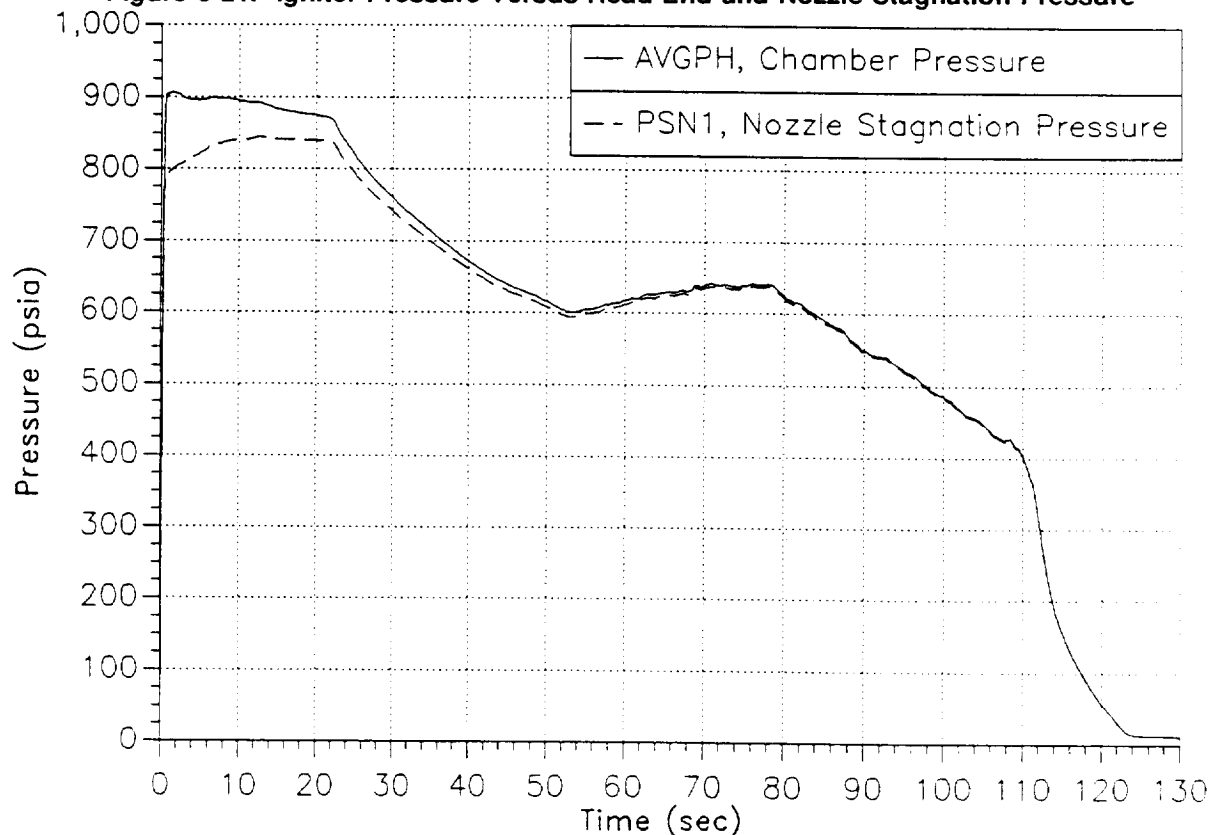


Figure 6-22. Measured Head-End and Nozzle Stagnation Pressure Time Histories

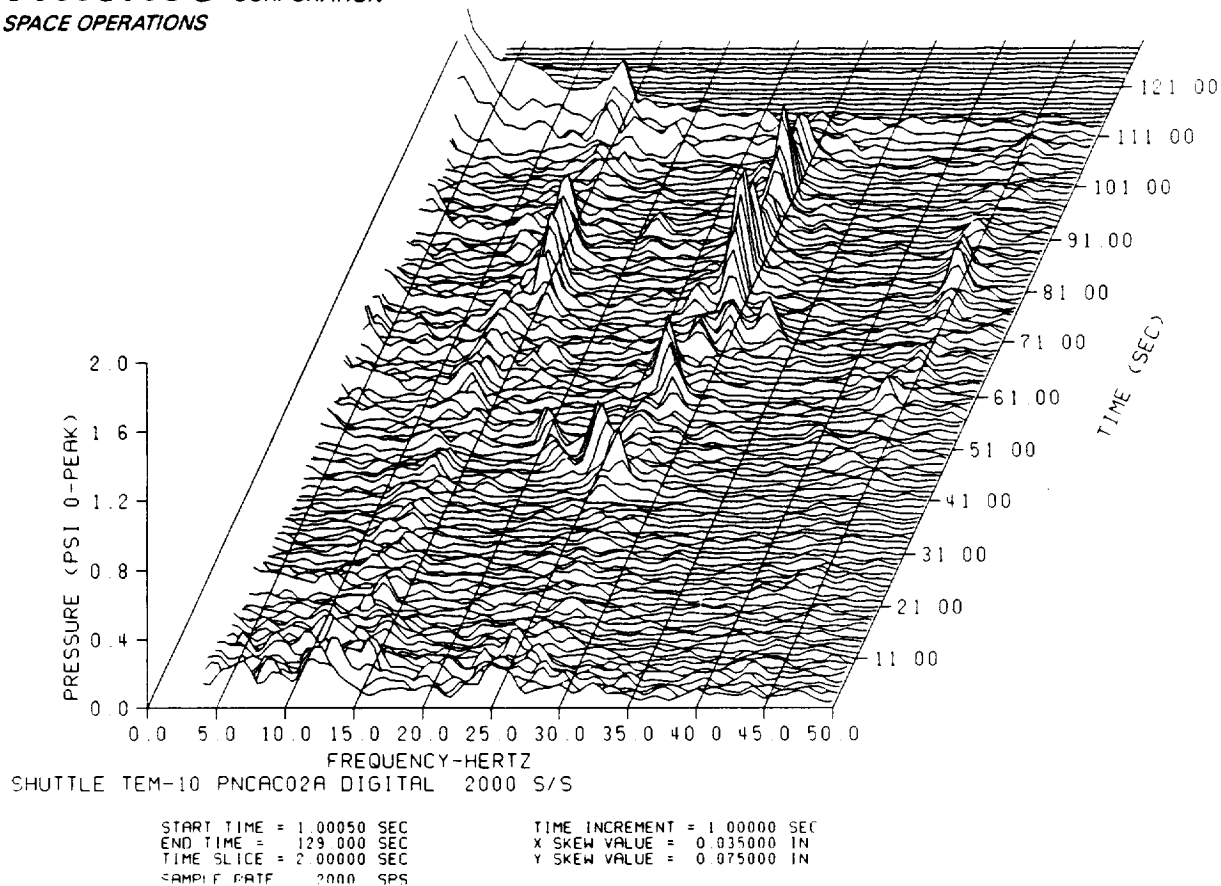


Figure 6-23. PNCAC002 Waterfall Plot

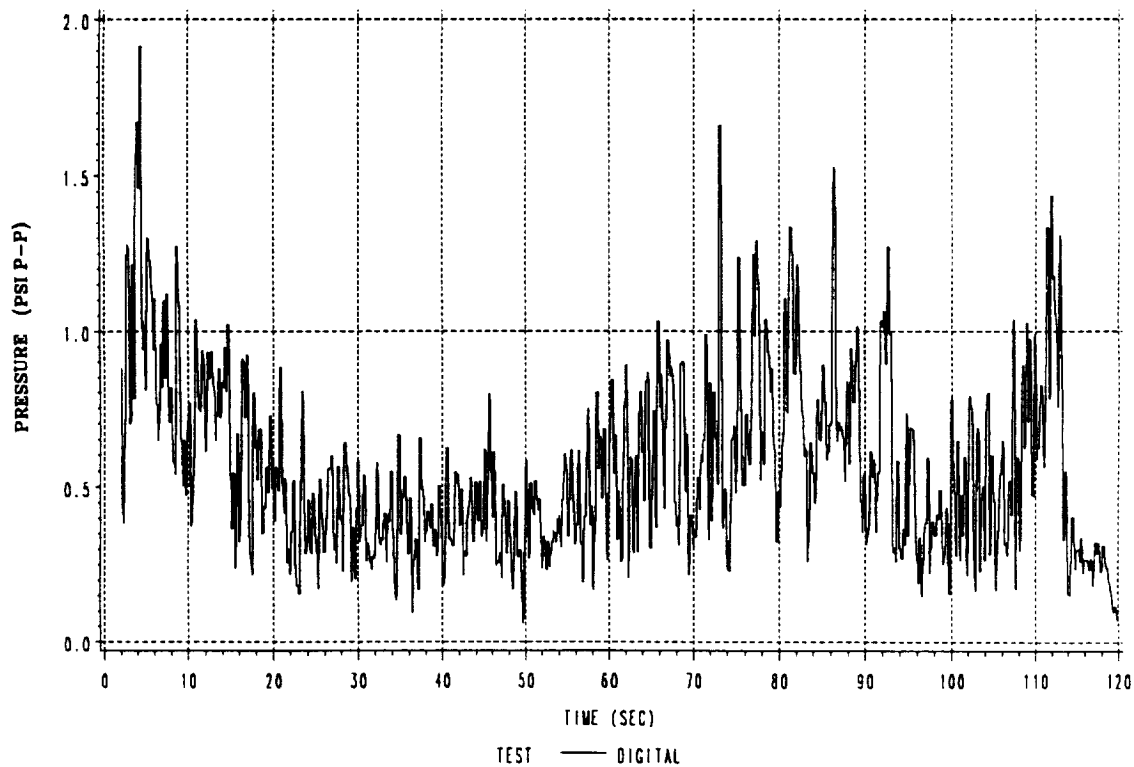


Figure 6-24. Maximum Oscillation Amplitudes--PNCAC002 1-L Acoustic Mode

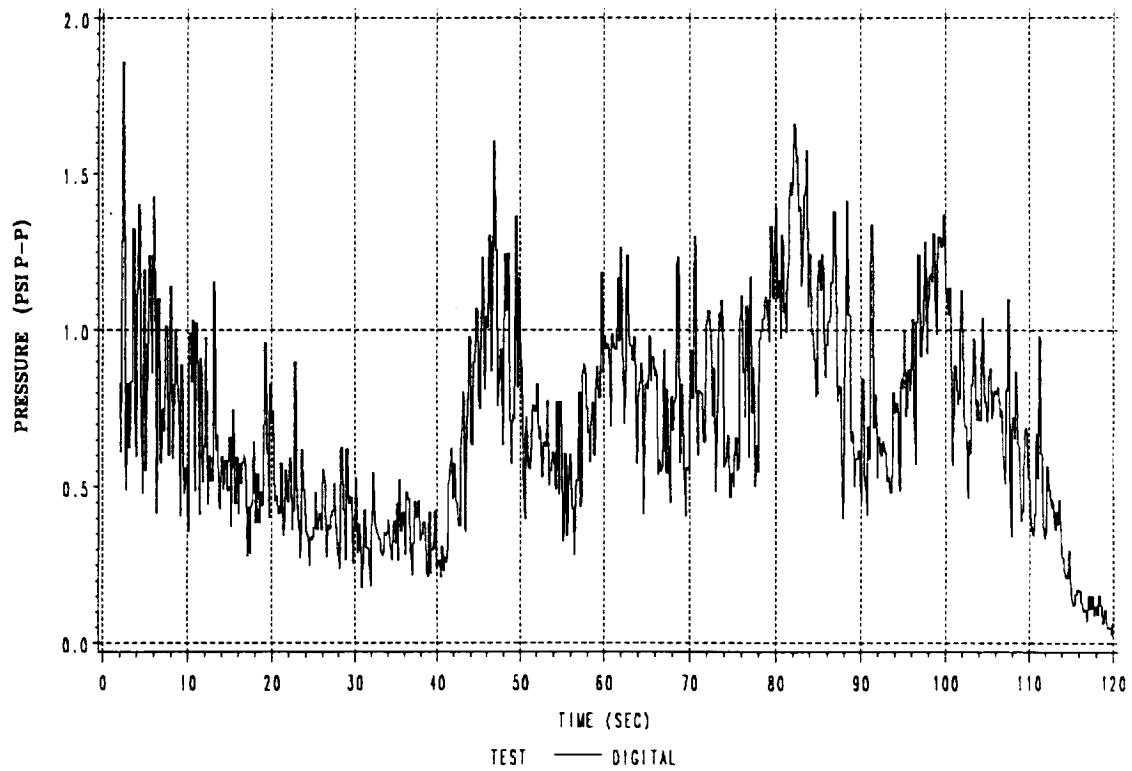


Figure 6-25. Maximum Oscillation Amplitudes--PNCAC002 2-L Acoustic Mode

Table 6-10. Maximum Pressure Oscillation Amplitude Comparison

| Motor | Source of Measurement | Mode | Time of Measurement | Frequency (Hz) | Max Pressure (psi 0-to-peak) |
|-------------------|------------------------|------|---------------------|----------------|------------------------------|
| TEM-10 | Waterfall PNCAC002 | 1-L | 82 | 15.5 | 0.47 |
| | | 2-L | 83 | 29.5 | 0.69 |
| FSM-3* | Waterfall PNCAC016 | 1-L | 103 | 14.5 | 0.51 |
| | | 2-L | 79 | 29.5 | 0.59 |
| TEM-9 | Waterfall PNCAC002 | 1-L | 81 | 15.5 | 0.65 |
| | | 2-L | 83 | 29.5 | 0.59 |
| FSM-2* | Waterfall PNCAC001 | 1-L | 107 | 14.5 | 0.51 |
| | | 2-L | 93 | 29.5 | 0.62 |
| TEM-8 | Waterfall PNCAC002 | 1-L | 81 | 16.0 | 0.55 |
| | | 2-L | 97 | 29.5 | 0.60 |
| TEM-7 | Waterfall PNCAC002 | 1-L | 85 | 15.5 | 0.54 |
| | | 2-L | 100 | 29.5 | 0.53 |
| FSM-1* | Waterfall PNCAC001 | 1-L | 100 | 14.0 | 0.64 |
| | | 2-L | 79 | 29.5 | 0.74 |
| TEM-6 | Waterfall PNCAC001 | 1-L | 92 | 15.0 | 0.41 |
| | | 2-L | 98/99 | 29.5 | 0.67 |
| TEM-6 (Aft) | Waterfall PNNAR005 | 1-L | 92 | 15.0 | 0.31 |
| | | 2-L | 98/99 | 29.5 | 0.44 |
| TEM-5 | Waterfall PNCAC005 | 1-L | 81 | 16.0 | 0.46 |
| | | 2-L | 100 | 29.5 | 0.57 |
| TEM-4 | Waterfall | 1-L | 115 | 14.5 | 0.37 |
| | | 2-L | 87 | 29.5 | 0.96 |
| TEM-3 | Waterfall | 1-L | 106 | 15.0 | 0.36 |
| | | 2-L | 102 | 30.0 | 0.58 |
| STS-29 (left) | Waterfall AC OPT | 1-L | 86 | 15.5 | 0.31 |
| | | 2-L | 89 | 28.0 | 0.44 |
| STS-29 (right) | Waterfall AC OPT | 1-L | 85 | 15.5 | 0.38 |
| | | 2-L | 83 | 29.5 | 0.54 |
| TEM-2 | Waterfall | 1-L | 78 | 16.0 | 0.43 |
| | | 2-L | 100 | 29.5 | 0.68 |
| QM-8* | Waterfall (P000002) | 1-L | 104 | 14.5 | 1.32 |
| | | 2-L | 55 | 27.5 | 0.47 |
| TEM-1 | Waterfall | 1-L | 79 | 15.5 | 0.37 |
| | | 2-L | 95 | 29.5 | 0.78 |
| STS-27 (left) | Waterfall AC OPT | 1-L | 82 | 15.5 | 0.37 |
| | | 2-L | 82 | 29.5 | 0.60 |

Table 6-10. Maximum Pressure Oscillation Amplitude Comparison (cont)

| Motor | Source of Measurement | Mode | Time of Measurement | Frequency (Hz) | Max Pressure (psi 0-to-peak) |
|----------------|-----------------------|------|---------------------|----------------|------------------------------|
| STS-27 (right) | Waterfall AC OPT | 1-L | 82 | 15.5 | 0.57 |
| | | 2-L | 83 | 29.5 | 0.72 |
| STS-26 (left) | Waterfall AC OPT | 1-L | 79 | 16.0 | 0.70 |
| | | 2-L | 95 | 29.5 | 0.87 |
| STS-26 (right) | Waterfall AC OPT | 1-L | 83 | 15.0 | 0.54 |
| | | 2-L | 94 | 30.0 | 0.47 |
| PVM-1* | Waterfall | 1-L | 99 | 14.5 | 1.23 |
| | | 2-L | 79 | 29.5 | 0.77 |
| QM-7* | Waterfall P000001 | 1-L | 93 | 14.5 | 1.40 |
| | | 2-L | 79 | 29.5 | 0.95 |
| QM-6* | Waterfall | 1-L | 107 | 14.5 | 1.05 |
| | | 2-L | 85 | 29.5 | 0.53 |
| DM-9* | Waterfall | 1-L | 107 | 14.5 | 0.81 |
| | | 2-L | 96 | 30.0 | 0.64 |
| DM-8* | Waterfall | 1-L | 78 | 16.0 | 0.58 |
| | | 2-L | 97 | 29.5 | 0.62 |
| ETM-1A | Waterfall | 1-L | 84 | 15.5 | 0.45 |
| | | 2-L | 101 | 29.5 | 0.61 |
| DM-7** | Waterfall | 1-L | 77 | 15.5 | 0.90 |
| | | 2-L | 96 | 29.0 | 0.62 |
| DM-6** | Waterfall | 1-L | 76 | 15.5 | 0.51 |
| | | 2-L | 86 | 29.0 | 0.78 |
| QM-4 | Waterfall | 1-L | 81 | 15.5 | 0.31 |
| | | 2-L | 80 | 29.5 | 0.30 |

* RSRM static test motors.

** FWC HPMs

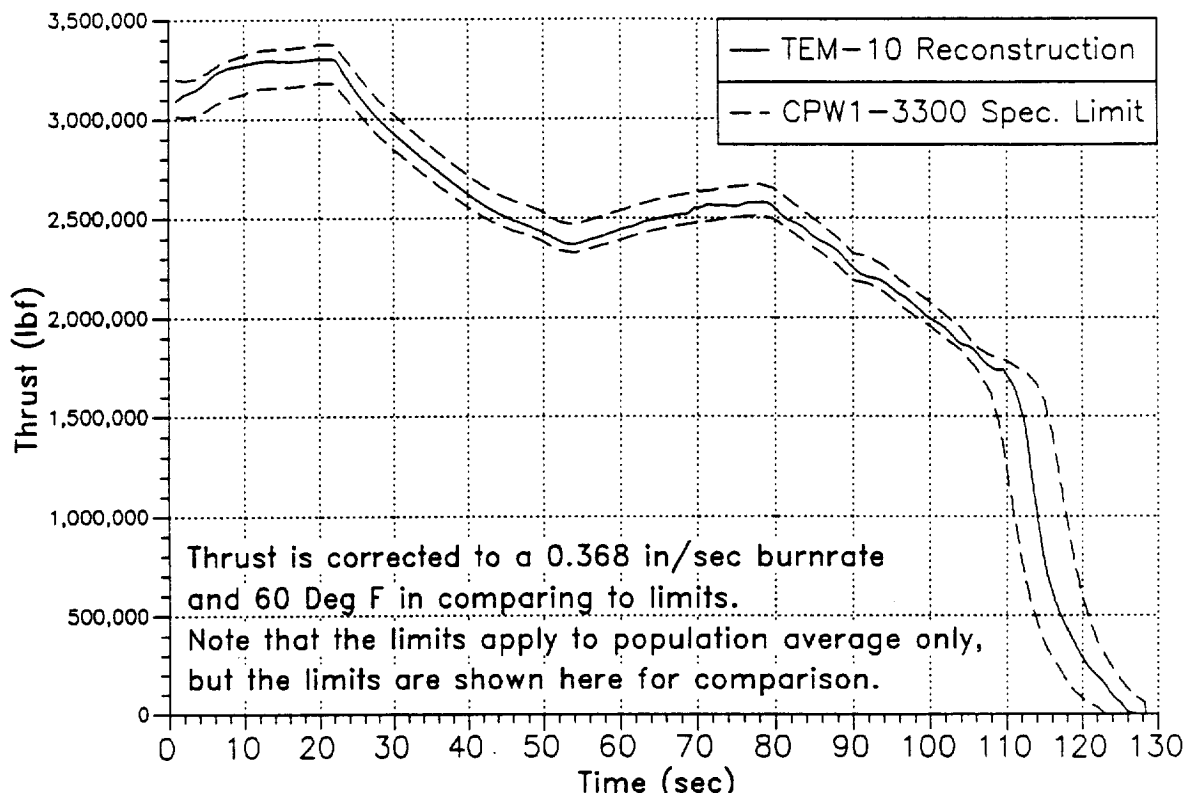


Figure 6-26. Reconstructed Thrust Compared to CEI Limits

6.10 PRESSURE PERTURBATION SUMMARY

6.10.1 Introduction

To better understand the small pressure fluctuations experienced during motor operation, additional instrumentation was incorporate into the TEM-10 static test.

6.10.2 Objectives/Conclusions

| Objective | Conclusion |
|--|--|
| F. Obtain RTR, acceleration, IR plume, sound pressure, and strain data in support of the RSRM-29 pressure anomaly investigation. | <i>Obtained.</i> This section specifically addresses the strain data, calorimeter/radiometer data, and the RTR data portions of the objective. |

6.10.3 Recommendations

The TEM-10 motor pressure perturbation was benign relative to the pressure perturbations recorded on flight motors.

Valuable instrumentation and RTR data were gathered on TEM-10; therefore, it is recommended that every opportunity to gain knowledge on the pressure perturbations be aggressively pursued on future full-scale static test motors.

6.10.4 Results/Discussion

This section documents the calorimeter and radiometer data analysis; a time correlation between the RTR film, video, and high speed film; a correlation between the nozzle strain gages and identified pressure perturbations; and an accelerometer data correlation with identified pressure perturbations.

6.10.4.1 Calorimeter/Radiometer Data. A calorimeter and radiometer were placed on the axis of the motor a foot above the floor in front the motor pit. They were pointed to just below the exit cone of the nozzle down the axis of the motor (Figure 6-27). The calorimeter data followed the radiometer data very closely (Figures 6-28 and 6-29). The calorimeter/radiometer data roughness tends to follow the motor pressure roughness. The turbulence of the plume also shows up in the heat flux plots.

A linear relationship exists between calorimeter/radiometer data and head-end motor chamber pressure when plotted on a log-log plot (Figure 6-30). The results of removing the effects of pressure from the calorimeter data are shown in Figures 6-31 and 6-32.

Two events in the calorimeter data have been looked at carefully. At 74.7 sec there was an increase in heat flux measured by the calorimeter/radiometer data, which is currently believed to be from a nozzle impact event or an internal high-speed ejecta event (Figure 6-33). The event correlates well with events in the pressure, accelerometer, and strain gage data. At 108.4 sec there was an increase in the heat flux as measured by the calorimeter/radiometer (Figure 6-34).

6.10.4.2 Nozzle Strain Gage Correlation to Identified Pressure Events. Pressure perturbations (blips) have been identified at approximately 74.5 and 108 sec into motor operation. A more detailed examination of the nozzle strains at these times for the 2,000 SPS gage data is shown in Figures 6-35 through 6-50.

Figures 6-45 through 6-48 show the hoop strain, and Figures 6-39 through 6-42 the meridional strain, measured on the fixed housing at station 1867.0 between 72 and 76 sec during motor operation.

Each figure shows a single strain gage plotted against the chamber pressure measured at gage PNCAC002. Strain data from the 2,000 SPS gages located at the 80-, 170-, 260-, and 350-deg locations were used, and show up as the heavy black line in each plot.

These figures show that at approximately 74.5 sec the chamber pressure increased approximately 4 psi and the nozzle fixed housing strains reacted. Internal pressure is the primary load causing strain in the fixed housing metal.

Figures 6-43 through 6-46 show the hoop strain, and Figures 6-47 through 6-50 the meridional strain, measured on the fixed housing at station 1867.0 between 102 and 110 sec during motor operation.

Each figure shows a single strain gage plotted against the chamber pressure measured at gage PNCAC002. Strain data from the 2,000 SPS gages located at the 80-, 170-, 260-, and 350-deg locations were used and show up as the heavy black line in each plot.

These figures show that at approximately 108 sec the chamber pressure increased by as much as 10 psi and the nozzle fixed housing strains reacted. Internal pressure is the primary load causing strain in the fixed housing metal.

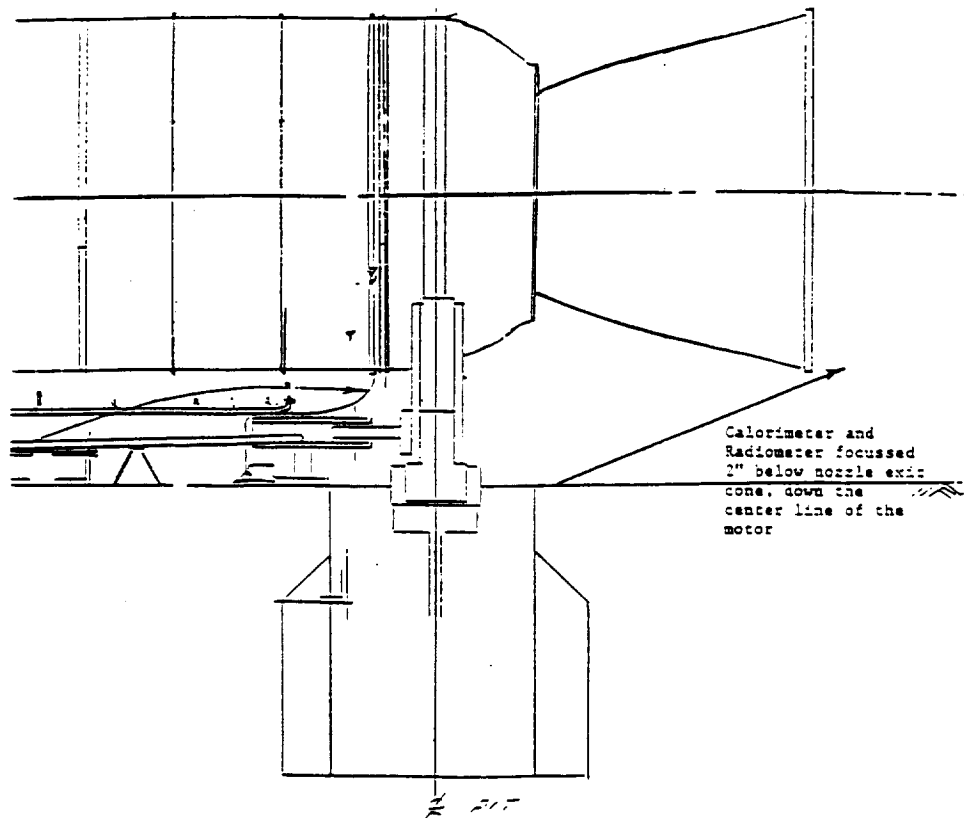


Figure 6-27. Calorimeter/Radiometer Location

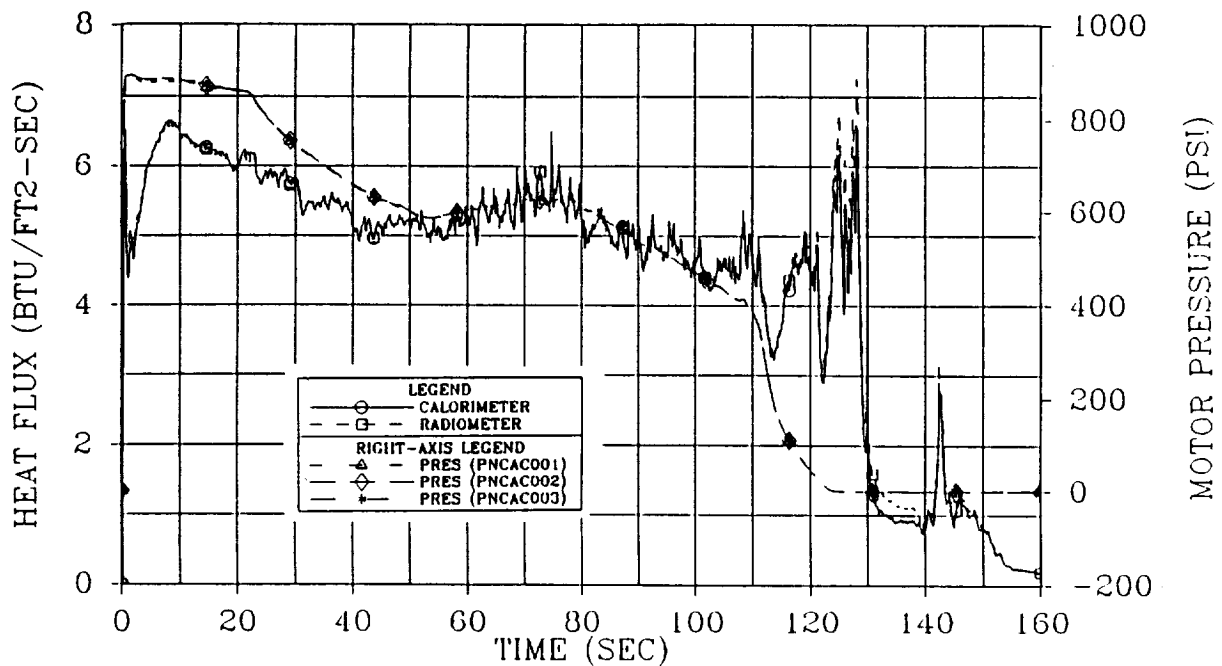


Figure 6-28. Calorimeter/Radiometer Data Versus Time (0-160 sec)

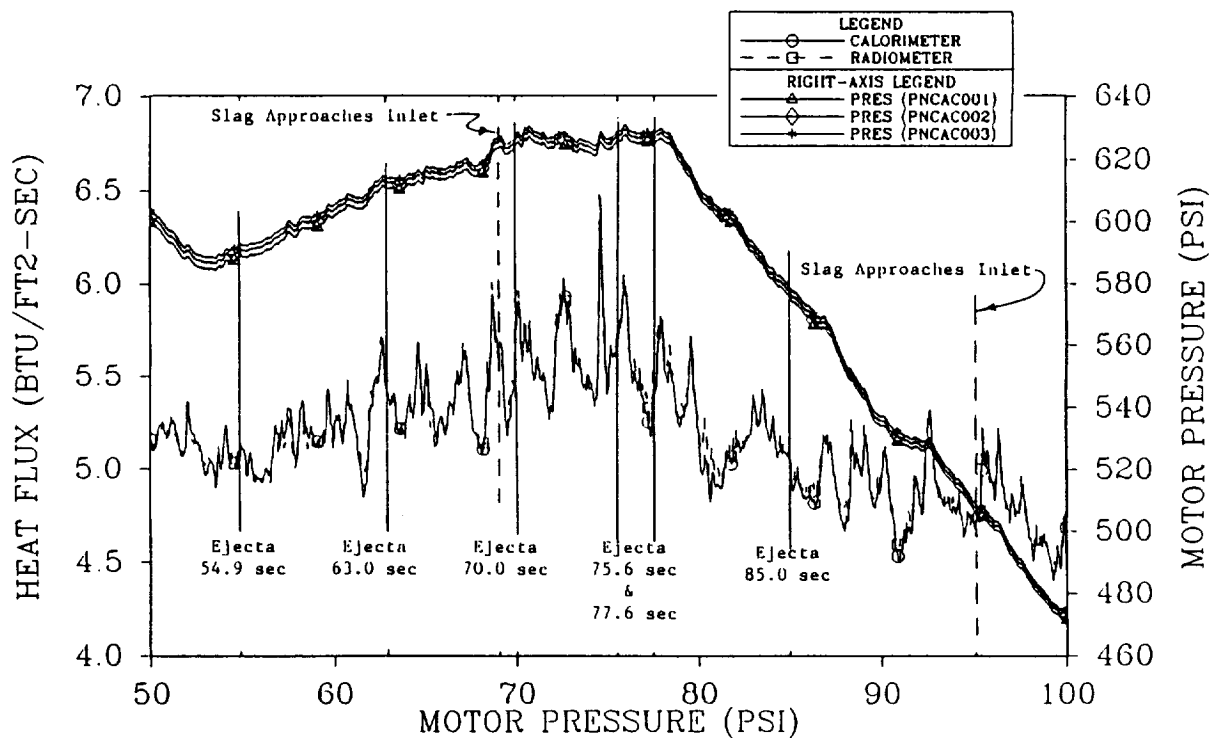


Figure 6-29. Calorimeter/Radiometer Data Versus Time (50-100 sec)

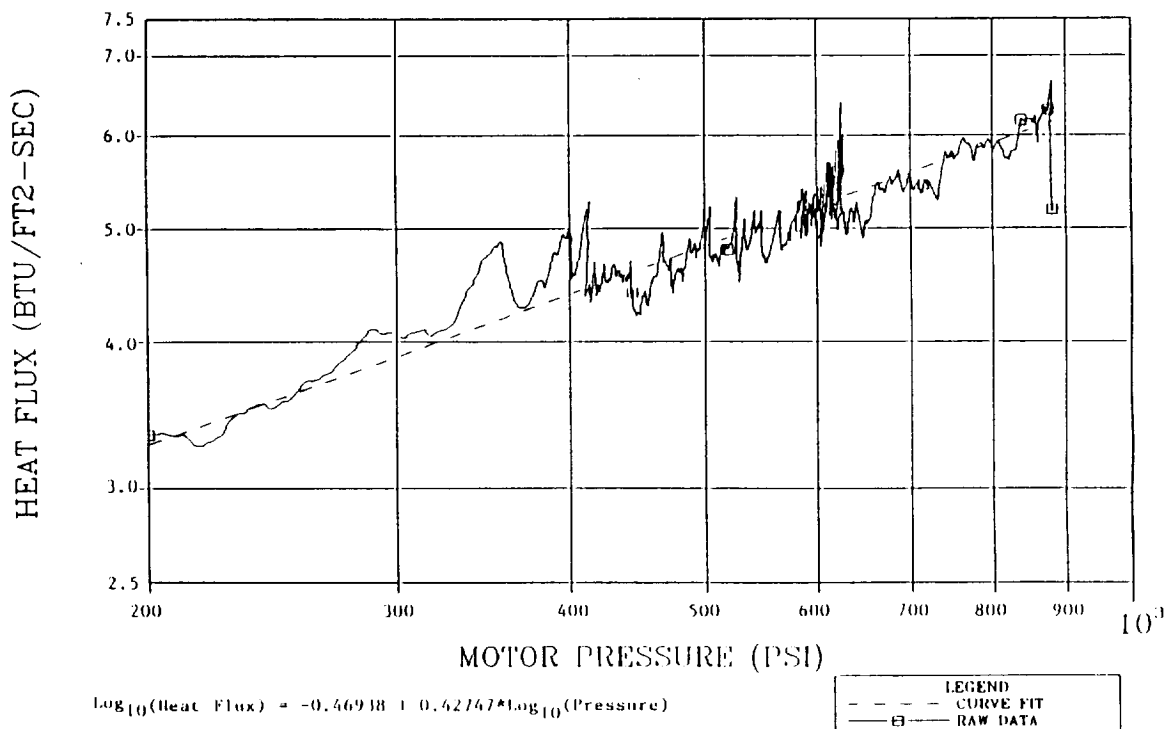


Figure 6-30. Calorimeter Versus Motor Pressure

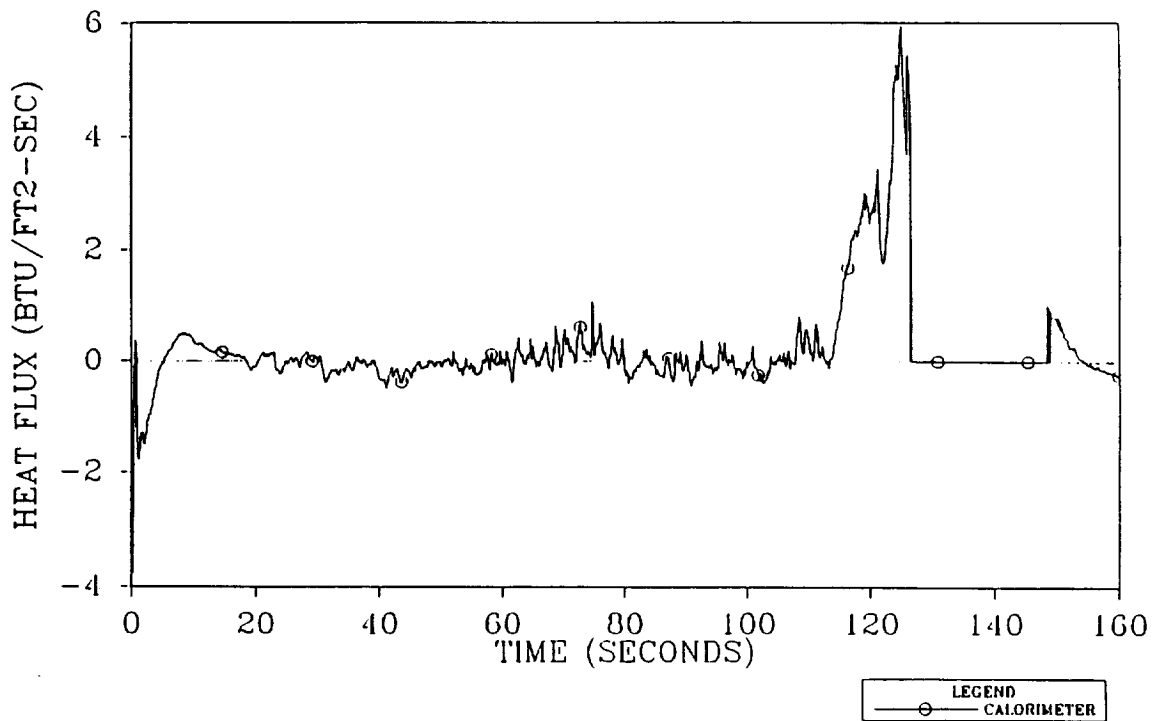


Figure 6-31. Calorimeter Data Minus Predicted Versus Time (0-160 sec)

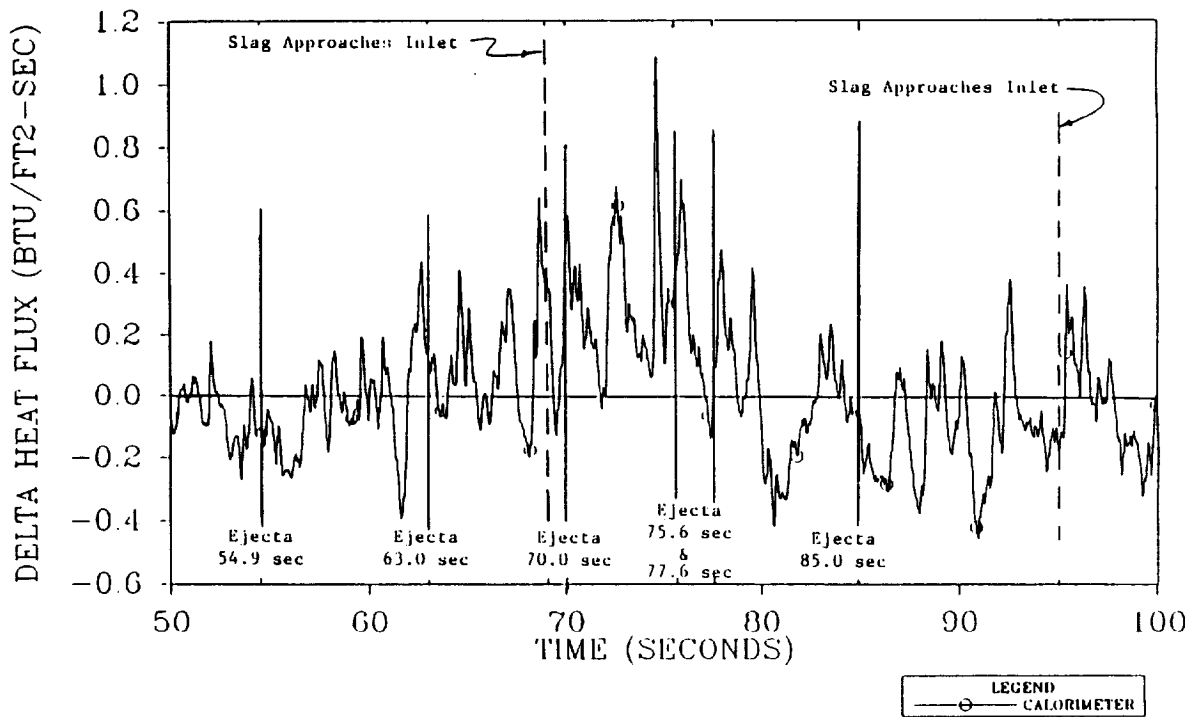


Figure 6-32. Calorimeter Data Minus Predicted Versus Time (50-100 sec)

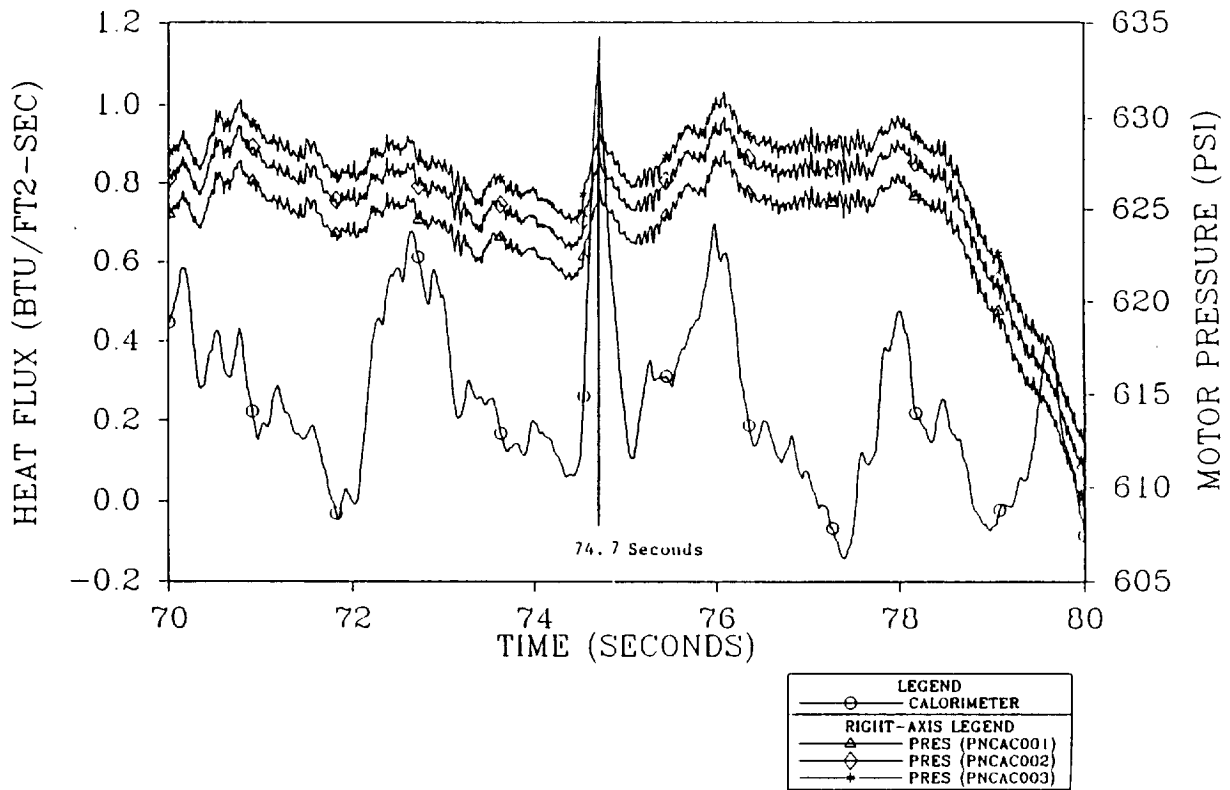


Figure 6-33. Calorimeter Data Minus Predicted Versus Time (70-80 sec)

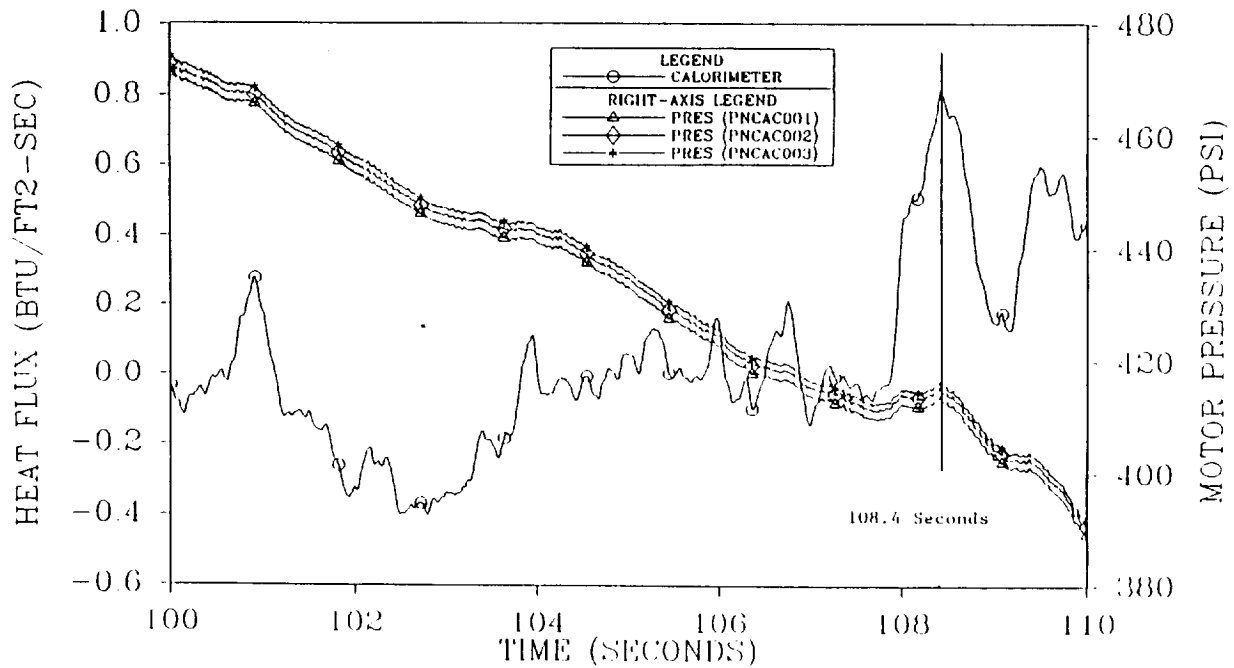


Figure 6-34. Calorimeter Data Minus Predicted Versus Time (100-110 sec)

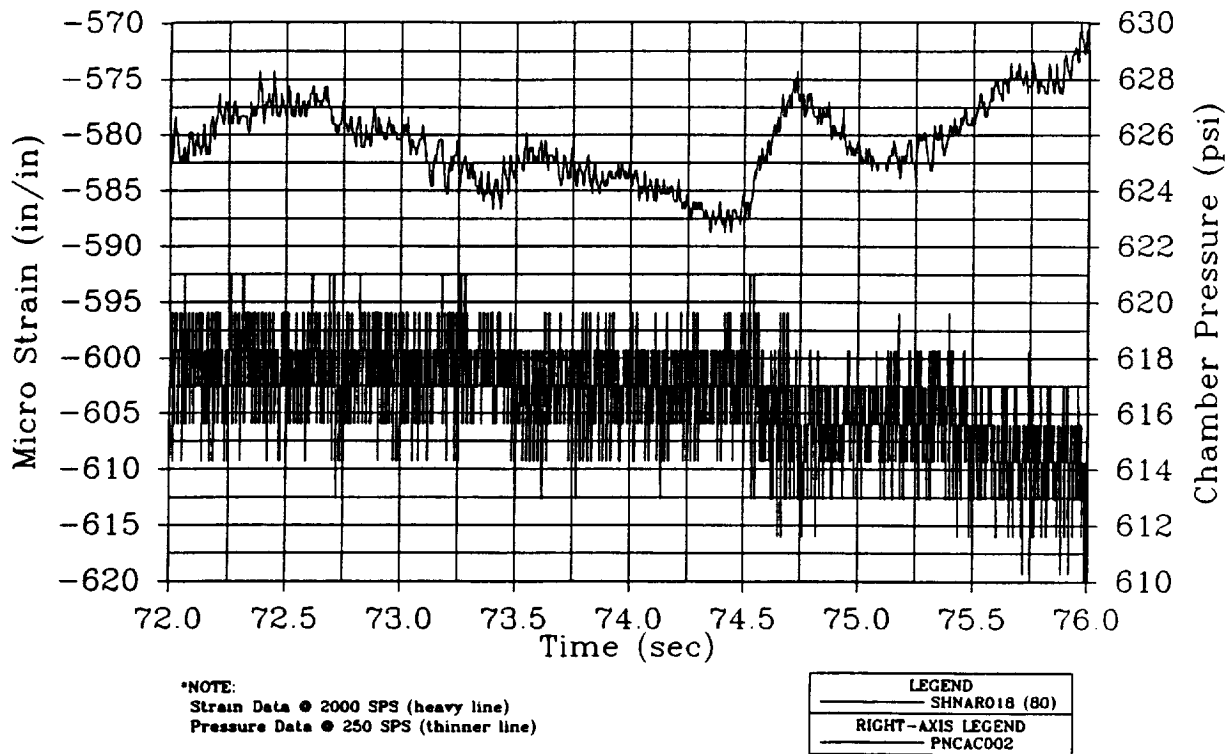


Figure 6-35. Nozzle Fixed Housing Hoop Strain Versus Chamber Pressure at 72-76 sec (80 deg)

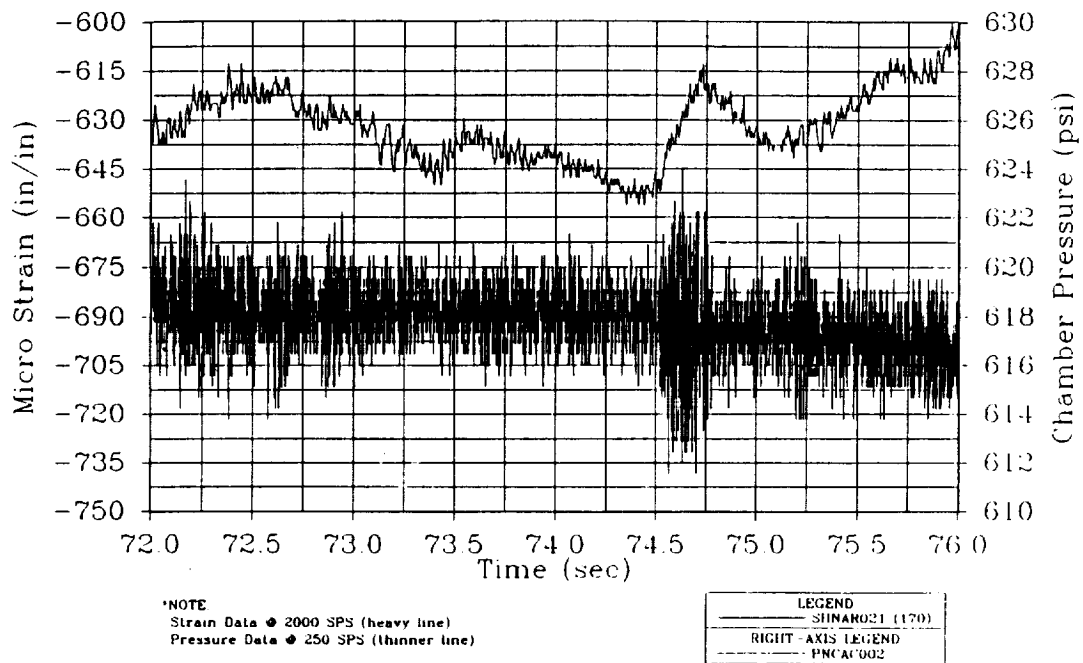


Figure 6-36. Nozzle Fixed Housing Hoop Strain Versus Chamber Pressure at 72-76 sec (170 deg)

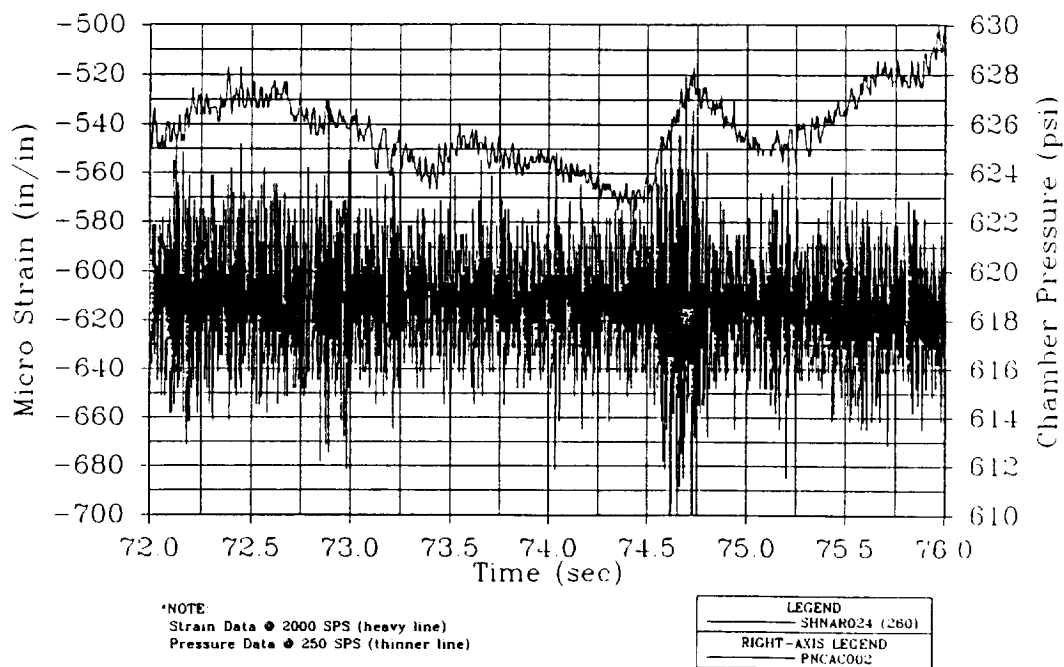


Figure 6-37. Nozzle Fixed Housing Hoop Strain Versus Chamber Pressure at 72-76 sec (260 deg)

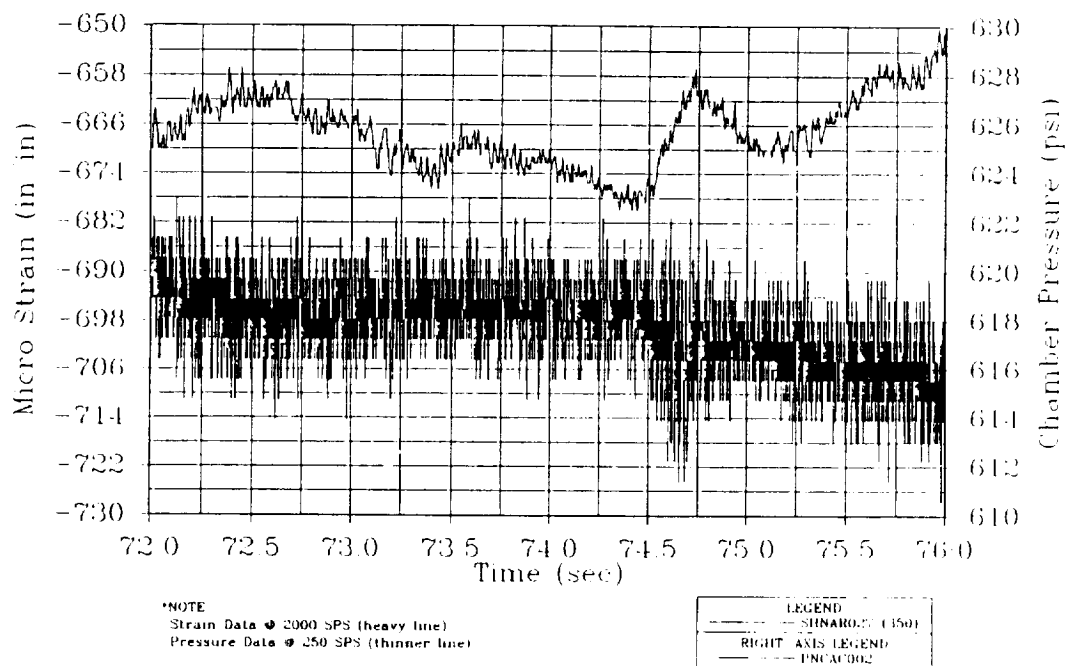


Figure 6-38. Nozzle Fixed Housing Hoop Strain Versus Chamber Pressure at 72-76 sec (350 deg)

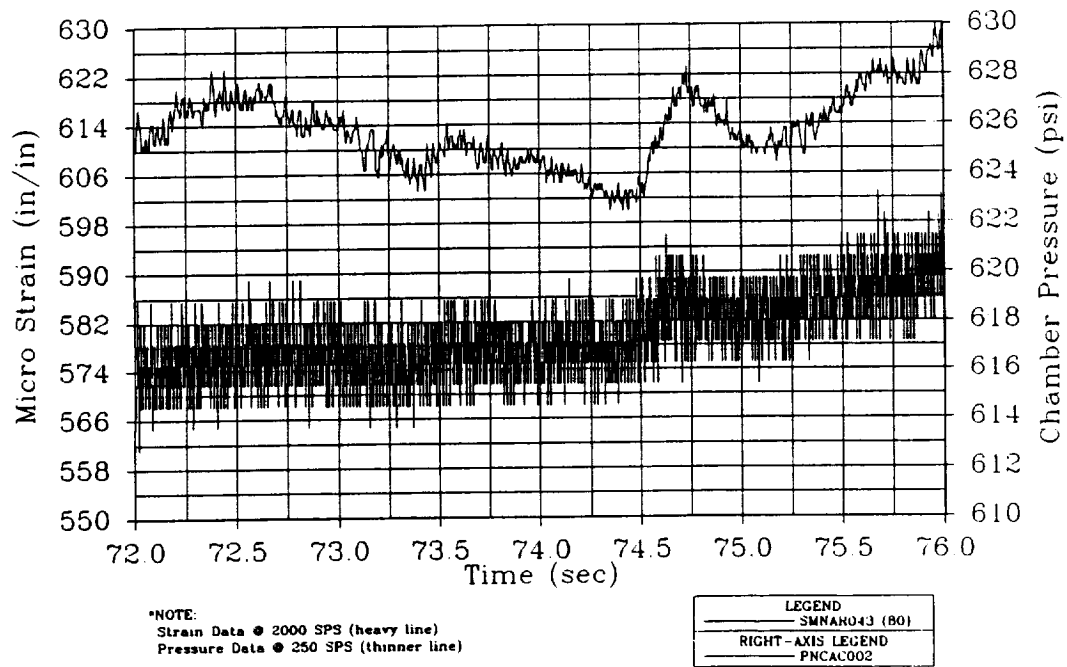


Figure 6-39. Nozzle Fixed Housing Meridional Strain Versus Chamber Pressure at 72-76 sec (80 deg)

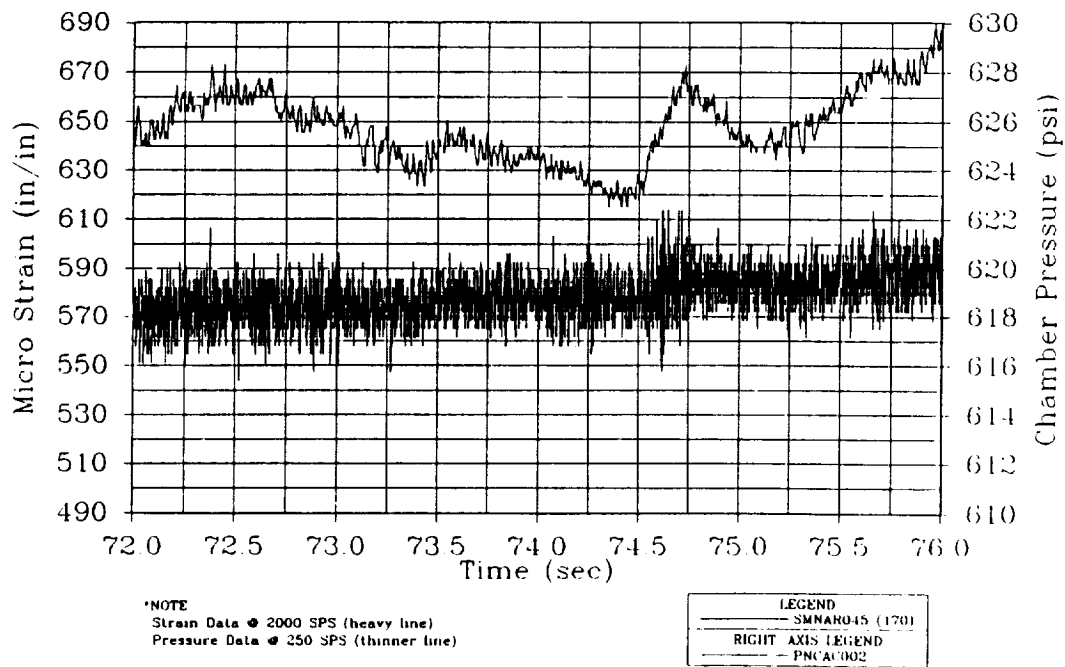


Figure 6-40. Nozzle Fixed Housing Meridional Strain Versus Chamber Pressure at 72-76 sec (170 deg)

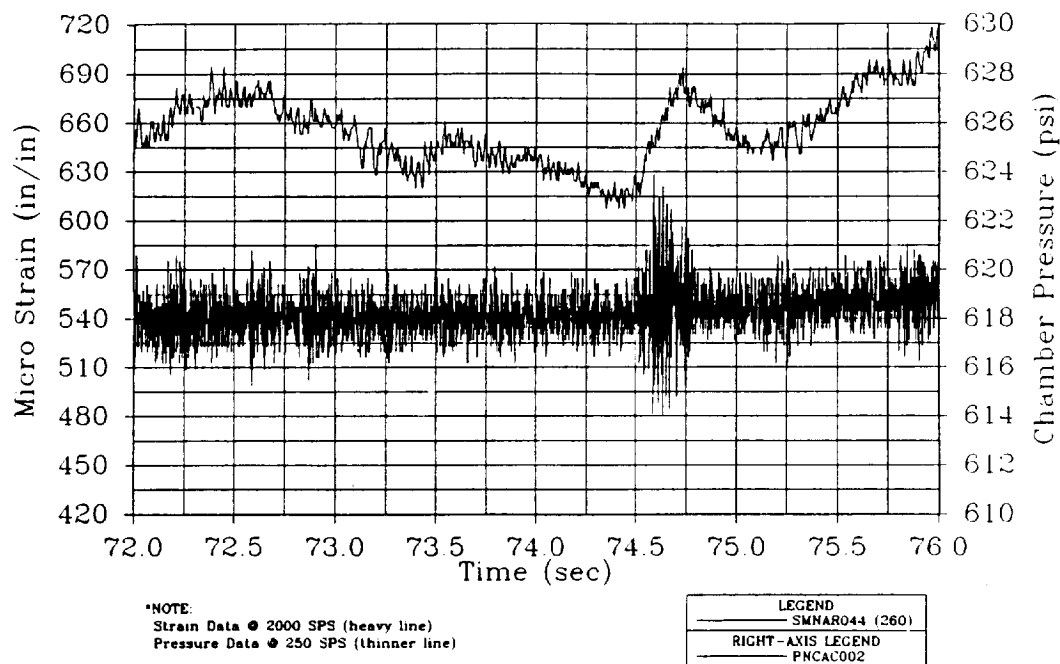


Figure 6-41. Nozzle Fixed Housing Meridional Strain Versus Chamber Pressure at 72-76 sec (260 deg)

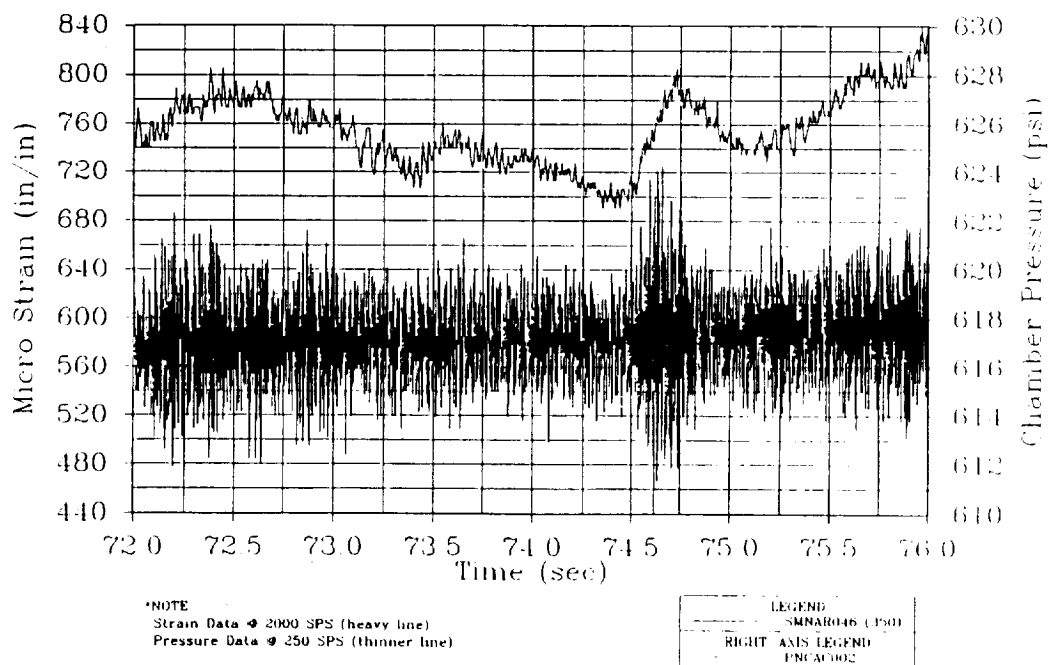


Figure 6-42. Nozzle Fixed Housing Meridional Strain Versus Chamber Pressure at 72-76 sec (350 deg)

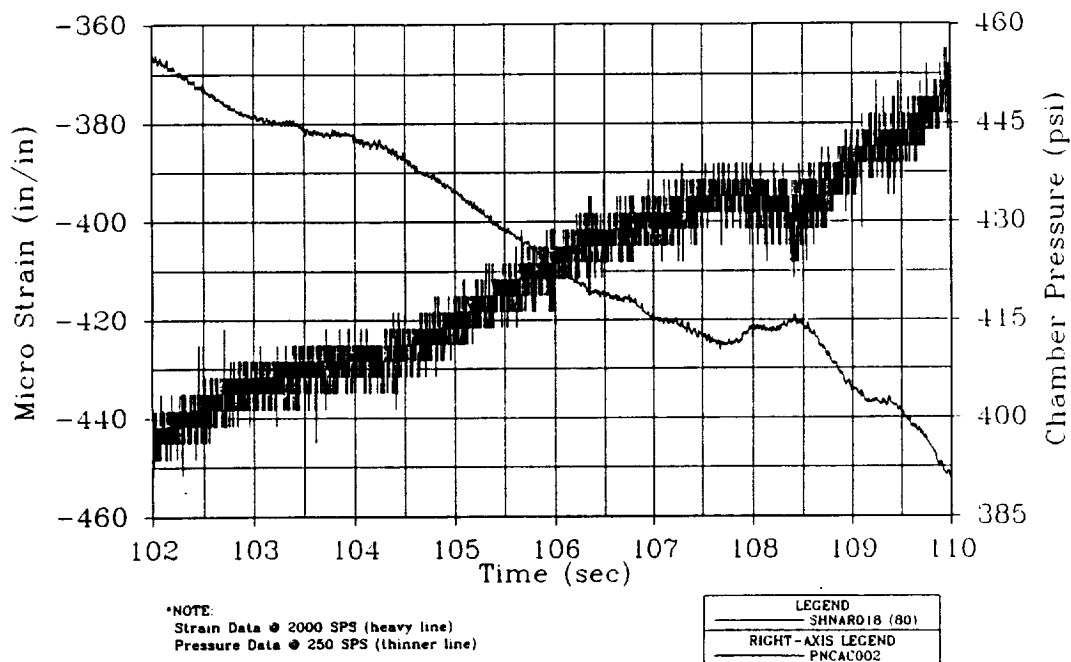


Figure 6-43. Nozzle Fixed Housing Hoop Strain Versus Chamber Pressure at 102-110 sec (80 deg)

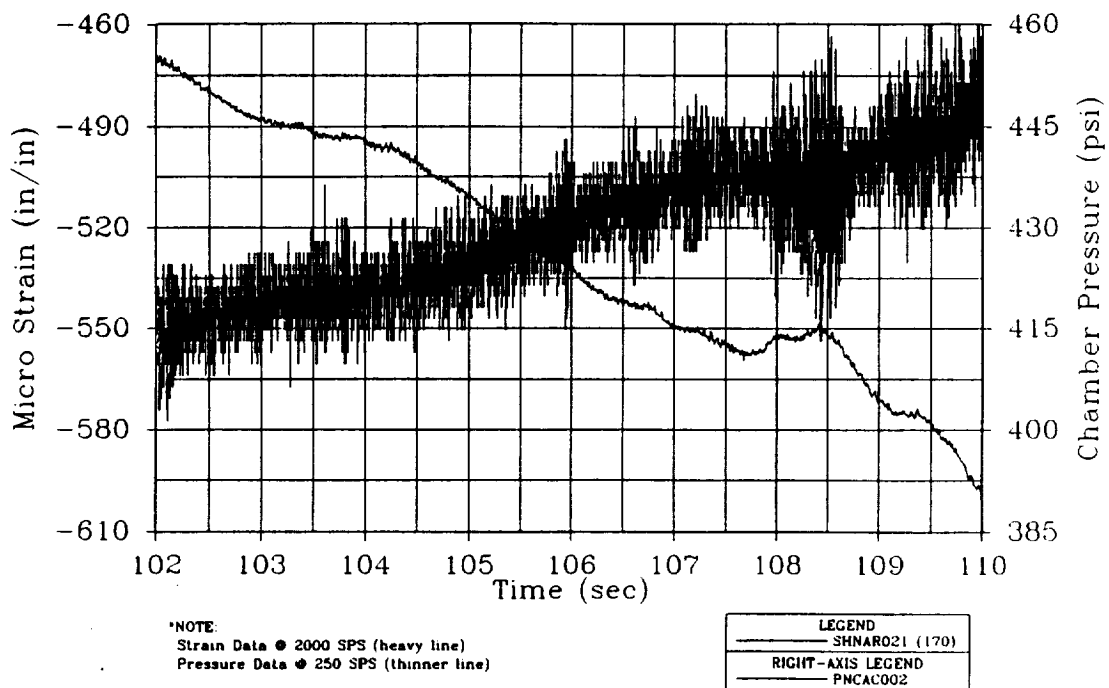


Figure 6-44. Nozzle Fixed Housing Hoop Strain Versus Chamber Pressure at 102-110 sec (170 deg)

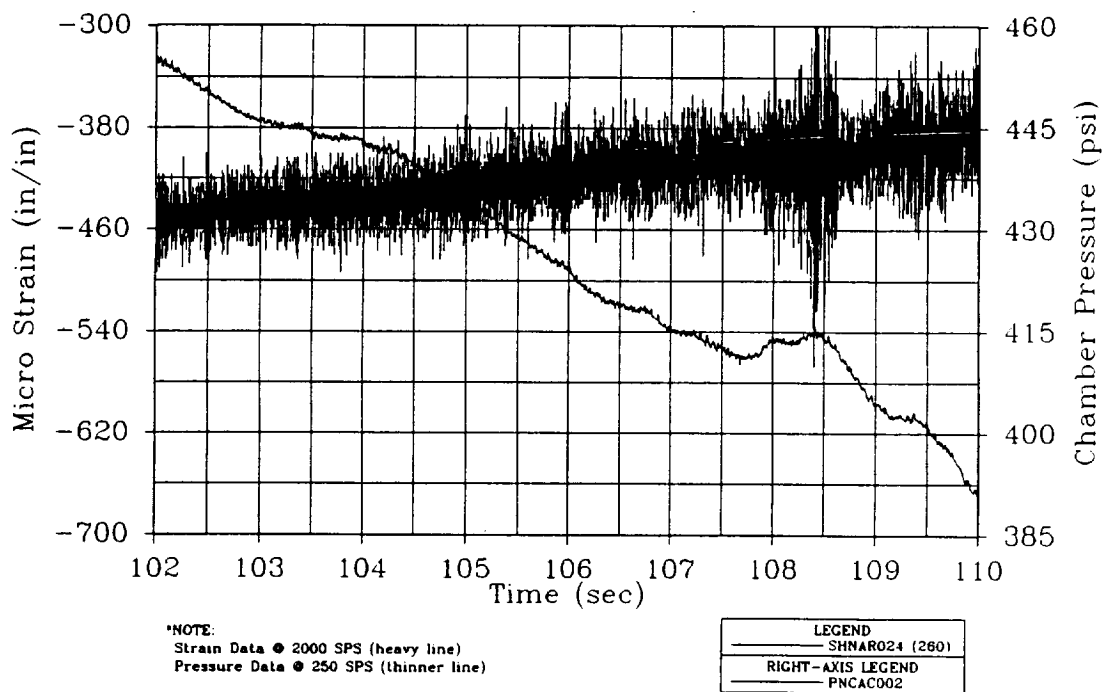


Figure 6-45. Nozzle Fixed Housing Hoop Strain Versus Chamber Pressure at 102-110 sec (260 deg)

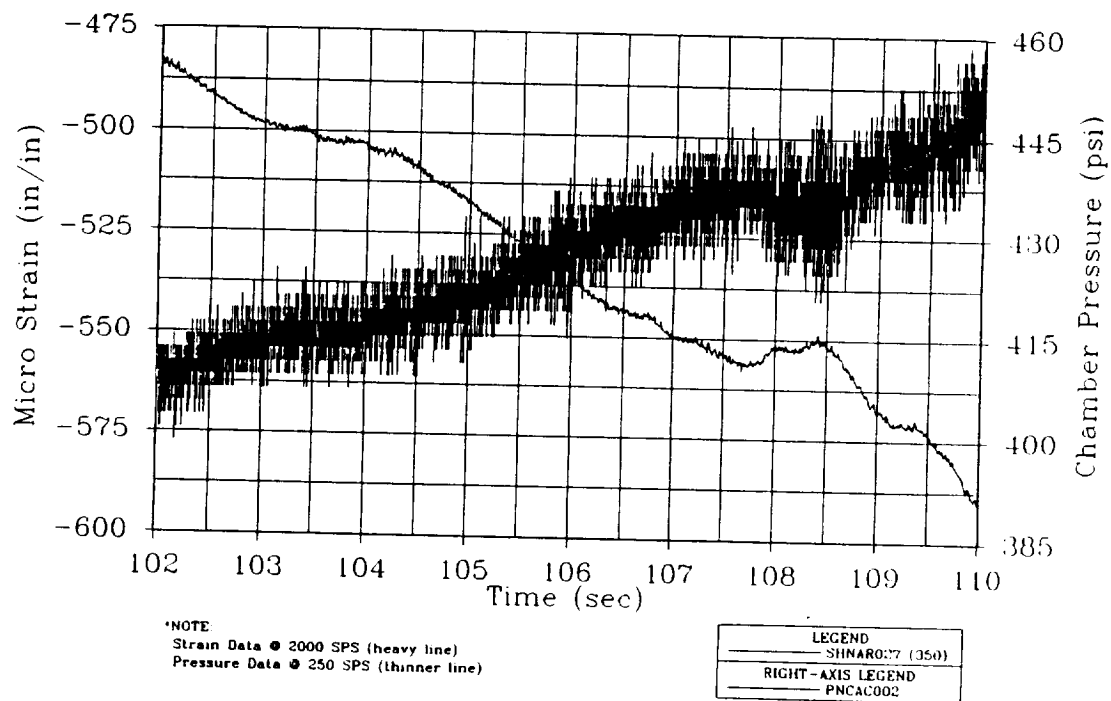


Figure 6-46. Nozzle Fixed Housing Hoop Strain Versus Chamber Pressure at 102-110 sec (350 deg)

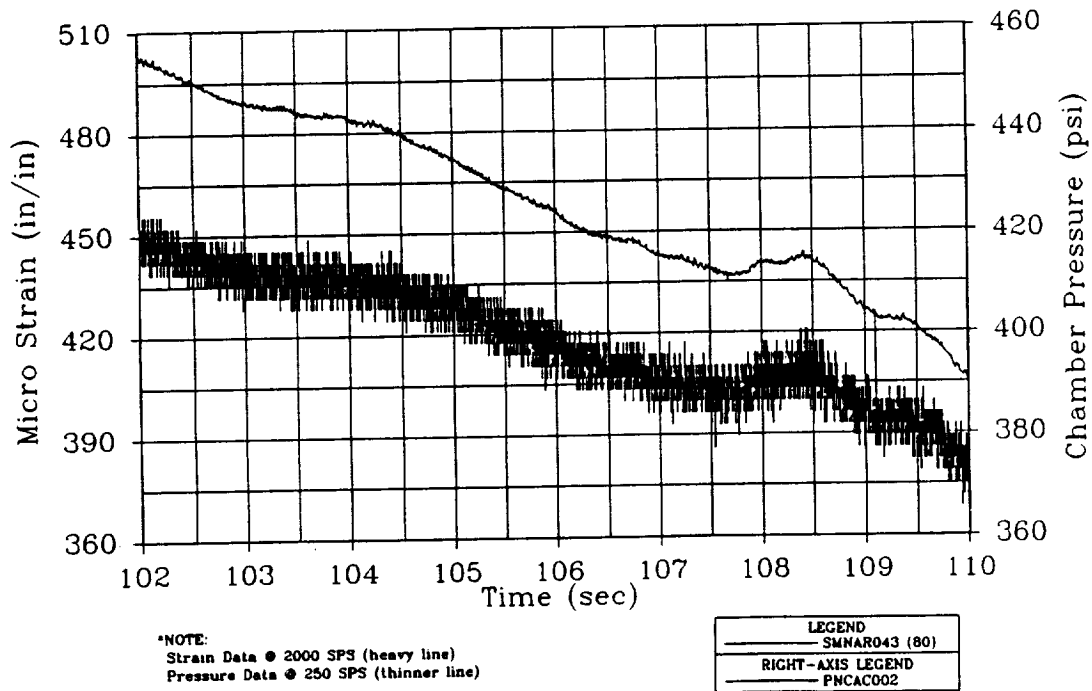


Figure 6-47. Nozzle Fixed Housing Meridional Strain Versus Chamber Pressure at 102-110 sec (80 deg)

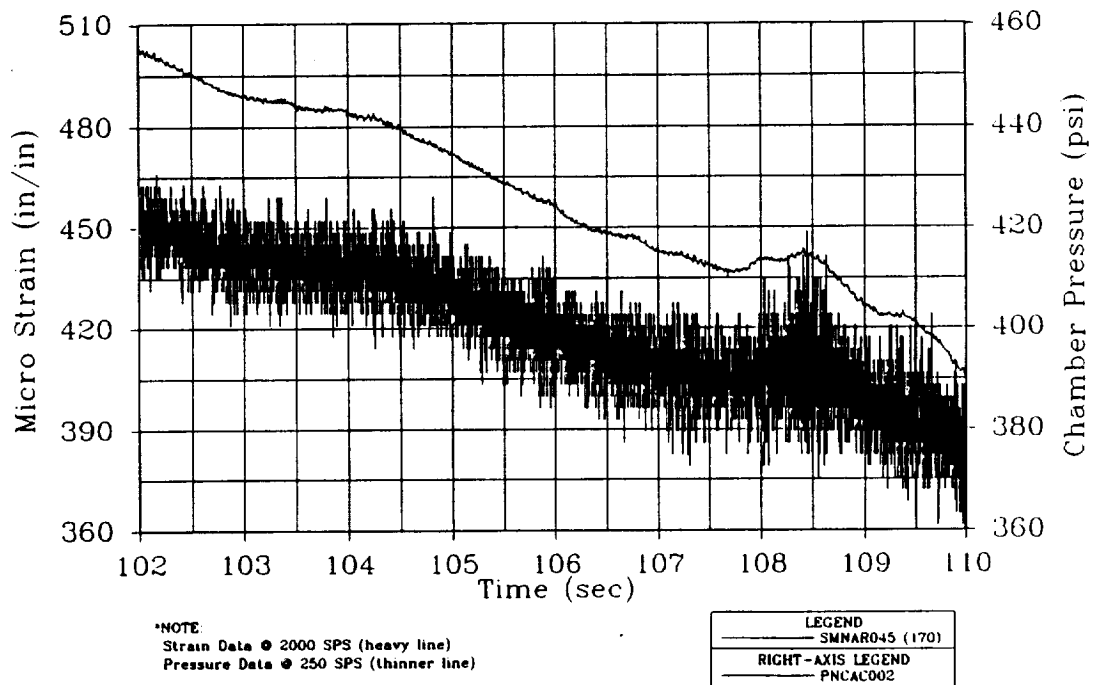


Figure 6-48. Nozzle Fixed Housing Meridional Strain Versus Chamber Pressure at 102-110 sec (170 deg)

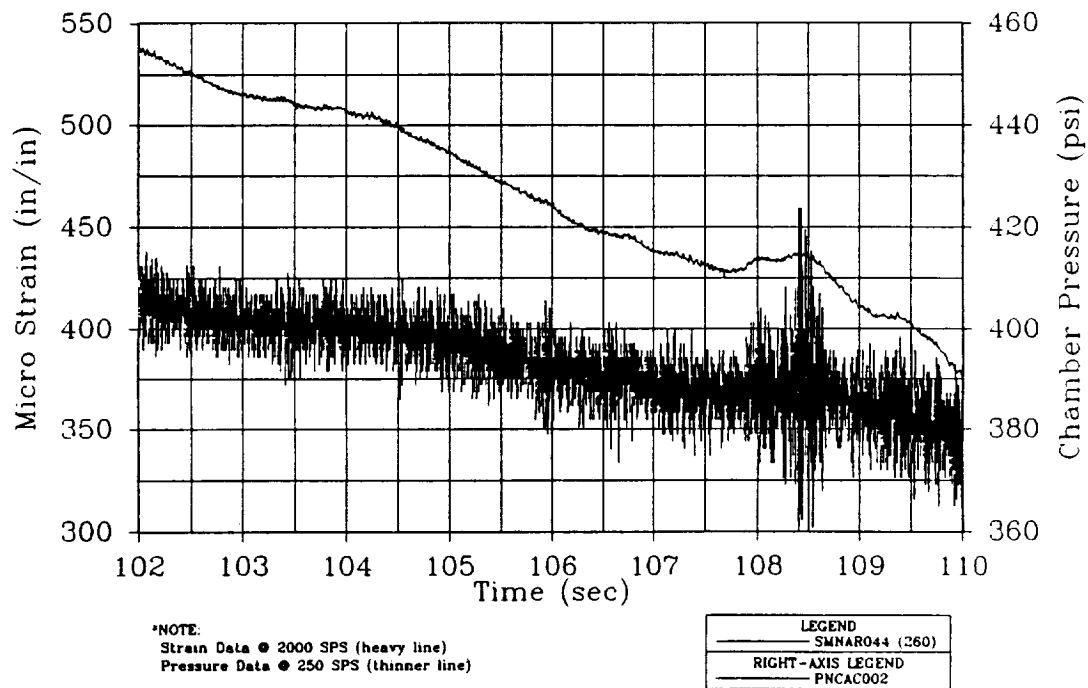


Figure 6-49. Nozzle Fixed Housing Meridional Strain Versus Chamber Pressure at 102-110 sec (260 deg)

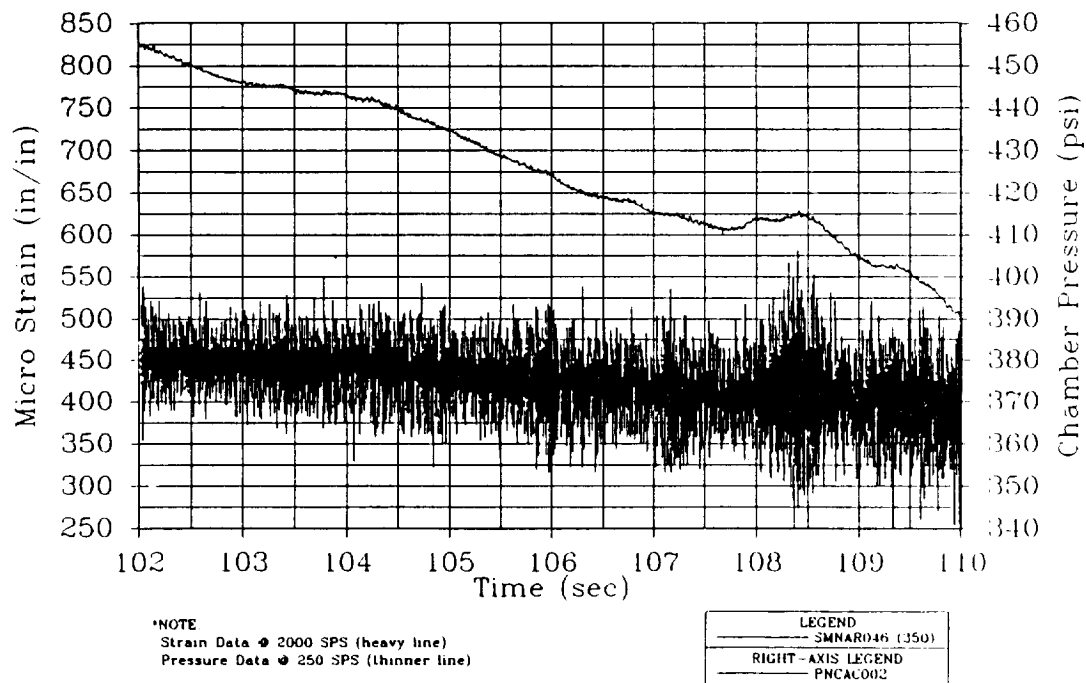


Figure 6-50. Nozzle Fixed Housing Meridional Strain Versus Chamber Pressure at 102-110 sec (350 deg)

6.10.4.3 Accelerometer Correlation to Identified Pressure Events. The accelerometers on the case and nozzle tracked the pressure events very well (Figures 6-51 and 6-52). Frequency waterfall plots for all axial accelerometers on the case and nozzle have been produced and are being studied.

One of the interesting features is the 74- to 75-sec event that excites the entire frequency band, with the largest magnitudes occurring at the higher frequencies on the nozzle (above 400 Hz) (Figure 6-53). This event also shows up in the aft region of the case, but to a lesser extent. Two possible causes for this event are a nozzle impact event and/or internal high-speed eject event.

Timeline of Events--In order to better track and correlate the various events and channel activity, a timeline was constructed (Appendix C). The timeline shows that the 68-69.5-sec and the 74.5-sec event caused a response in almost all of the gages. It also shows the activity to have a periodicity of approximately 1.5 sec.

Accelerometer Analysis--Three accelerometers were installed on the aft center segment to gather standard dynamic vibration data in the three motor axis. These data channels were all nominal. Analysis of the data is included in TWR-63827.

In support of pressure perturbation study, four triaxial accelerometers were installed midway on the case segments and one each uniaxial accelerometer on the forward and aft domes. The following accelerometers were installed on the nozzle: one triaxial on the aft exit cone, six uniaxial on aft exit cone, and six uniaxial on the forward exit cone (TWR-63827). The intent of these measurements was to track any disturbance within the motor. One of these accelerometers (AANAV011) was intermittent during the motor firing.

The accelerometer response tracks the pressure activity well and tends to peak on the up slope of the pressure rise (see Figures 6-51 and 6-52). The maximum accelerometer response occurred on the nozzle with diminishing amplitude forward of the nozzle toward the front end of the motor. The activity was largest at the 0-deg location (closest to the ground) as compared to the 180-deg location.

Since the nozzle accelerometers were more active than the case accelerometers a detailed pressure blip-by-blip comparison to the nozzle accelerometers was made (Figures 6-54 through 6-60). This comparison yielded three possible anomalies. Two of the accelerometer events seem uncharacteristically large as compared to the pressure trace. These occurred at 57.1 and 95.5 sec. The third anomaly occurred at 73.5 sec. At this time there seems to be a small pressure blip that the accelerometers do not respond to. This anomaly occurs just prior to the largest accelerometer response at 74.6 sec.

The frequency content of the accelerometers indicate a broad band of activity during a pressure blip (Figure 6-53 and TWR-63827). The maximum amplitude of this excitation occurs between 200 and 600 Hz.

The nozzle accelerometers responded very well to the pressure events. As a result of the information gathered on TEM-10 it is recommended to continue and expand on the number of nozzle accelerometers used for TEM-11.

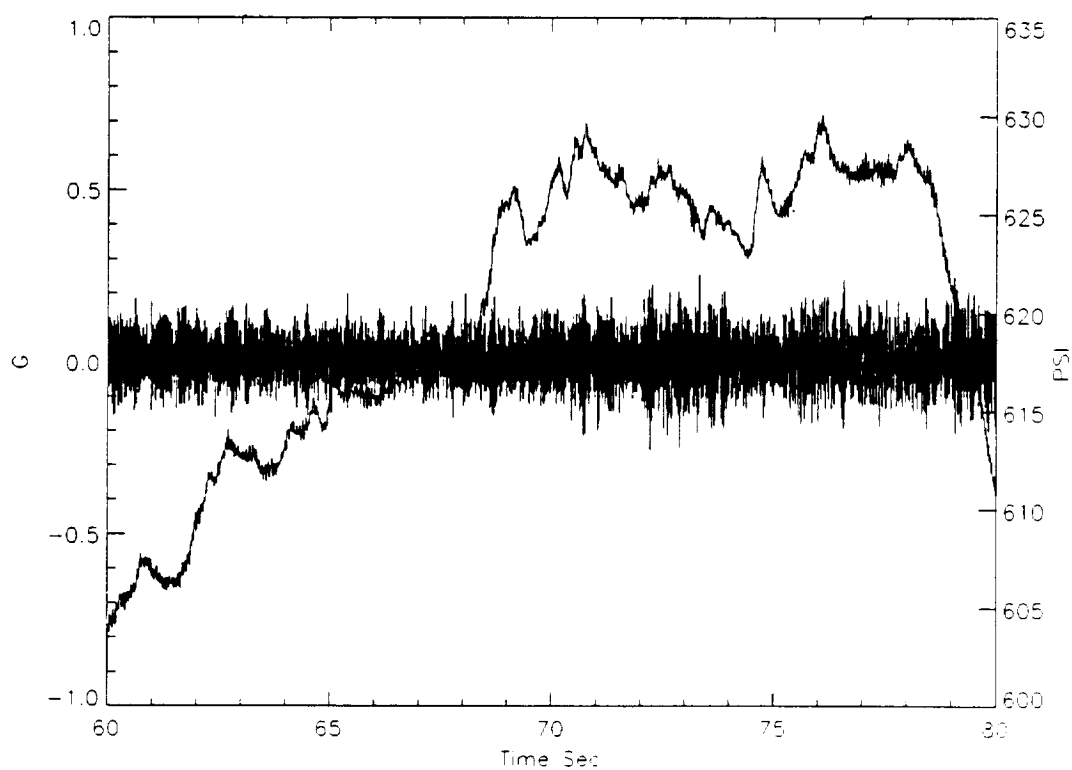


Figure 6-51. Case Accelerometer Versus Pressure (typical)

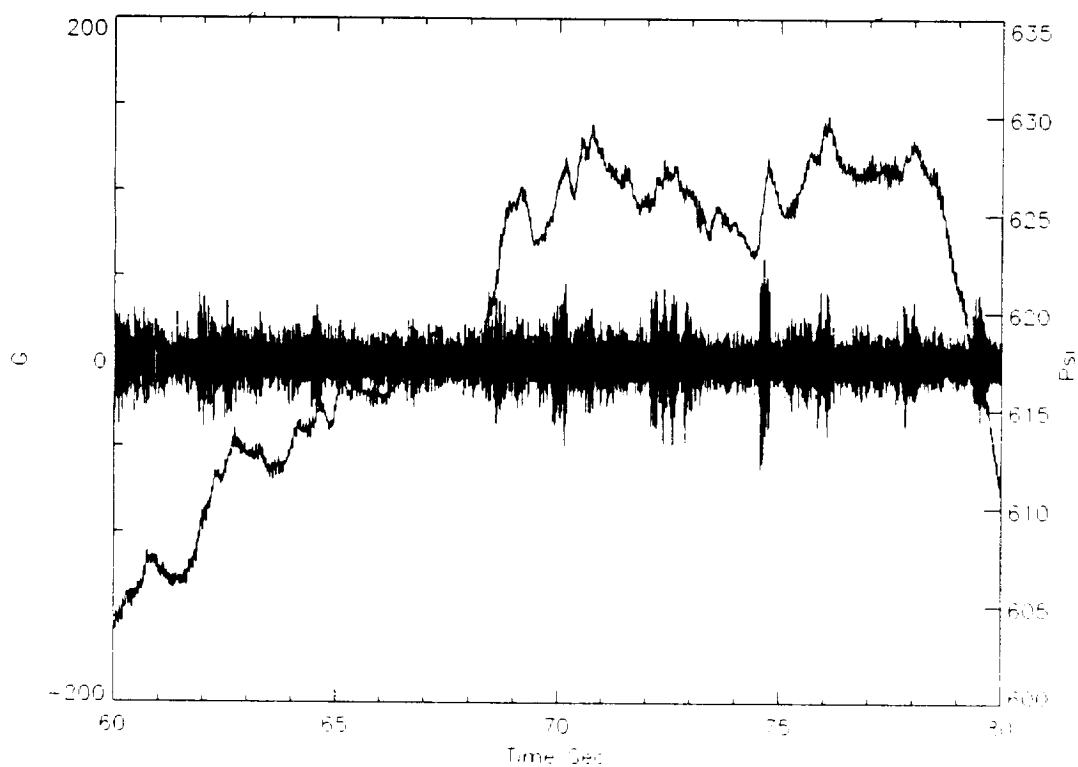


Figure 6-52. Nozzle Accelerometer Versus Pressure (typical)

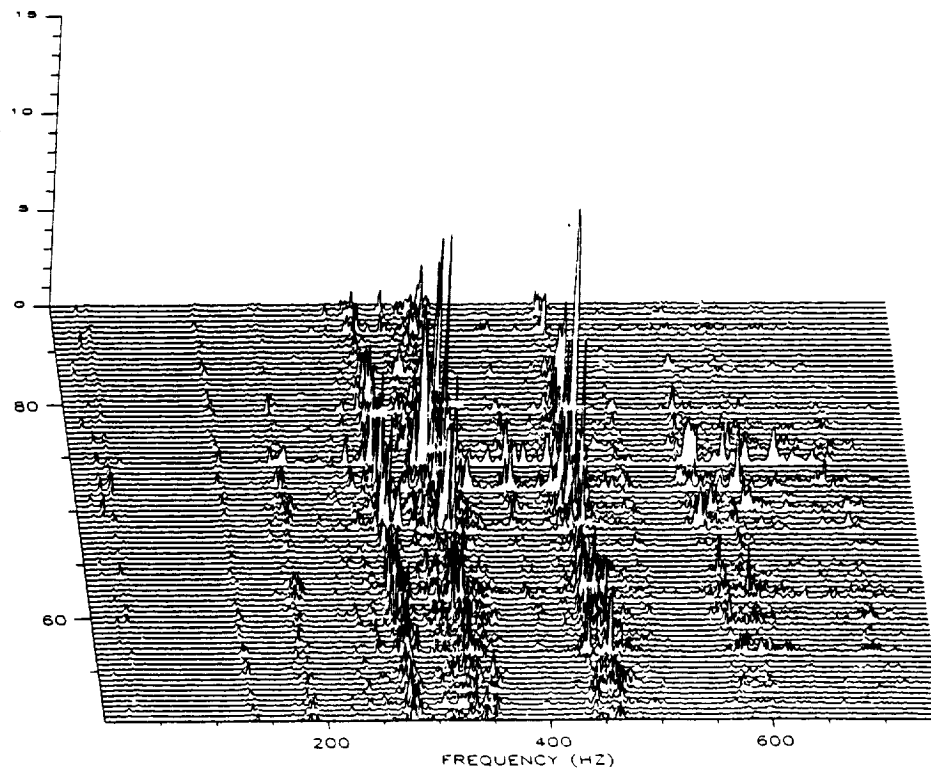


Figure 6-53. Nozzle Accelerometer Waterfall Plot

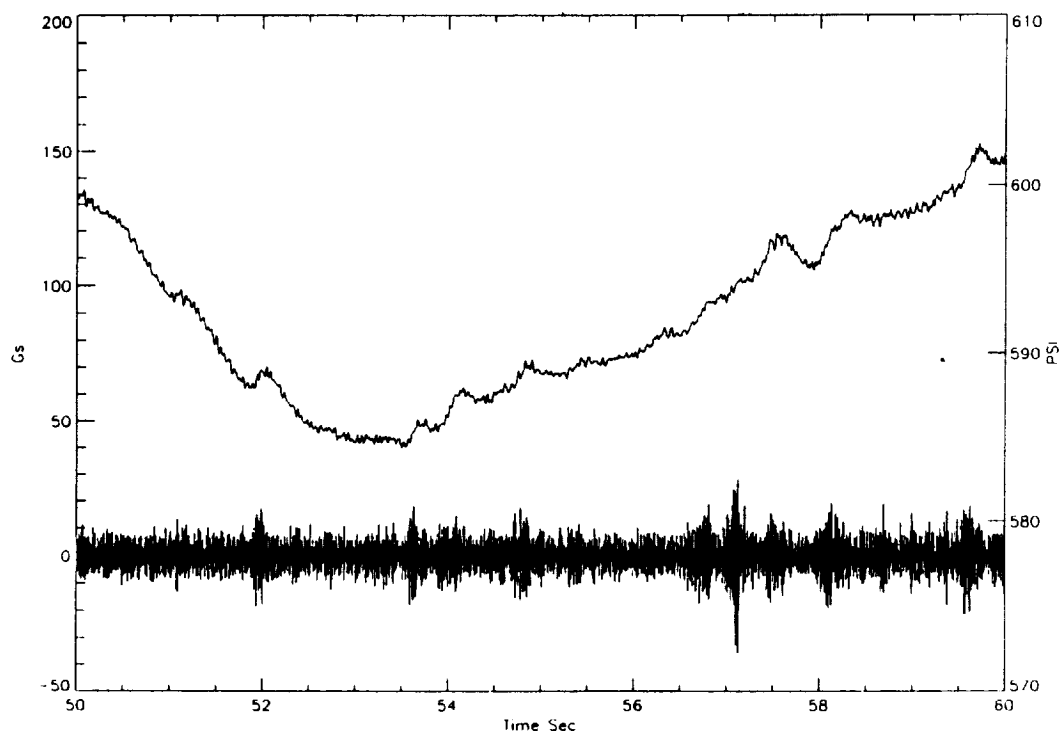


Figure 6-54. Nozzle Accelerometer Compared With Motor Pressure (50-60 sec)

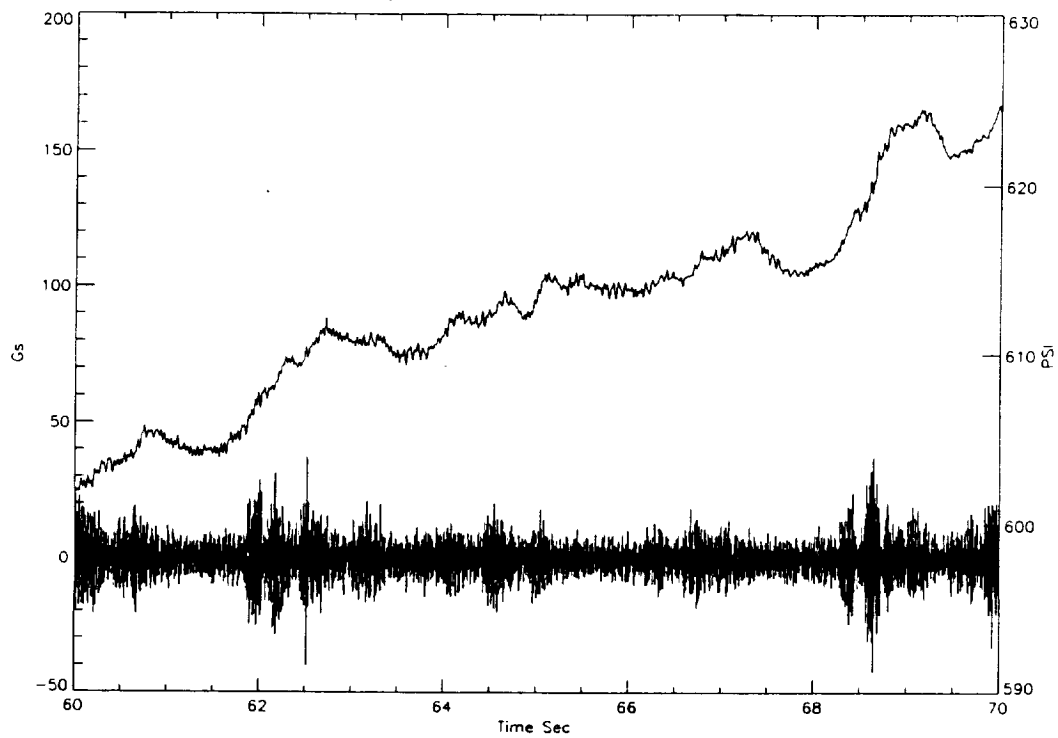


Figure 6-55. Nozzle Accelerometer Compared With Motor Pressure (60-70 sec)

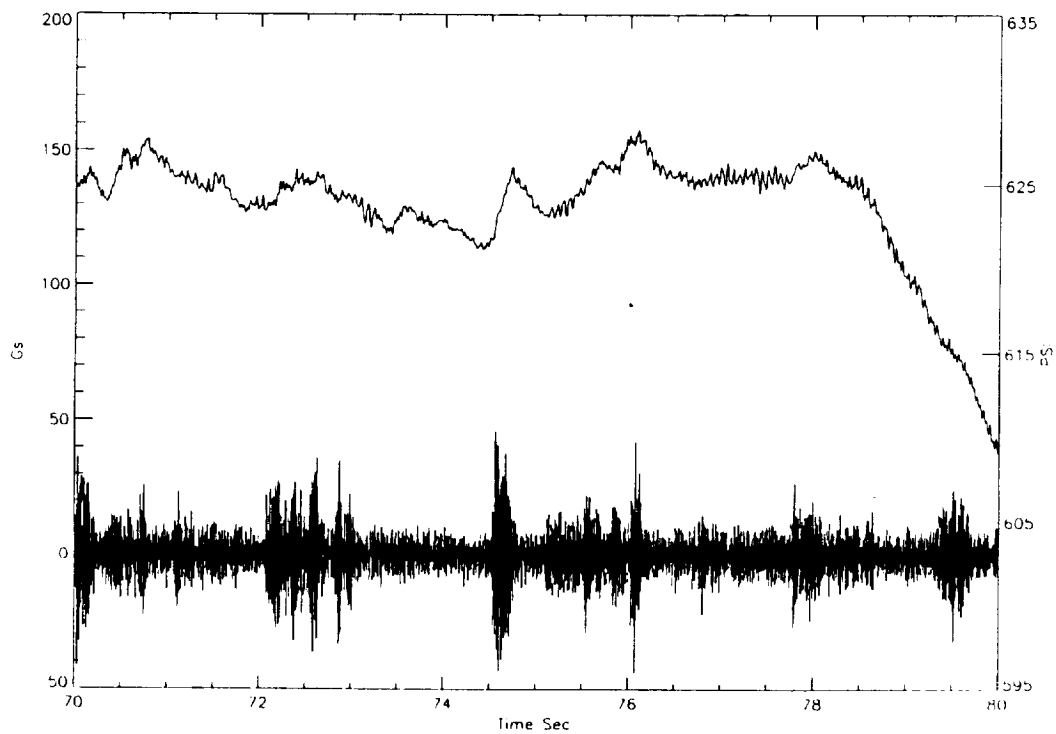


Figure 6-56. Nozzle Accelerometer Compared With Motor Pressure (70-80 sec)

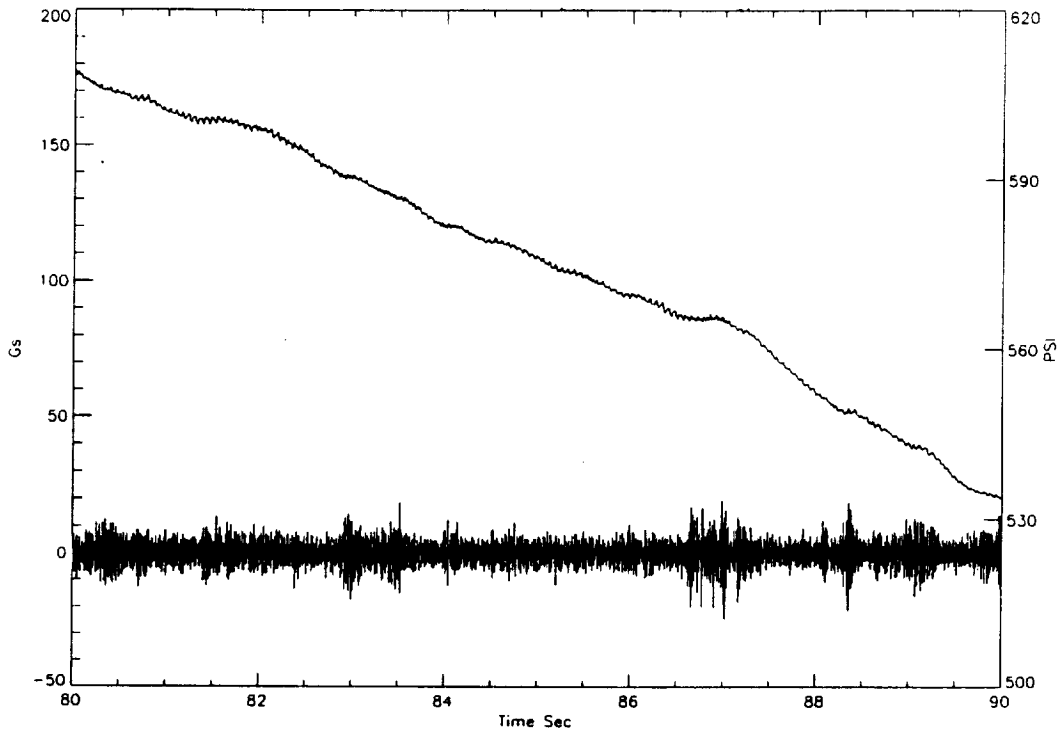


Figure 6-57. Nozzle Accelerometer Compared With Motor Pressure (80-90 sec)

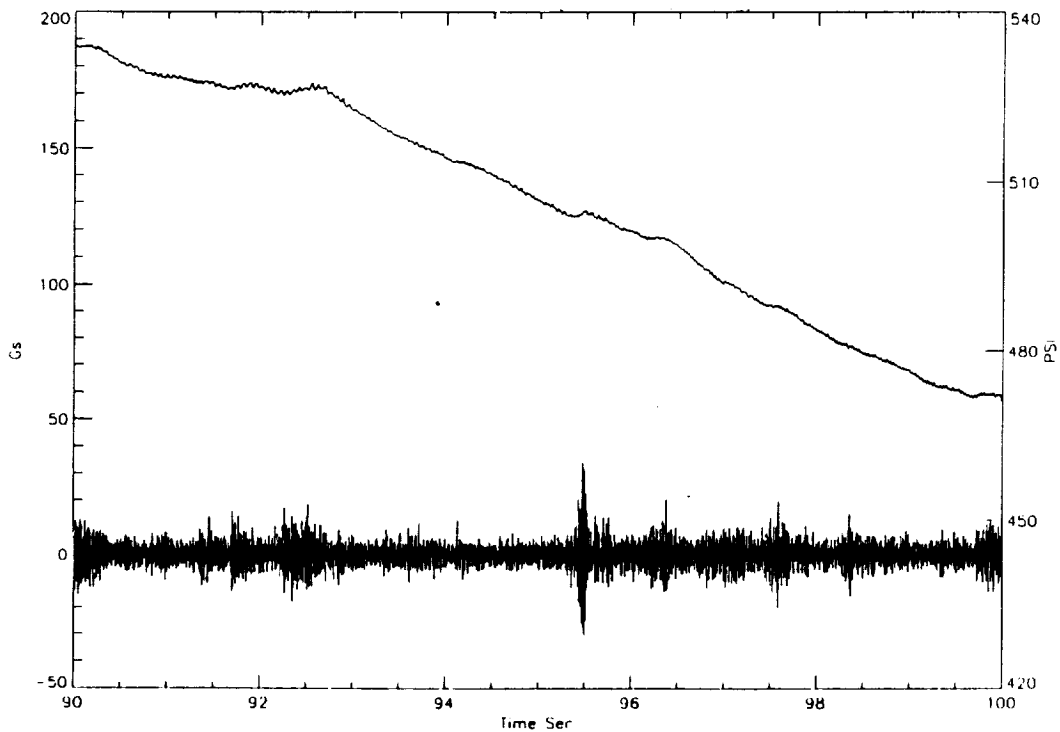


Figure 6-58. Nozzle Accelerometer Compared With Motor Pressure (90-100 sec)

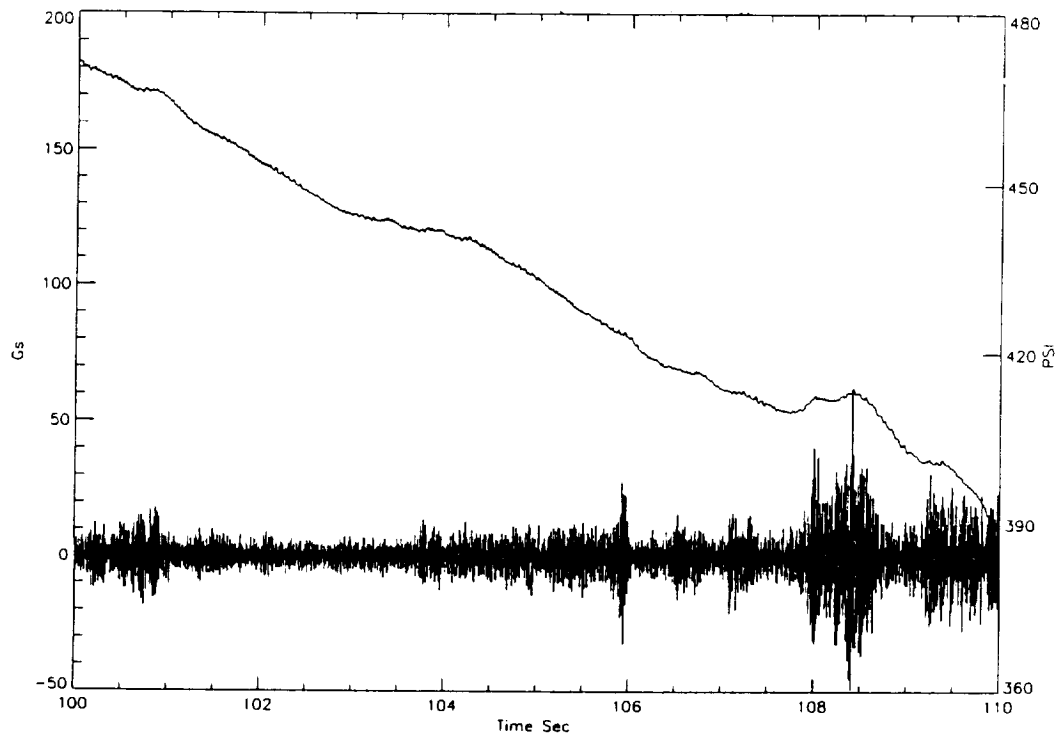


Figure 6-59. Nozzle Accelerometer Compared With Motor Pressure (100-110 sec)

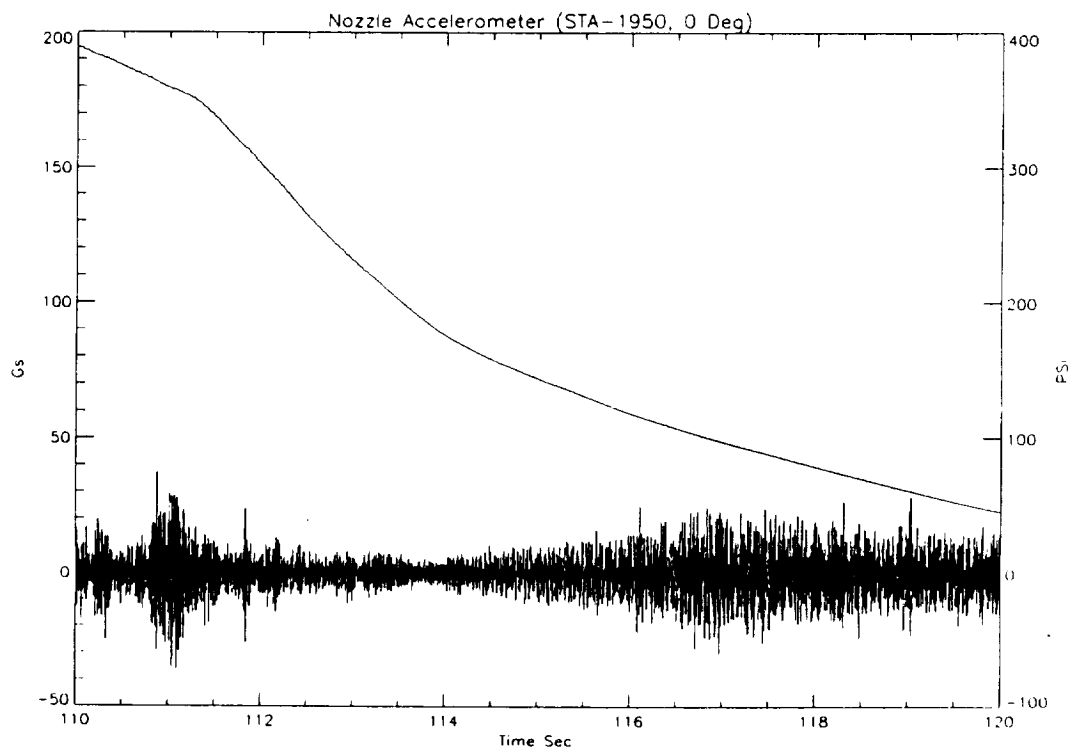


Figure 6-60. Nozzle Accelerometer Compared With Motor Pressure (110-120 sec)

6.10.4.4 RTR Observations. RTR was a beneficial tool for better understanding internal motor operation events. Figure 6-61 shows the RTR configuration for the test.

Figure 6-62 shows the four camera views on the forward joint. These views consist of 1) the upper overall view, 2) the lower overall view, 3) the upper zoomed view, and 4) the lower zoomed view. The first forward field joint castable inhibitor movement began at approximately 50 sec into the burn. At this time, The castable inhibitor bent across the slot toward the NBR inhibitor. It is clear that the inhibitors were not in contact from 80 sec to the end of the burn (approximately 120 sec).

Figure 6-63 shows the two camera views on the aft dome factory joint region. The slag motion first occurred as a swirling motion in the lower camera region at 49 sec. Slag motion continued from this time until motor depressurization. At depressurization, the slag began to settle into pools.

In the upper camera viewing area, slag motion first appeared at approximately 68 sec. The propellant burned completely out of the upper camera view at 77 sec. From 107 sec to the end of burn, slag moved through the upper camera area.

Perceptics Corporation of Salt Lake City, Utah, performed a standard deviation calculation on intensity to give a numerical value to approximate amount of slag/slag activity with respect to time from the RTR digitized data. These data were plotted with the calorimeter data in Figures 6-64 and 6-65 for the lower view and upper view, respectively. Figures 6-66 and 6-67 show the data of regions of interest between 70 and 80 sec and between 104 and 114 sec, respectively. Figures 6-68 and 6-69 show the upper view RTR data more closely. Clearly there is more activity at the T+74- and T+108-sec timeframes in the upper RTR which was picked up in the radiometer and calorimeter data.

Looking at the frequency content of the upper view and lower view standard deviation RTR data (Figures 6-70 and 6-71), radiometer/calorimeter data (Figure 6-72) and the pressure data (Figure 6-73) the same build up of the 0.5 Hz content is noticed. This indicates that the slag motion in the submerged region, the motor pressure, and the heat flux to the radiometer/calorimeter are all closely interrelated.

Aft-End RTR Slag Movement Analysis--Part of the post-test analysis of the aft RTR included image enhancements performed by Perceptics Corporation (TWR-63827). Part of their analysis included using statistical modeling to better quantify increased slag movement activity. See Figures 6-74 and 6-75 for the upper and lower views, respectively.

The lower RTR showed significantly more slag activity than the upper RTR (Figures 6-74 and 6-75). Both of the views showed a significant event around the 73-76-sec timeframe (Figure 6-76). During this time the upper view peaked at around 73 sec and the lower view peaked at around 75.4 sec. Another timeframe of interest occurred between 102 and 114 sec (Figure 6-77). During this time both views again showed an increase in activity.

The data reduction that Perceptics performed was very beneficial in showing the slag activity. It is recommended that a similar analysis be performed on future RTR activity.

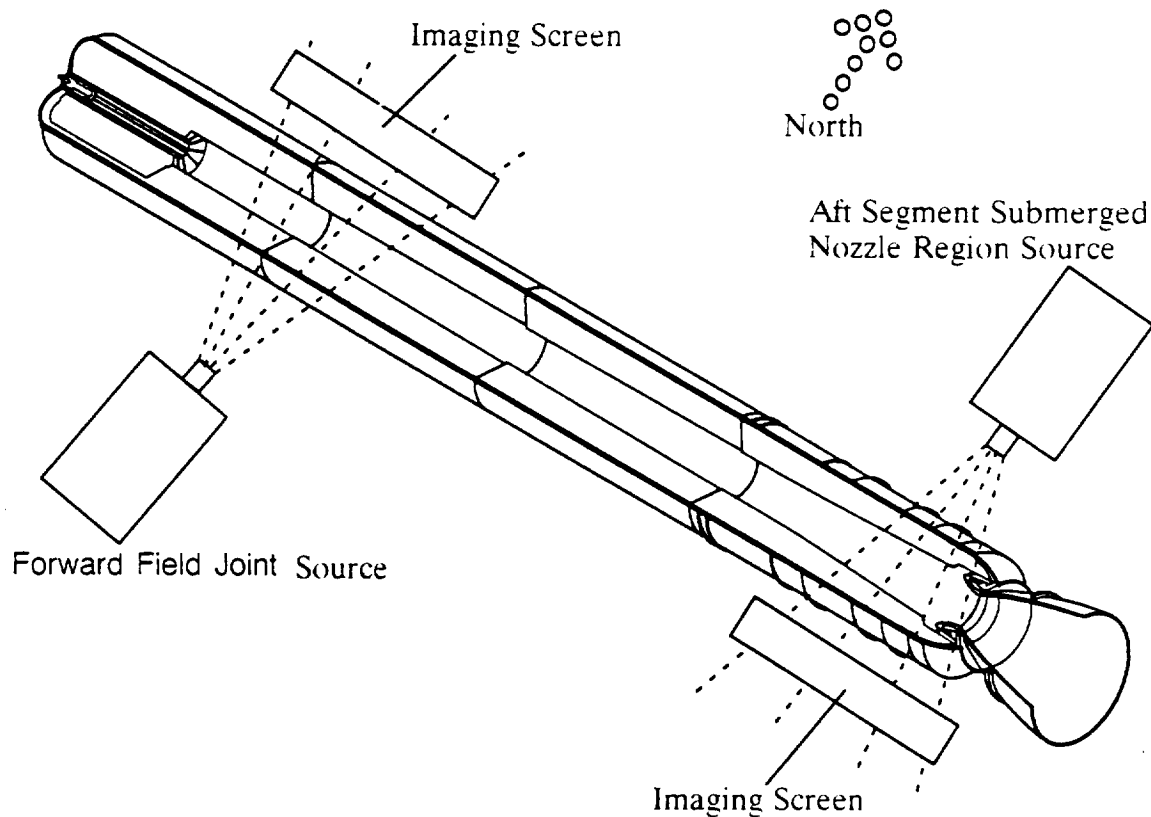


Figure 6-61. RTR Locations

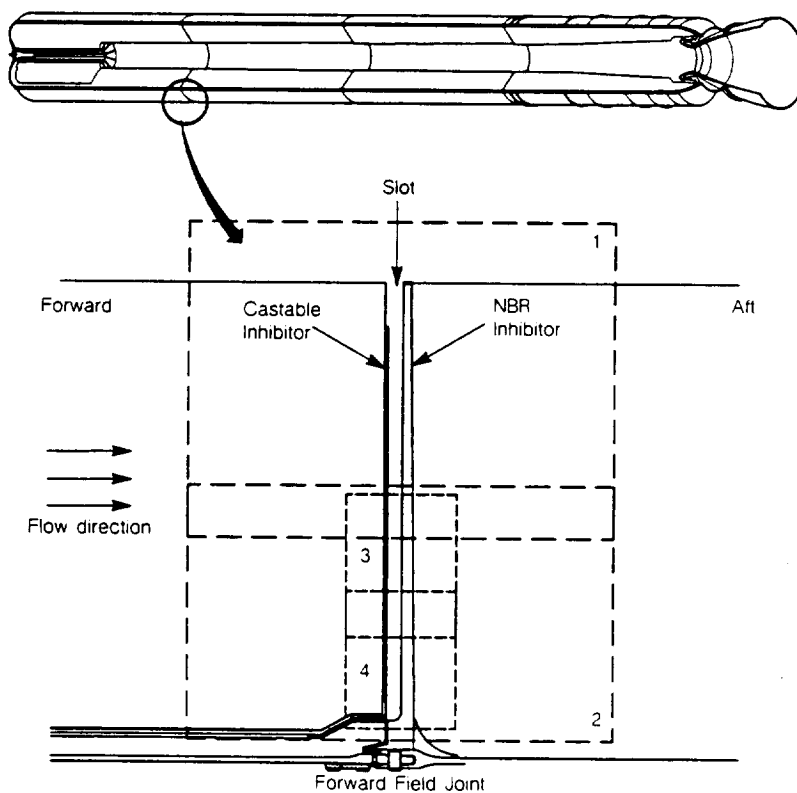


Figure 6-62. Forward Field Joint

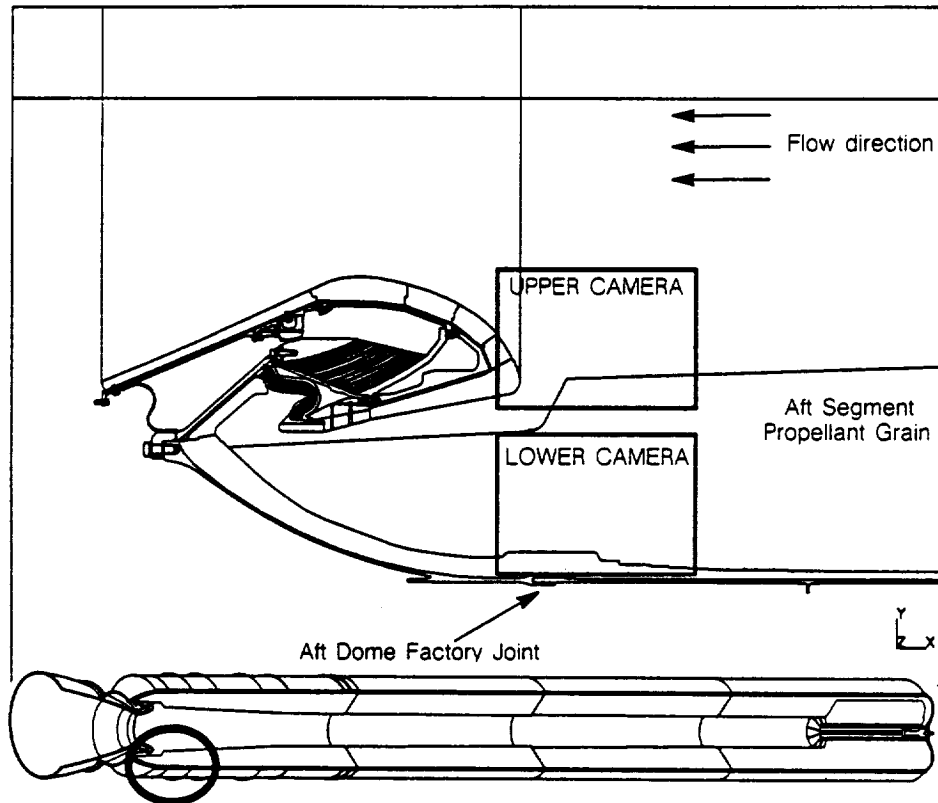


Figure 6-63. Aft Dome Factory Joint

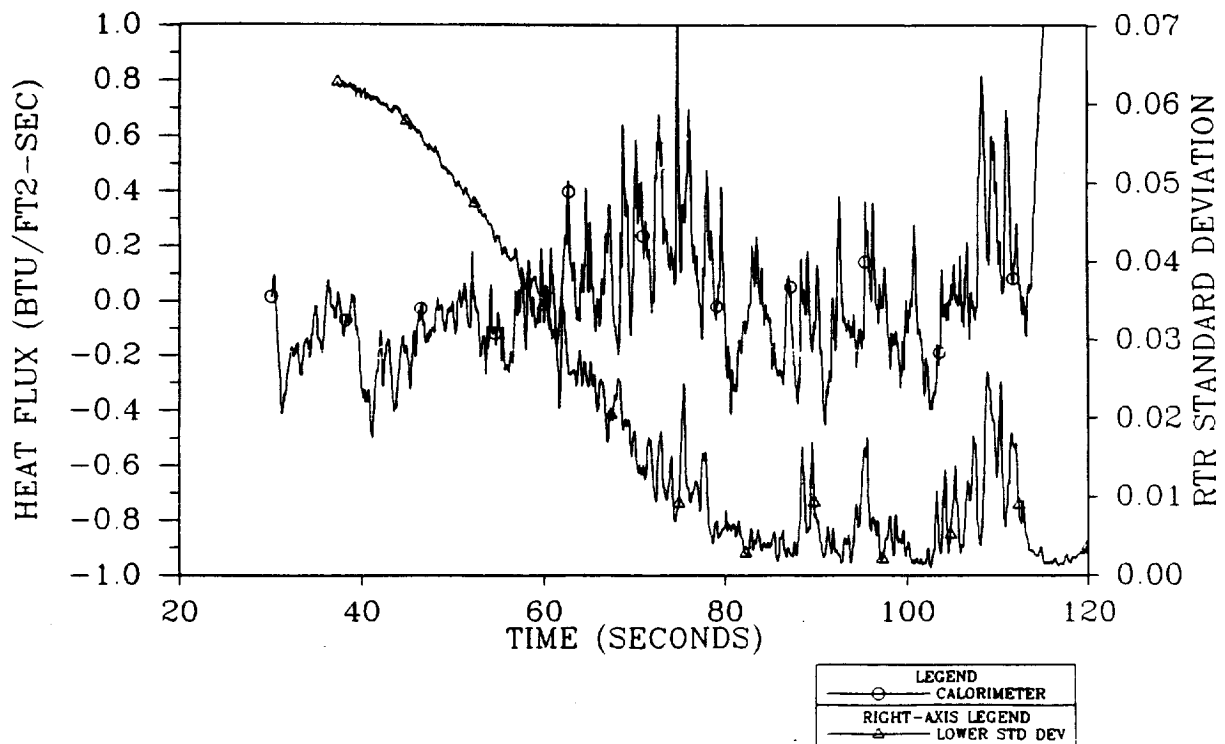


Figure 6-64. Lower View RTR Data Plotted With Calorimeter Data (20-120 sec)

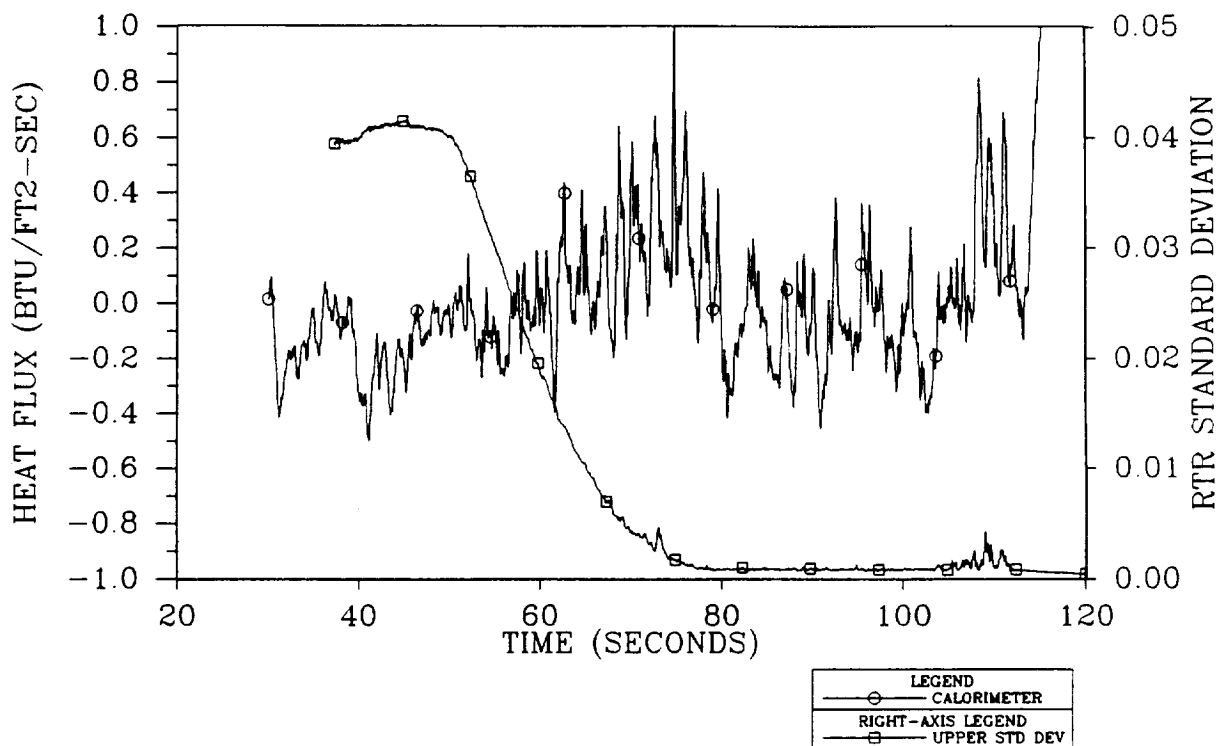


Figure 6-65. Upper View RTR Data Plotted With Calorimeter Data (20-120 sec)

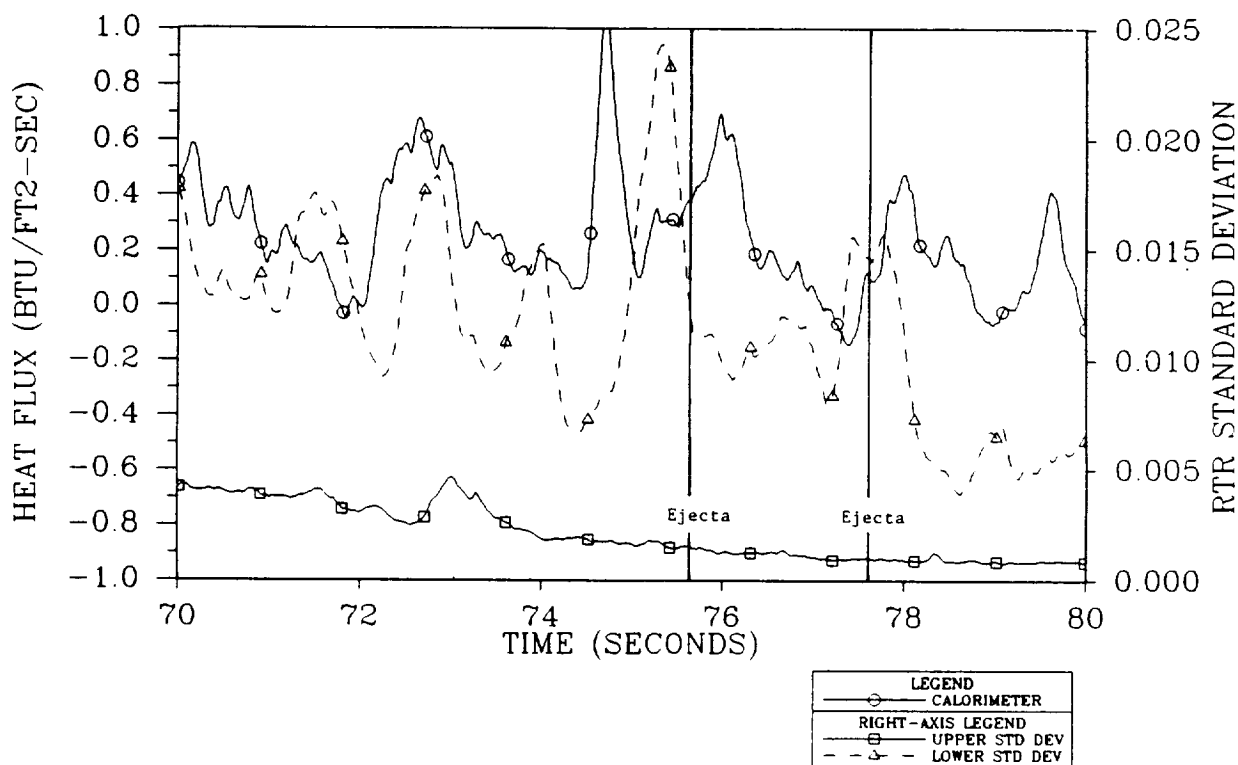


Figure 6-66. Upper and Lower RTR Data Plotted With Calorimeter Data (70-80 sec)

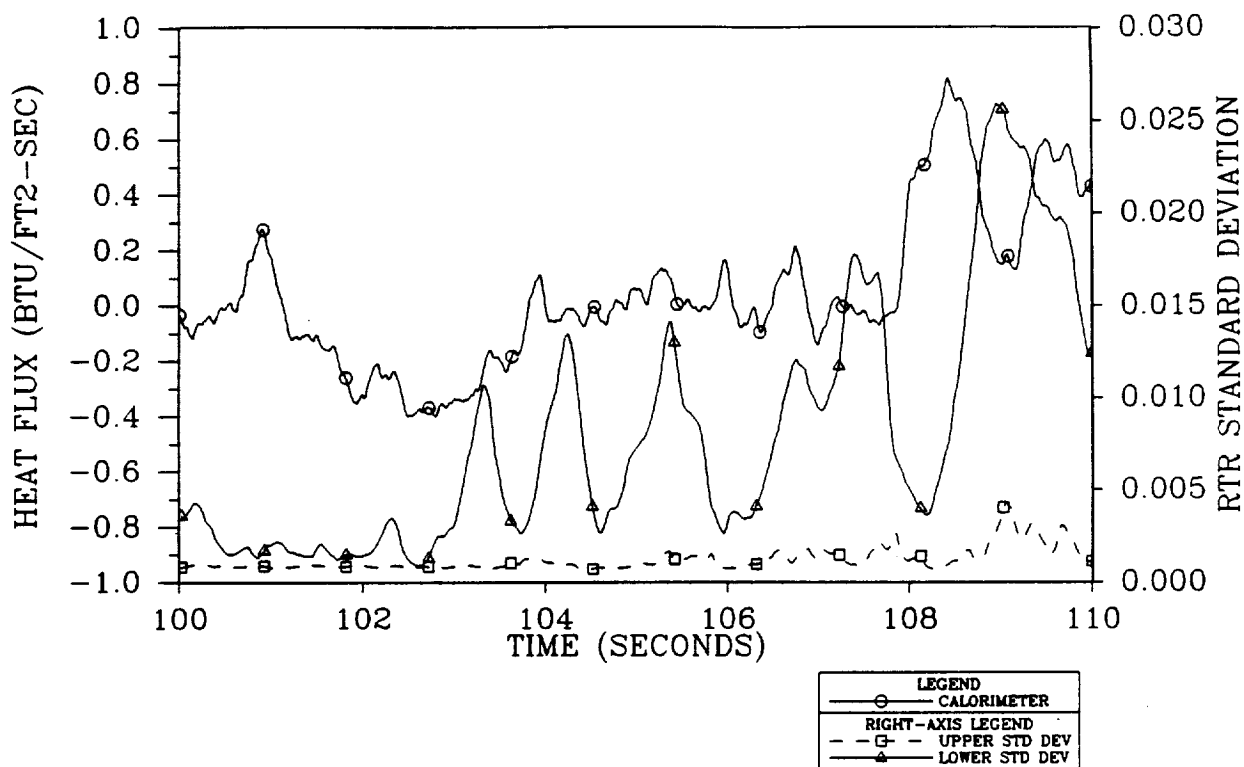


Figure 6-67. Upper and Lower RTR Data Plotted With Calorimeter Data (104-114 sec)

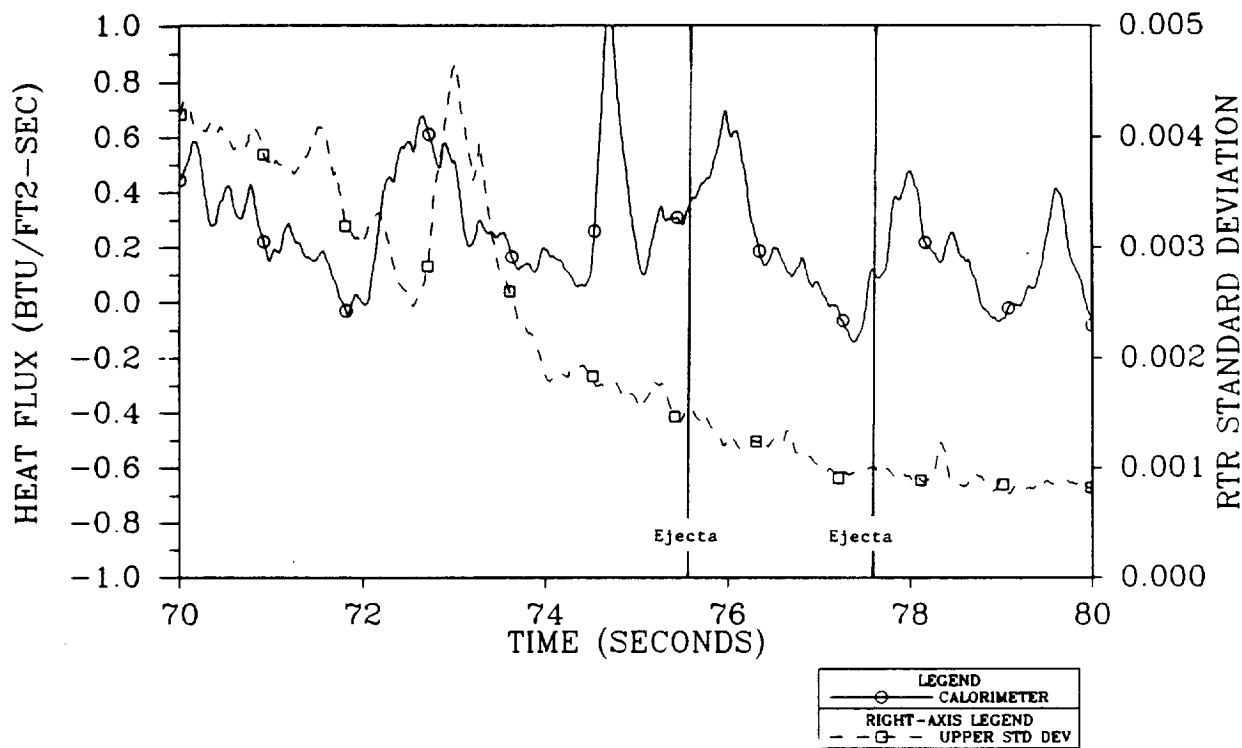


Figure 6-68. Upper RTR Data Plotted With Calorimeter Data (70-80 sec)

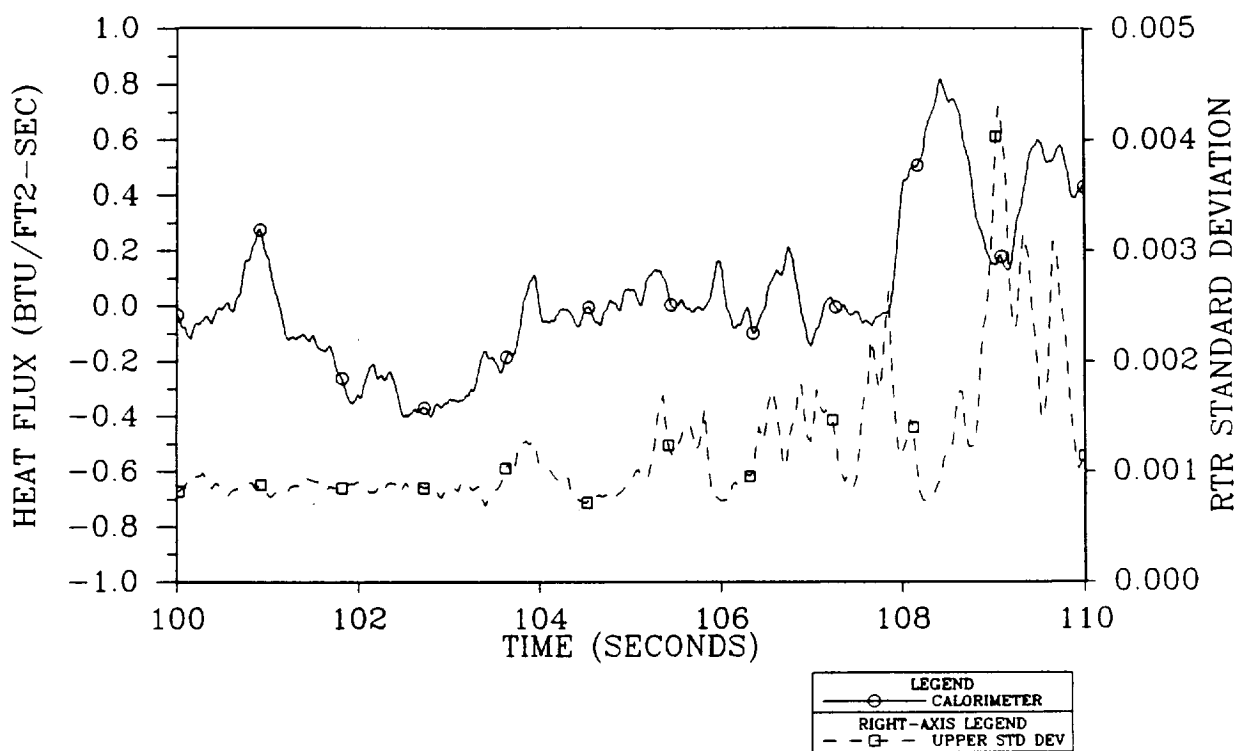


Figure 6-69. Upper RTR Data Plotted With Calorimeter Data (104-114 sec)

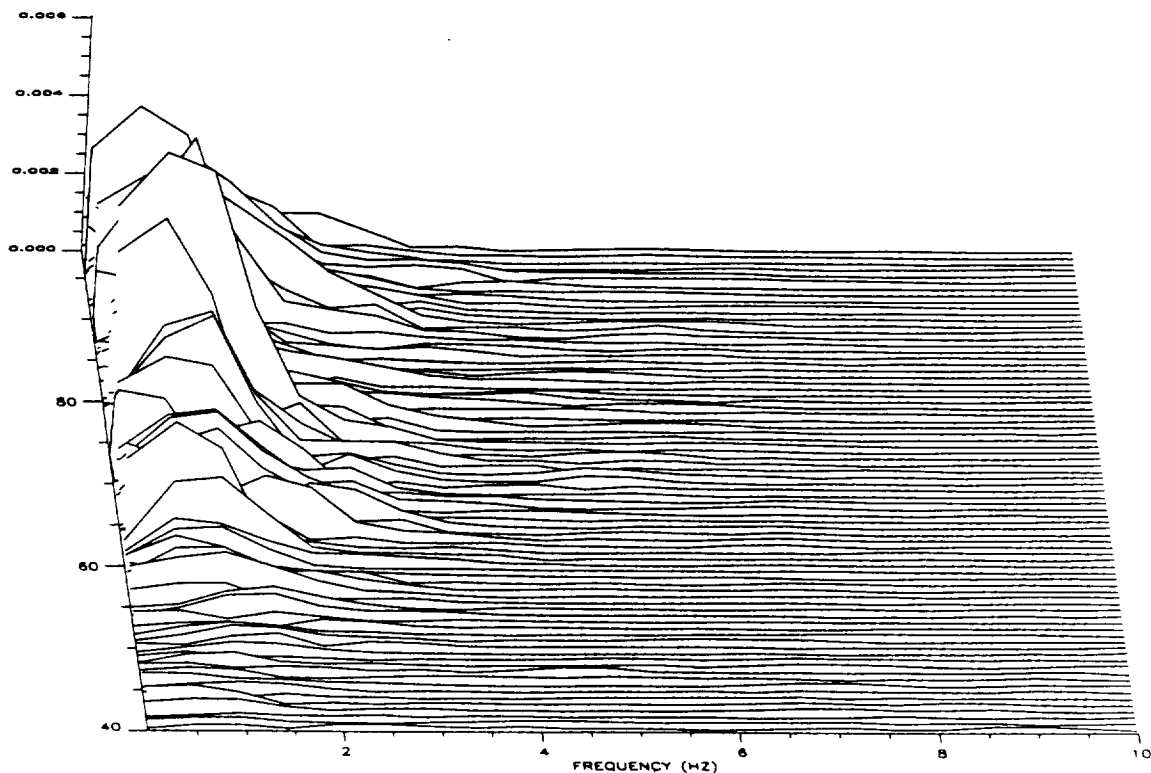


Figure 6-70. Lower RTR Waterfall Plot

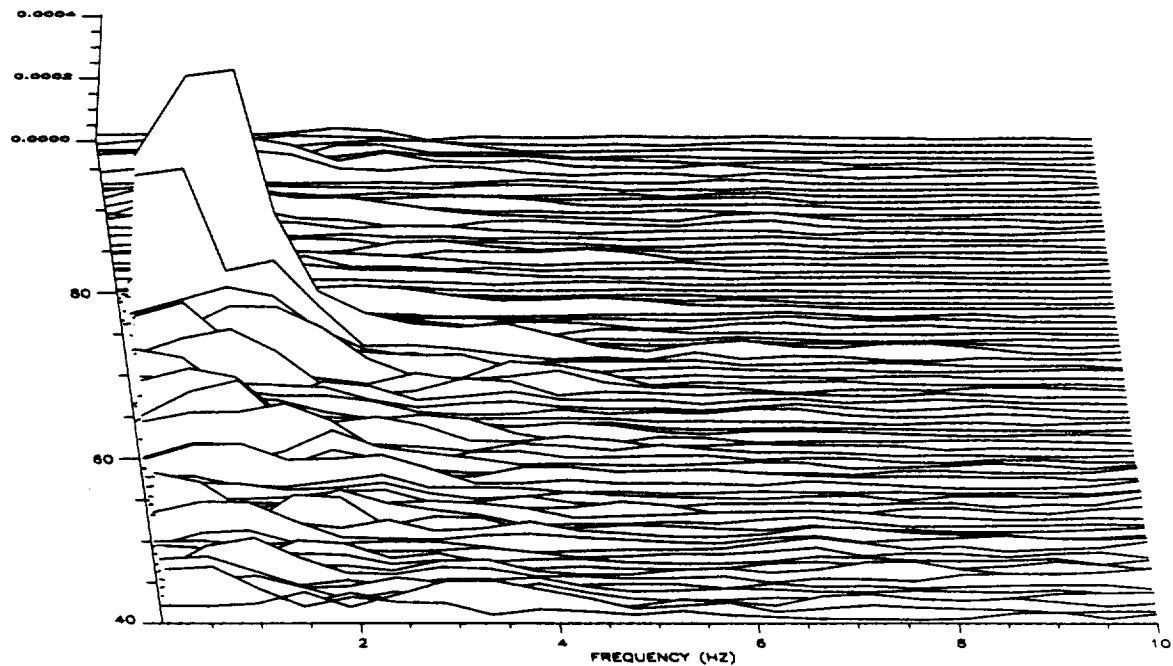


Figure 6-71. Upper RTR Waterfall Plot

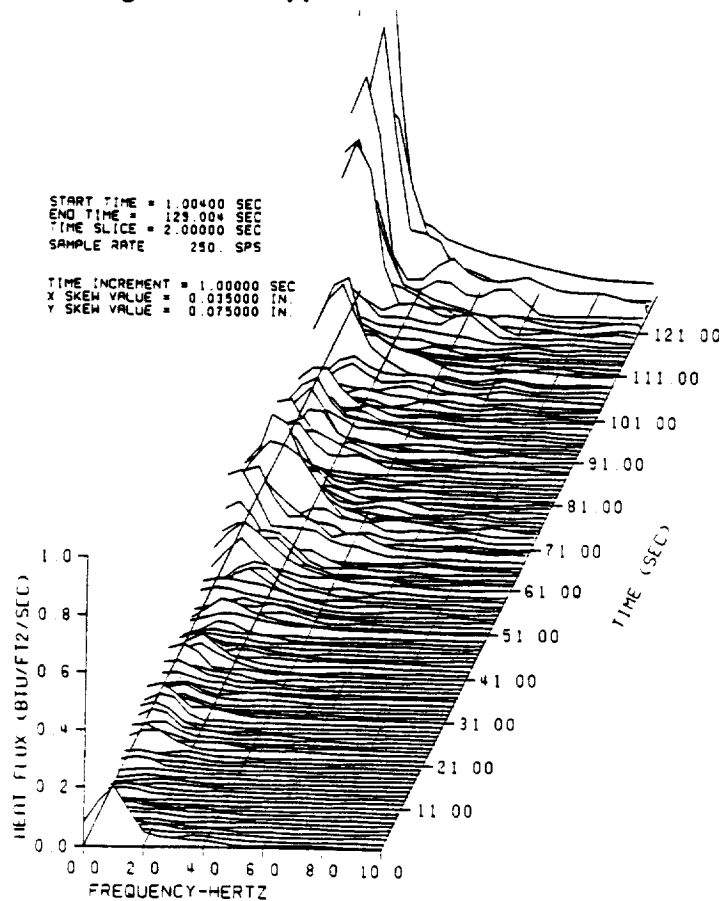


Figure 6-72. Calorimeter/Radiometer Waterfall Plot

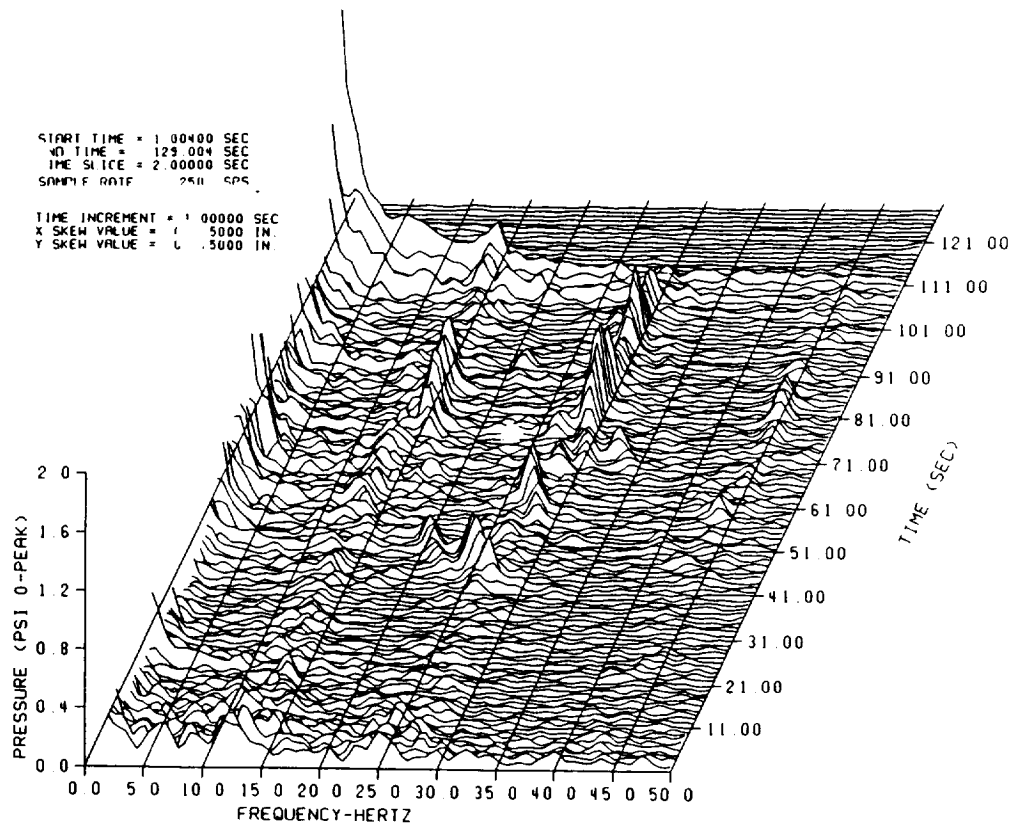


Figure 6-73. Motor Pressure Waterfall Plot

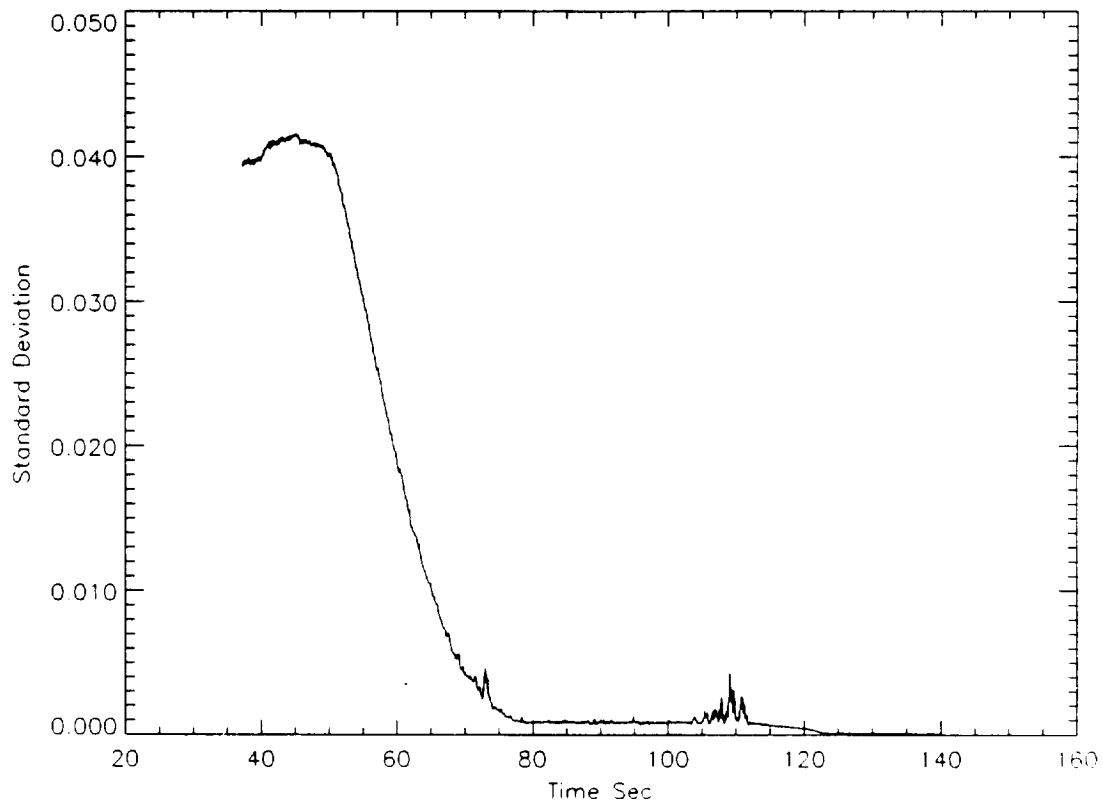


Figure 6-74. Upper RTR Slag Movement Activity

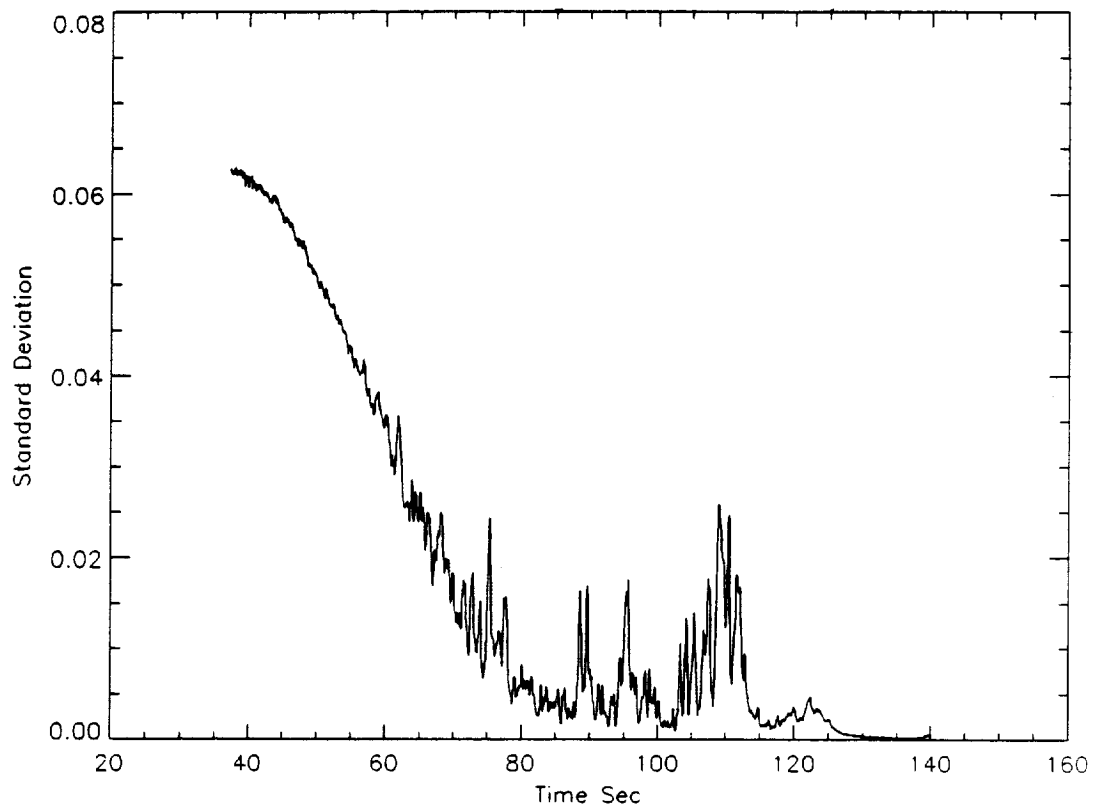


Figure 6-75. Lower RTR Slag Movement Activity

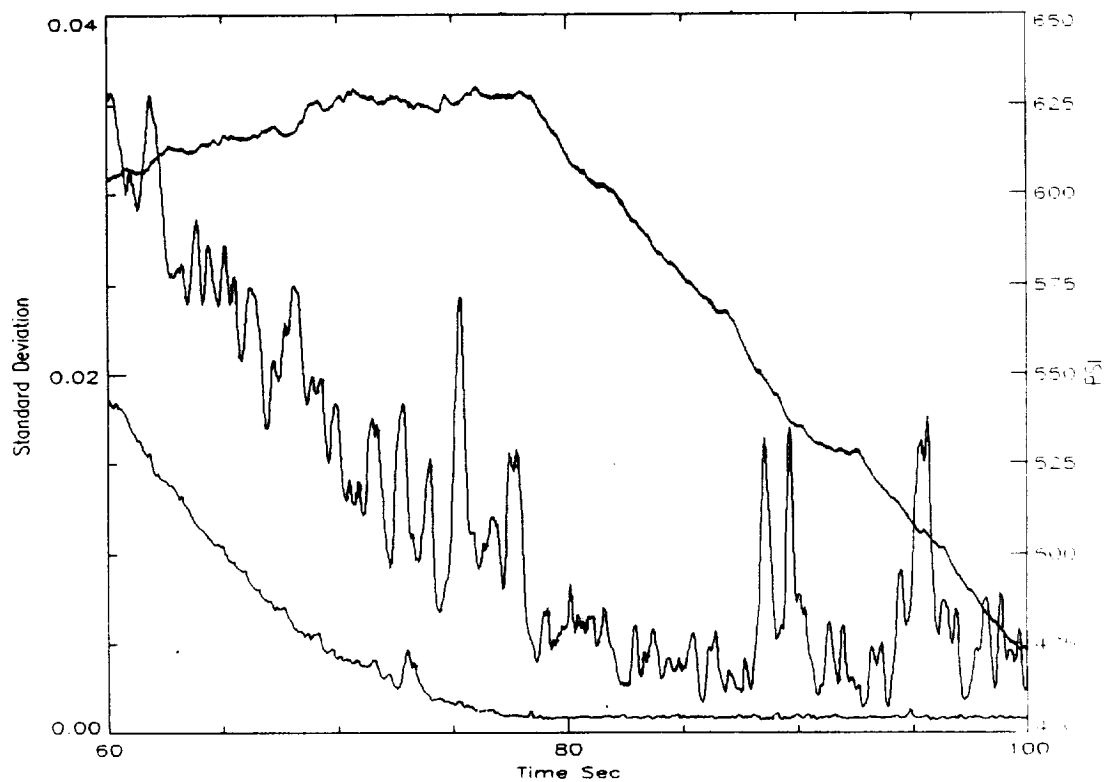


Figure 6-76. RTR Slag Movement Data (60-100 sec)

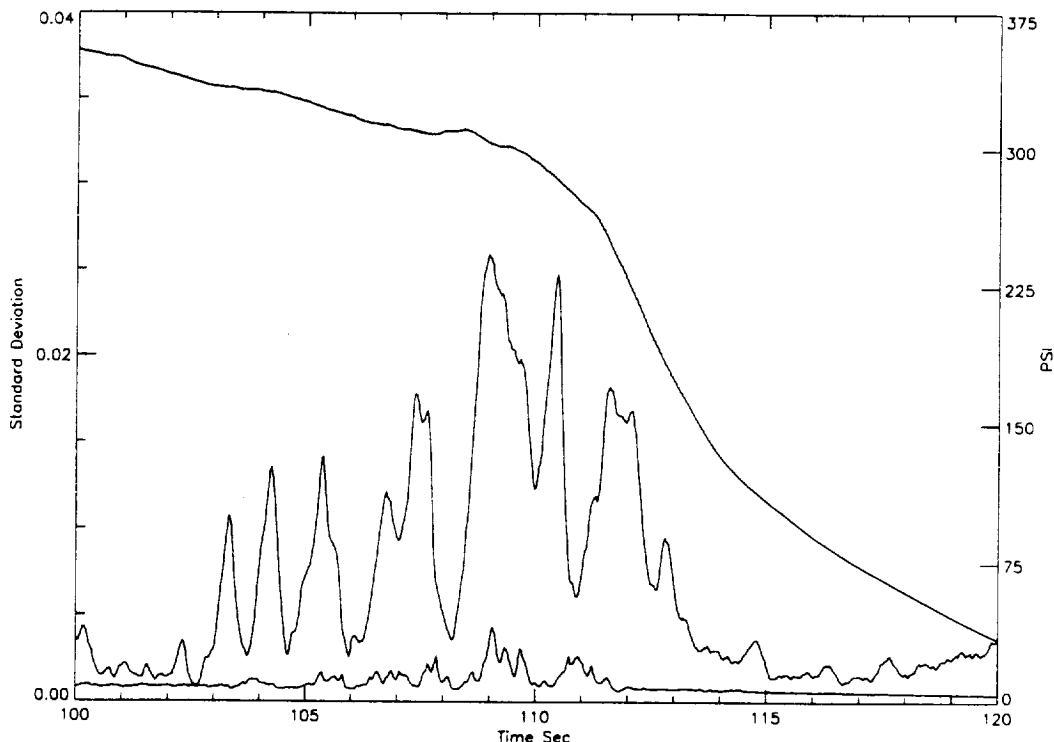


Figure 6-77. RTR Slag Movement Data (100-120 sec)

6.11 STATIC TEST SUPPORT EQUIPMENT

6.11.1 Introduction

The deluge system performed adequately with no indication of excessive case heating. No unusual or unexpected temperatures were recorded during or after the static motor test. The final PMBT at the time of motor firing (13:49 on 27 April 1993) was 69°F.

6.11.2 Objectives/Conclusions

There are no objectives from Section 2 concerning static test support equipment.

6.11.3 Recommendations

None.

6.11.4 Results/Discussion

This section documents the operation of the deluge system, the case temperature summary, and the nozzle region heat soak histories.

6.11.4.1 Deluge System Operation. The deluge system performed as expected as far as can be determined at this time. No hardware was lost due to heat soak from the aluminum oxide slag. The deluge system instrumentation showed no anomalous data prior to, during, or following motor operation.

6.11.4.2 Case Temperature. The initial TEM-10 case temperature was 50°F with a maximum case temperature of 196° F recorded 7.7 minutes after motor ignition (Figure 6-78). Figure 6-79 shows the peak minus initial case temperature versus slag weight for several static motor firings. Only those test motors fired since the redesign of the deluge system are included.

6.11.4.3 Nozzle Region Heat Soak Histories. The long-term heat soak effect was measured at the nozzle-to-case joint and at the fixed housing locations. Table 6-11 shows the maximum temperature increases, their times of occurrence, and T+8 hour temperature readings for these two locations. Fixed housing instrumentation was added as a result of postfire debond concerns resulting from heat soak. Both measurement locations were on the external surface of structural component surfaces. Temperature response data were consistent at each station. A database is being developed to include this postfire temperature response data which will aid in identifying unusual nozzle component temperature responses.

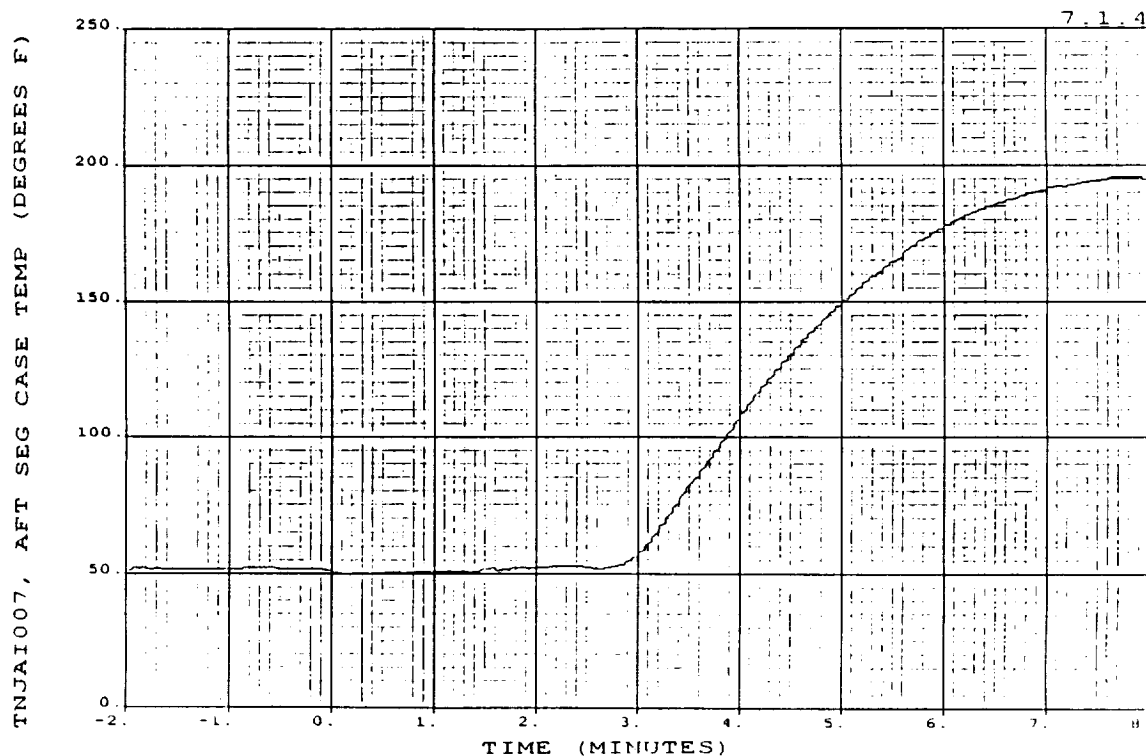
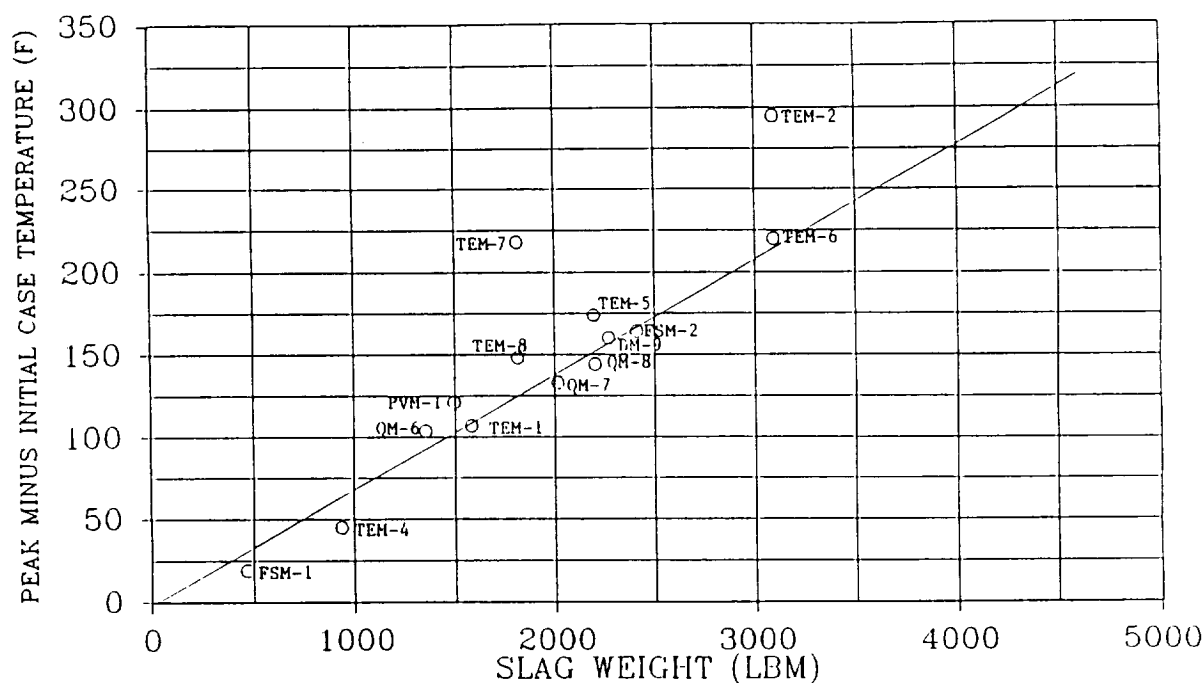


Figure 6-78. Maximum Case Temperature Versus Time



*NOTE: PREDICTED WORST CASE SLAG WEIGHT IS 4800 LBM

Figure 6-79. Maximum Case Temperatures Versus Slag Weight

Table 6-11. TEM-10 Nozzle Component Postfire Heat Soak Data

| Nozzle Component/ Sensor ID | Station | Angle | Temperatures (°F) | | | | Time of Maximum Temperature Peak (hr) |
|--------------------------------|---------|-------|-------------------|---------|-------|--------|---|
| | | | Initial | Maximum | Delta | T+8 hr | |
| Nozzle-to-Case Joint | | | | | | | |
| TNNAR070 | 1876.60 | 0 | 78 | 117 | 39 | 90 | 2.15 |
| TNNAR071 | 1876.60 | 120 | 77 | 116 | 39 | 89 | 2.10 |
| Fixed Housing | | | | | | | |
| TNNAR075 | 1841.25 | 0 | 75 | 215 | 140 | 80 | 0.65 |
| TNNAR076 | 1841.25 | 90 | 78 | 210 | 132 | 94 | 0.67 |
| TNNAR077 | 1841.25 | 180 | 78 | 200 | 122 | 95 | 0.60 |
| TNNAR078 | 1841.25 | 270 | 77 | 198 | 121 | 93 | 0.63 |

11/11/11

7 / APPLICABLE DOCUMENTS

The latest revision of the following documents, unless otherwise specified, are applicable to the extent specified herein.

| <u>Drawings</u> | <u>Title</u> |
|-----------------|---|
| 1U50088 | Housing, Nozzle--Fixed |
| 1U50159 | Plug, Leak Check Port, Nozzle |
| 1U50188 | Transducer, Motional Pickup Pressure |
| 1U50543 | Segment, Rocket Motor, Center--Thermal Protection |
| 1U50532 | Exit Cone Assembly, Forward Section |
| 1U50717 | Case Segment, Cylinder--Lightweight |
| 1U51055 | Pin Straight Headless |
| 1U51899 | Retainer, Pin Field Joint, SRM |
| 1U52501 | Stiffener Ring, Insulated |
| 1U52565 | Segment, Rocket Motor, Forward--Thermal Protection |
| 1U52566 | Segment, Rocket Motor, Center--Thermal Protection |
| 1U52568 | Segment, HPM, Loaded, Aft |
| 1U52840 | Flex Bearing Assembly |
| 1U75801 | Packing, Lubricated |
| 1U76034 | Bolt, Case-to-Nozzle |
| 1U76425 | Adjustable Vent Port Plug |
| 1U76778 | Exit Cone Assembly, Aft-Modified |
| 1U77075 | Cable Assembly, Special Purpose, Electrical, Branched--Systems Tunnel |
| 1U77252 | Heater--Field Joint |
| 1U77253 | Heater--Igniter-to-Case Joint |
| 1U77356 | Bolt, Special |
| 1U77358 | Bolt Inner, Igniter |
| 1U77359 | Bolt, S&A Device |
| 1U77387 | S&A Device Assembly, Rocket Motor |
| 1U77452 | Adapter, Igniter Quench Port |
| 1U77453 | Adapter Assembly-Quench, Igniter-Insulated |
| 1U77460 | Bolt, Outer, Igniter |
| 1U77463 | Modified Outer Gasket |
| 1U77472 | Preload Indicating Washer Assembly |
| 1U77555 | Forward Segment Assembly |
| 1U77584 | Nozzle Assembly, Final |
| 1U77609 | Test Assembly, TEM-10 |
| 1U77611 | Motor Assembly, TEM |
| 1U77613 | Nozzle Assembly, Aft Segment |
| 1U77636 | Igniter, Test Configuration |
| 1U82840 | Band Pin Assembly Retainer |
| 1U100269 | Plug, Machine Thread |

| <u>Drawings (cont)</u> | <u>Title</u> |
|------------------------|--|
| 2U65151 | Static Test Arrangement--T-24 |
| 2U65686 | Transducer Leak Test Fixture |
| 2U65848 | Leak Test Assembly--B-B Assembly, S&A Device |
| 2U132179 | CO ₂ Quench System--T-24 |
| 2U129749 | Water Deluge System |
| 2U129714 | Assembly, RSRM Joint Leak Check System |
| 2U129760 | Static Test Arrangement--T24 |
| 2U132180 | Aft Test Stand Assembly |
| 2U132116 | Adjustable Link Kit |
| 2U132880 | SII Arming Cable Installation Kit |
| 4U69505 | Shield, Deluge System |
| 7U76902 | Transducer Assembly, Pressure |
| 7U76924 | Fixed Link Support Assembly |
| 7U77254 | Heater--Nozzle-to-Case Joint |
| 7U77349 | Cable Assembly--Refurbished |
| 7U77607 | Joint Protection System, TEM |
| 7U77681 | Retainer, Tapered, Pin-Field Joint, RSRM |
| 7U77684 | Pin, Custom |
| 8U75902 | Leak Check System, Installation |
| 8U76500 | Leak Check System, S&A Device, Installation |

| <u>Specifications</u> | <u>Title</u> |
|-----------------------|--|
| CPW1-3600A | Prime Equipment Contract End Item Detail Specification |
| CTP-0110 | Space Shuttle Technical Evaluation Motor No. 10 (TEM-10) Static Fire Test Plan |
| STW4-2621 | Insulation, Acrylonitrile Butadiene Rubber, Asbestos and Silicon Dioxide-Filled |
| STW4-2868 | Thermal Insulation, Ethylene Propylene Diene Monomer--Neoprene Rubber, Carbon Fiber-Filled |
| STW4-3266 | Putty and Caulking or Glazing Compounds, Other |
| STW5-2833 | TP-H1178 Propellant, SRM, Igniter Space Shuttle Project |
| STW5-3223 | Inhibitor, UF-3267, SRM, Space Shuttle Projects |
| STW5-3224 | Liner, SRM, Space Shuttle Project |
| STW5-3343 | Propellant, SRM, TP-H1148 |
| STW5-3479 | Adhesive, Pressure-Sensitive, Solvent Dispersed |
| STW7-2831 | Inspection and Process Finalization |
| No Change | Criteria, Insulated Components, Space Shuttle SRM |
| STW7-2853 | Leak Test, Pressure Transducer Assemblies, Space Shuttle Project SRM |
| STW7-3682 | Leak Testing, Field and Case-to-Nozzle Joints, Space Shuttle RSRM |
| STW7-3688 | Grease Application and O-Ring Installation, Field and Case-to-Nozzle Joints |
| STW7-3745 | Putty, Aft Segment and Nozzle Assembly Joint; Application of |

Specifications

Title

| | |
|-----------|--|
| STW7-3746 | Putty, Vacuum Seal, Field Joint Assembly; Application of |
| STW7-3894 | Leak Test, Redesigned Inner and Outer Igniter Joints Baseline Design, Space Shuttle RSRM |
| STW7-3895 | Leak Testing, Redesigned Safe and Arm Joint Baseline Design, Space Shuttle RSRM |
| STW7-3896 | Leak Testing, Barrier-Booster Redundant Seals, Space Shuttle RSRM, Igniter Redesign |
| STW7-9008 | Igniter J-joint Insulation, Preparation and Adhesive Application |

Documents

Title

| | |
|-----------|--|
| TWR-19124 | Predicted Ballistic Performance Characteristics for TEM-10 |
| TWR-19841 | Technical Evaluation Motor No. 10 (TEM-10) Performance Information Summary |
| TWR-55088 | Preliminary Statement of Work Igniter Seal Redesign Phase I |
| TWR-60273 | TEM Postfire Engineering Evaluation Plan |
| TWR-63821 | Postfire Hardware Special Issues TEM-10 |
| TWR-63827 | TEM-10 Dynamic Data Analysis |
| TWR-64992 | TEM-10 Bore Inspection/Field Joint Putty Tamping |

APPENDIX A

TEM-10 Drawing Tree

DRAWING TREES

TEM-10

REV S

DATE 16 OCT 1992

A-3

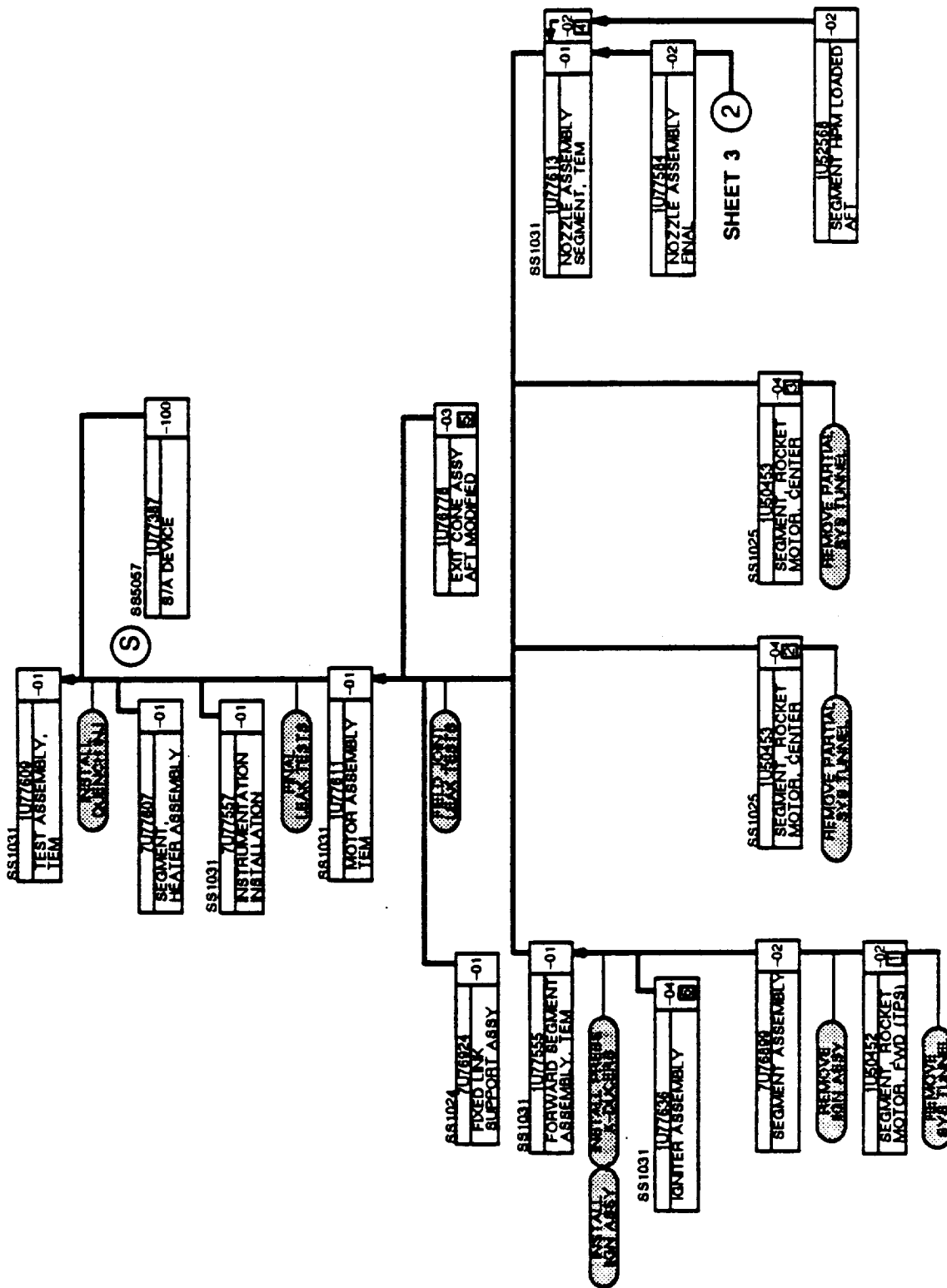
APPROVED BY: Daniel Foreman 10/16/92 H.E.

INTEGRATION DESIGN

APPROVED BY: William P. Ponder 10-27-12

CMT PROJECT ENGINEER

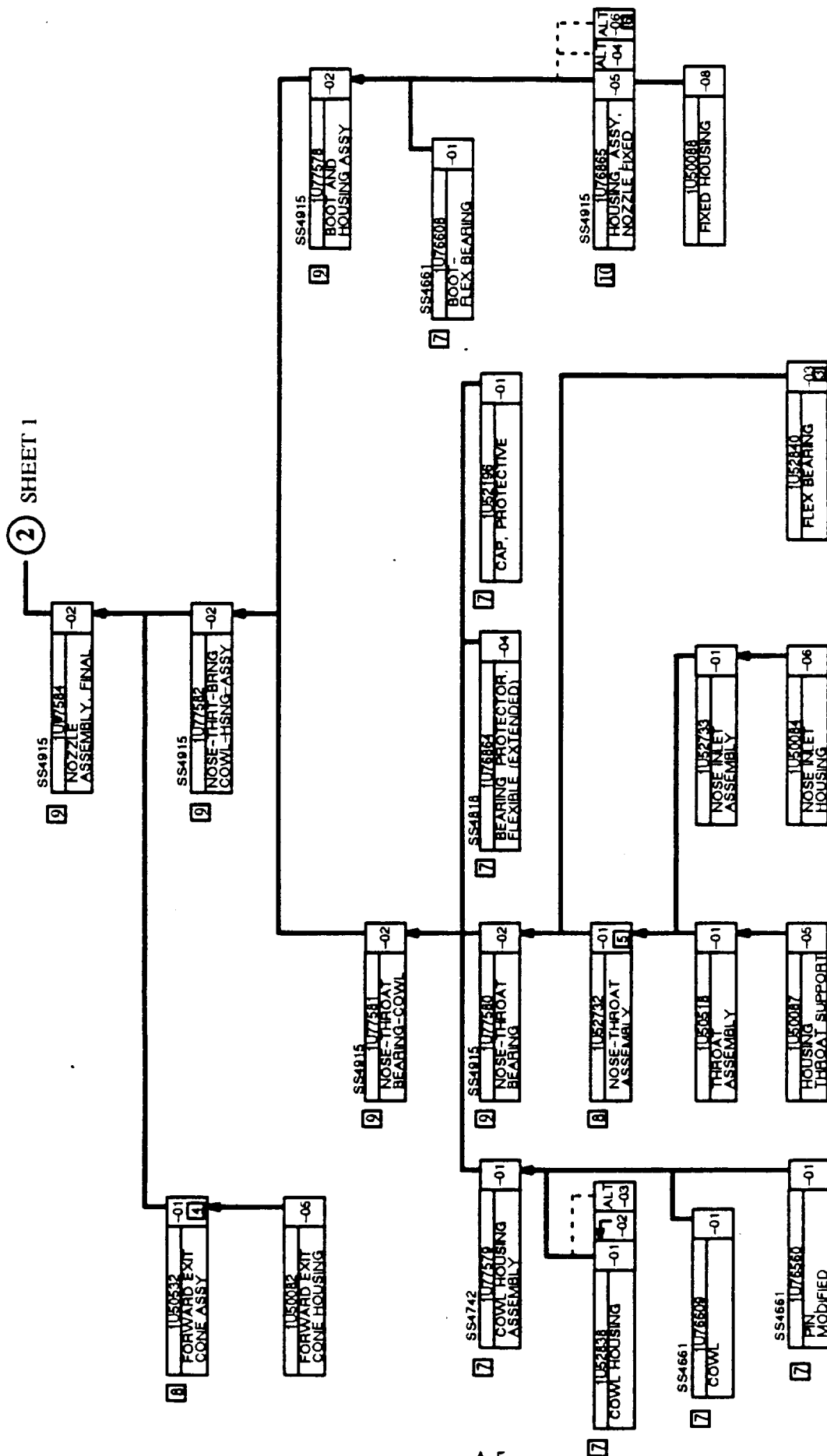
PRECEDING PAGE BLANK NOT FILMED



A-4

- 1 MAKE FROM 1U50452-01, S/N0000030 (26B)
- 2 MAKE FROM 1U50453-01, S/N0000047 (25A)
- 3 MAKE FROM 1U50453-01, S/N0000054 (26B)
- 4 MAKE FROM 1U52568-02, (907) S/N0000001 (27A)
- 5 MAKE FROM 1U50524-01, (901) S/N0000008
- 6 SEE IGNITER REDESIGN DRAWING TREE

NOZZLE ASSEMBLY

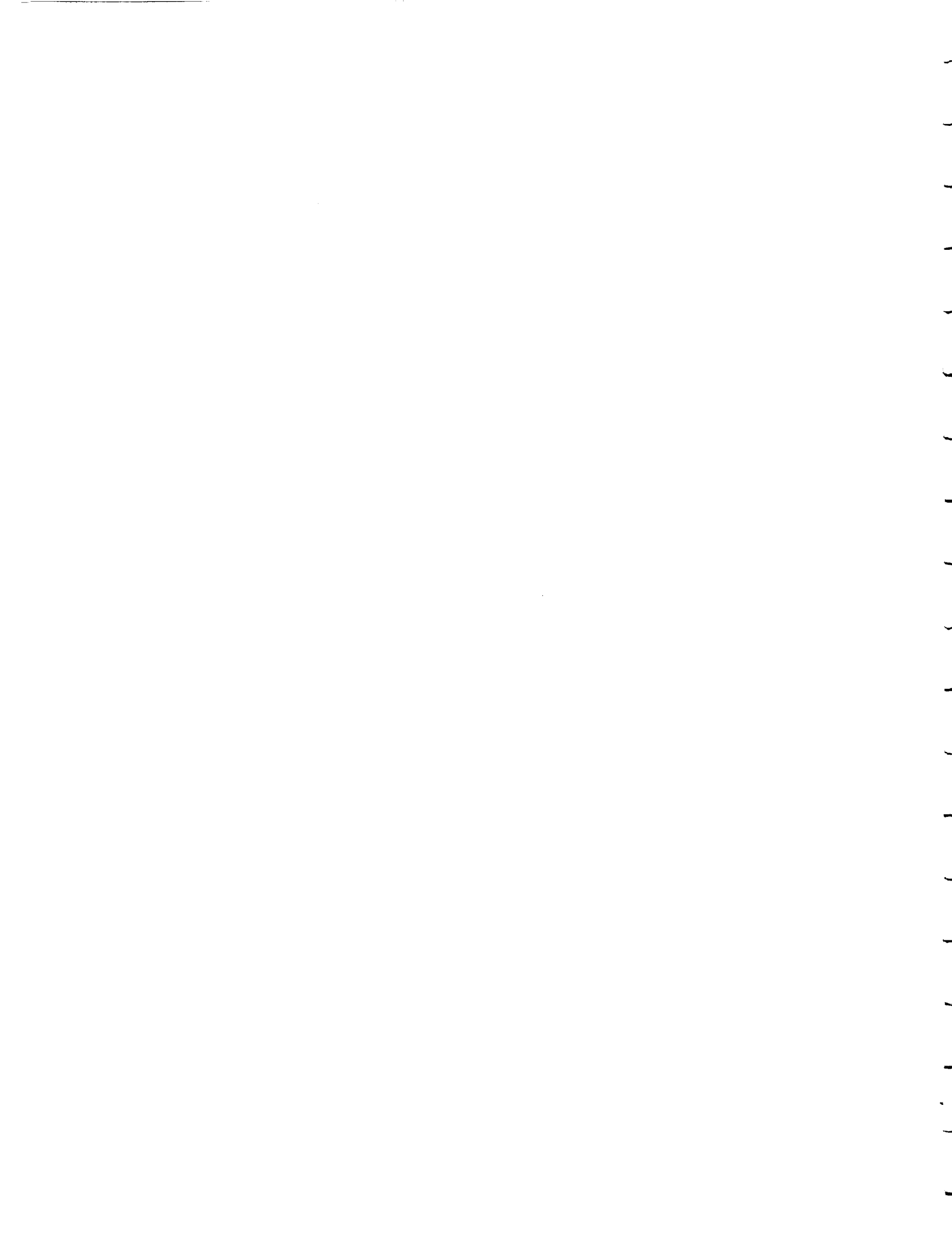


7 FSM-3 CONFIGURATION
8 HPM CONFIGURATION
9 FSM-3 REVISED CONFIGURATION
10 HPM REVISED CONFIGURATION

| | |
|---|--|
| 1 | -03 MAKE FROM 1U51060-01, -07, -10, OR -12 |
| 2 | -01 MAKE FROM (906) S/N00000002 |
| 3 | -01 MAKE FROM (912) S/N00000002 |
| 4 | -06 MAKE FROM 1U50519-01 (902) S/N00000004 |

APPENDIX B

Summary of Measured Ballistic and Nozzle Performance Data



0000 010000

THIOL CORPORATION SRM STATIC TEST 15M-10 27 APRIL 1993 5

A. AMBIENT CONDITIONS

DATE & TIME AT FIRE PULSE 15.8 - 4 - 27 - 1993 DEG F
 AMBIENT TEMPERATURE 88.60 DEG F
 MEASURED AMBIENT PRESSURE 12.38 PSIA

B. WEIGHT DATA

TOTAL LOADED PROPELLANT WEIGHT 1110138.0 LBS
 TOTAL EXPENDED PROPELLANT RESIDUE 2530.0 LBS
 UNEXPENDED PROPELLANT RESIDUE 2530.0 LBS
 EXPENDED INERT WEIGHT 2530.0 LBS
 A FORWARD SEGMENT 718.0 LBS
 B FORWARD CENTER SEGMENT 508.0 LBS
 C AFT SEGMENT 942.0 LBS
 D AFT SEGMENT INCLUDING NOZZLE 4072.0 LBS
 FROM FIELD JOINT FORWARD 6350.0 LBS

E. TOTAL EXPENDED INERTS

TOTAL EXPENDED PROPELLANT WEIGHT 1110138.0 LBS

C. NOZZLE DATA

INITIAL THROAT AREA 2279.0 SQ IN
 FINAL THROAT AREA 2476.8 SQ IN
 WEIGHT TIME AVERAGE THROAT AREA 2381.9 SQ IN
 ACTION TIME AVERAGE THROAT AREA 2391.4 SQ IN
 INITIAL TIP AREA 17589.8 SQ IN
 FINAL TIP AREA 17528.0 SQ IN
 WEIGHT TIME AVERAGE TIP AREA 17558.9 SQ IN
 ACTION TIME AVERAGE TIP AREA 17558.9 SQ IN
 TOTAL TIME AVERAGE THROAT RADIAL EROSION RATE 0.01004 IN/SEC
 TOTAL TIME AVERAGE THROAT RADIAL EROSION RATE 0.00933 IN/SEC
 TOTAL TIME AVERAGE THROAT RADIAL EROSION RATE 0.00928 IN/SEC
 INITIAL EXPANSION RATIO 7.7118
 WEIGHT TIME AVERAGE EXPANSION RATIO 7.3718
 ACTION TIME AVERAGE EXPANSION RATIO 7.3430
 TOTAL TIME AVERAGE NOZZLE EFFICIENCY 0.97481
 ACTION TIME AVERAGE NOZZLE EFFICIENCY 0.97486

0000 010000

THIOL CORPORATION SRM STATIC TEST 15M-10 27 APRIL 1993 5

D. TIME AND BALLISTIC DATA

TIME AT FIRST INDICATION OF HEAD END PRESSURE 0.028 SEC
 IGNITION DELAY TIME 0.050 SEC
 TIME AT 50% MAX IGNITER PRESSURE 0.050 SEC
 IGNITION INTERVAL TIME 0.622 SEC
 TIME WHEN HEAD END CHAMBER PRESSURE ACHIEVES 50% PSIA DURING IGNITION 0.735 SEC
 TIME AT LAST INDICATION OF HEAD END PRESSURE 10.418 SEC
 TIME IT WPH RECEPTOR 10.418 SEC

TITLE THIOL CORPORATION SRM
 MISSILE TEST/NUM NUMBER 0000
 SOURCE YCCD TYPE ST

NUMBER CHANNEL UNITS MM
 TYPE SECONDS
 SPIN 0
 0 0000000

NUM CHANNEL MM CHANNEL
 LINE 01 PHAS
 0 0000000

TITLE THIOL CORPORATION SRM S
 MISSILE TEST/NUM NUMBER 00000
 SOURCE YCCD TYPE STA
 NUMBER CHANNEL UNITS MM
 TYPE SECONDS
 SPIN 0
 0 0000000

PRECEDING PAGE BLANK NOT FILMED

and Date

| | |
|------------------------|---------------------------|
| TITLE | THIOL CORPORATION SRM SLP |
| MISILE TEST/RUN NUMBER | 000000X |
| SOURCE YCD | TYPE STAT |
| NUMBER CHANNEL UNITS | MURGE |

| | | | | | | | | | |
|---|--|--|--|--|--|--|--|--|--|
| THIKOL CORPORATION SRM STATIC TEST IEM-10 27 APRIL 1993 5 | | | | | | | | | |
| E. IMPULSE DATA | | | | | | | | | |
| M-IMPULSE TOTAL IMPULSE | | | | | | | | | |
| 277.205 MILLION LB-SEC | | | | | | | | | |
| M-IMPULSE CORRECTED TO VACUUM | | | | | | | | | |
| 297.180 MILLION LB-SEC | | | | | | | | | |
| M-IMPULSE CORRECTED TO VACUUM | | | | | | | | | |
| 261.585 MILLION LB-SEC | | | | | | | | | |
| M-IMPULSE CORRECTED TO VACUUM | | | | | | | | | |
| 160.900 MILLION LB-SEC | | | | | | | | | |
| M-IMPULSE CORRECTED TO VACUUM | | | | | | | | | |
| 173.938 MILLION LB-SEC | | | | | | | | | |
| M-IMPULSE CORRECTED TO VACUUM | | | | | | | | | |
| 265.568 MILLION LB-SEC | | | | | | | | | |
| M-IMPULSE CORRECTED TO VACUUM | | | | | | | | | |
| 271.081 MILLION LB-SEC | | | | | | | | | |
| M-IMPULSE CORRECTED TO VACUUM | | | | | | | | | |
| 267.092 MILLION LB-SEC | | | | | | | | | |
| M-IMPULSE CORRECTED TO VACUUM | | | | | | | | | |
| 266.056 SEC | | | | | | | | | |
| M-IMPULSE CORRECTED TO VACUUM | | | | | | | | | |
| 244.838 SEC | | | | | | | | | |
| M-IMPULSE CORRECTED TO VACUUM | | | | | | | | | |
| 266.972 SEC | | | | | | | | | |
| M-IMPULSE CORRECTED TO VACUUM | | | | | | | | | |
| 243.383 SEC | | | | | | | | | |
| M-IMPULSE CORRECTED TO VACUUM | | | | | | | | | |
| 266.056 SEC | | | | | | | | | |
| M-IMPULSE CORRECTED TO VACUUM | | | | | | | | | |
| 244.733 SEC | | | | | | | | | |
| M-IMPULSE CORRECTED TO VACUUM | | | | | | | | | |
| 268.184 SEC | | | | | | | | | |
| F. PRESSURE INTEGRAL DATA | | | | | | | | | |
| TOTAL TIME PRESSURE INTEGRAL | | | | | | | | | |
| 75755.2 LB/30 IN-SEC | | | | | | | | | |
| WEB TIME PRESSURE INTEGRAL | | | | | | | | | |
| 75872.9 LB/30 IN-SEC | | | | | | | | | |
| ACTION TIME PRESSURE INTEGRAL | | | | | | | | | |
| 75711.8 LB/30 IN-SEC | | | | | | | | | |

| | | | |
|---------------------------------|--|--|--|
| TITLE THIKOL CORPORATION SRM 51 | | | |
| MISSILE TEST/RUN NUMBER 000000 | | | |
| SOURCE TEST/TYPE 0001 | | | |
| NUMBER CHANNEL UNITS | | | |
| 355-1514 | | | |
| 355-1514 | | | |
| 355-1514 | | | |
| 355-1514 | | | |
| 355-1514 | | | |
| 355-1514 | | | |
| 355-1514 | | | |
| 355-1514 | | | |
| 355-1514 | | | |
| 355-1514 | | | |
| 355-1514 | | | |
| 355-1514 | | | |
| 355-1514 | | | |
| 355-1514 | | | |
| 355-1514 | | | |
| 355-1514 | | | |
| 355-1514 | | | |
| 355-1514 | | | |
| 355-1514 | | | |
| 355-1514 | | | |
| 355-1514 | | | |
| 355-1514 | | | |
| 355-1514 | | | |
| 355-1514 | | | |
| 355-1514 | | | |
| 355-1514 | | | |
| 355-1514 | | | |
| 355-1514 | | | |
| 355-1514 | | | |
| 355-1514 | | | |
| 355-1514 | | | |
| 355-1514 | | | |
| 355-1514 | | | |
| 355-1514 | | | |
| 355-1514 | | | |
| 355-1514 | | | |
| 355-1514 | | | |
| 355-1514 | | | |
| 355-1514 | | | |
| 355-1514 | | | |
| 355-1514 | | | |
| 355-1514 | | | |
| 355-1514 | | | |
| 355-1514 | | | |
| 355-1514 | | | |
| 355-1514 | | | |
| 355-1514 | | | |
| 355-1514 | | | |
| 355-1514 | | | |
| 355-1514 | | | |
| 355-1514 | | | |
| 355-1514 | | | |
| 355-1514 | | | |
| 355-1514 | | | |
| 355-1514 | | | |
| 355-1514 | | | |
| 355-1514 | | | |
| 355-1514 | | | |
| 355-1514 | | | |
| 355-1514 | | | |
| 355-1514 | | | |
| 355-1514 | | | |
| 355-1514 | | | |
| 355-1514 | | | |
| 355-1514 | | | |
| 355-1514 | | | |
| 355-1514 | | | |
| 355-1514 | | | |
| 355-1514 | | | |
| 355-1514 | | | |
| 355-1514 | | | |
| 355-1514 | | | |
| 355-1514 | | | |
| 355-1514 | | | |
| 355-1514 | | | |
| 355-1514 | | | |
| 355-1514 | | | |
| 355-1514 | | | |
| 355-1514 | | | |
| 355-1514 | | | |
| 355-1514 | | | |
| 355-1514 | | | |
| 355-1514 | | | |
| 355-1514 | | | |
| 355-1514 | | | |
| 355-1514 | | | |
| 355-1514 | | | |
| 355-1514 | | | |
| 355-1514 | | | |
| 355-1514 | | | |
| 355-1514 | | | |
| 355-1514 | | | |
| 355-1514 | | | |
| 355-1514 | | | |
| 355-1514 | | | |
| 355-1514 | | | |
| 355-1514 | | | |
| 355-1514 | | | |
| 355-1514 | | | |
| 355-1514 | | | |
| 355-1514 | | | |
| 355-1514 | | | |
| 355-1514 | | | |
| 355-1514 | | | |
| 355-1514 | | | |
| 355-1514 | | | |
| 355-1514 | | | |
| 355-1514 | | | |
| 355-1514 | | | |
| 355-1514 | | | |
| 355-1514 | | | |
| 355-1514 | | | |
| 355-1514 | | | |
| 355-1514 | | | |
| 355-1514 | | | |
| 355-1514 | | | |
| 355-1514 | | | |
| 355-1514 | | | |
| 355-1514 | | | |
| 355-1514 | | | |
| 355-1514 | | | |
| 355-1514 | | | |
| 355-1514 | | | |
| 355-1514 | | | |
| 355-1514 | | | |
| 355-1514 | | | |
| 355-1514 | | | |
| 355-1514 | | | |
| 355-1514 | | | |
| 355-1514 | | | |
| 355-1514 | | | |
| 355-1514 | | | |
| 355-1514 | | | |
| 355-1514 | | | |
| 355-1514 | | | |
| 355-1514 | | | |
| 355-1514 | | | |
| 355-1514 | | | |
| 355-1514 | | | |
| 355-1514 | | | |
| 355-1514 | | | |
| 355-1514 | | | |
| 355-1514 | | | |
| 355-1514 | | | |
| 355-1514 | | | |
| 355-1514 | | | |
| 355-1514 | | | |
| 355-1514 | | | |
| 355-1514 | | | |
| 355-1514 | | | |
| 355-1514 | | | |
| 355-1514 | | | |
| 355-1514 | | | |
| 355-1514 | | | |
| 355-1514 | | | |
| 355-1514 | | | |
| 355-1514 | | | |
| 355-1514 | | | |
| 355-1514 | | | |
| 355-1514 | | | |
| 355-1514 | | | |
| 355-1514 | | | |
| 355-1514 | | | |
| 355-1514 | | | |
| 355-1514 | | | |
| 355-1514 | | | |
| 355-1514 | | | |
| 355-1514 | | | |
| 355-1514 | | | |
| 355-1514 | | | |
| 355-1514 | | | |
| 355-1514 | | | |
| 355-1514 | | | |
| 355-1514 | | | |
| 355-1514 | | | |
| 355-1514 | | | |
| 355-1514 | | | |
| 355-1514 | | | |
| 355-1514 | | | |
| 355-1514 | | | |
| 355-1514 | | | |
| 355-1514 | | | |
| 355-1514 | | | |
| 355-1514 | | | |
| 355-1514 | | | |
| 355-1514 | | | |
| 355-1514 | | | |
| 355-1514 | | | |
| 355-1514 | | | |
| 355-1514 | | | |
| 355-1514 | | | |
| 355-1514 | | | |
| 355-1514 | | | |
| 355-1514 | | | |
| 355-1514 | | | |
| 355-1514 | | | |
| 355-1514 | | | |
| 355-1514 | | | |
| 355-1514 | | | |
| 355-1514 | | | |
| 355-1514 | | | |
| 355-1514 | | | |
| 355-1514 | | | |
| 355-1514 | | | |
| 355-1514 | | | |
| 355-1514 | | | |
| 355-1514 | | | |
| 355-1514 | | | |
| 355-1514 | | | |
| 355-1514 | | | |
| 355-1514 | | | |
| 355-1514 | | | |
| 355-1514 | | | |
| 355-1514 | | | |
| 355-1514 | | | |
| 355-1514 | | | |
| 355-1514 | | | |
| 355-1514 | | | |
| 355-1514 | | | |
| 355-1514 | | | |
| 355-1514 | | | |
| 355-1514 | | | |
| 355-1514 | | | |
| 355-1514 | | | |
| 355-1514 | | | |
| 355-1514 | | | |
| 355-1514 | | | |
| 355-1514 | | | |
| 355-1514 | | | |
| 355-1514 | | | |
| 355-1514 | | | |
| 355-1514 | | | |
| 355-1514 | | | |
| 355-1514 | | | |
| 355-1514 | | | |
| 355-1514 | | | |
| 355-1514 | | | |
| 355-1514 | | | |
| 355-1514 | | | |
| 355-1514 | | | |
| 355-1514 | | | |
| 355-1514 | | | |
| 355-1514 | | | |
| 355-1514 | | | |
| 355-1514 | | | |
| 355-1514 | | | |
| 355-1514 | | | |
| 355-1514 | | | |
| 355-1514 | | | |
| 355-1514 | | | |
| 355-1514 | | | |
| 355-1514 | | | |
| 355-1514 | | | |
| 355-1514 | | | |
| 355-1514 | | | |
| 355-1514 | | | |
| 355-1514 | | | |
| 355-1514 | | | |
| 355-1514 | | | |
| 355-1514 | | | |
| 355-1514 | | | |
| 355-1514 | | | |
| 355-1514 | | | |
| 355-1514 | | | |
| 355-1514 | | | |
| 355-1514 | | | |
| 355-1514 | | | |
| 355-1514 | | | |
| 355-1514 | | | |
| 355-1514 | | | |
| 355-1514 | | | |
| 355-1514 | | | |
| 355-1514 | | | |
| 355-1514 | | | |
| 355-1514 | | | |
| 355-1514 | | | |
| 355-1514 | | | |
| 355-1514 | | | |
| 355-1514 | | | |
| 355-1514 | | | |
| 355-1514 | | | |
| 355-1514 | | | |
| 355-1514 | | | |
| 355-1514 | | | |
| 355-1514 | | | |
| 355-1514 | | | |
| 355-1514 | | | |
| 355-1514 | | | |
| 355-1514 | | | |
| 355-1514 | | | |
| 355-1514 | | | |
| 355-1514 | | | |
| 355-1514 | | | |
| 355-1514 | | | |
| 355-1514 | | | |
| 355-1514 | | | |
| 355-1514 | | | |
| 355-1514 | | | |
| 355-1514 | | | |
| 355-1514 | | | |
| 355-1514 | | | |
| 355-1514 | | | |
| 355-1514 | | | |
| 355-1514 | | | |
| 355-1514 | | | |
| 355-1514 | | | |
| 355-1514 | | | |
| 355-1514 | | | |
| 355-1514 | | | |
| 355-1514 | | | |
| 355-1514 | | | |
| 355-1514 | | | |
| 355-1514 | | | |
| 355-1514 | | | |
| 355-1514 | | | |
| 355-1514 | | | |
| 355-1514 | | | |
| 3 | | | |

*** 02***

INIKOL CORPORATION SRM STATIC TEST TEN-10 27 APRIL 1993 8

CORRECTED TO 40 DEGREES

U. TIME AND BALLISTIC DATA

| | | |
|--|---------|------|
| TIME AT FIRST INDICATION OF HEAD END PRESSURE | 0.030 | SEC |
| TIME WHEN HEAD END CHAMBER PRESSURE | | |
| ACHIEVES 50% PSIA DURING IGNITION | 0.200 | SEC |
| TIME AT LAST INDICATION OF HEAD END PRESSURE | 127.334 | SEC |
| TIME AT WEB DISSECTION | 177.082 | SEC |
| WEB TIME | 112.811 | SEC |
| ACTION TIME | 112.811 | SEC |
| MAX MEASURED HEAD END PRESSURE | 076.37 | PSIA |
| TIME AT MAX HEAD END PRESSURE | 1.516 | SEC |
| MAXIMUM THRUST CORRECTED TO VACUUM | 323000 | LB |
| MAXIMUM STAGNATION PRESSURE | 225.8 | PSIA |
| WEB TIME AVERAGE HEAD END CHAMBER PRESSURE | 617.50 | PSIA |
| ACTION TIME AVERAGE HEAD END CHAMBER PRESSURE | 597.21 | PSIA |
| WEB TIME AVERAGE NOZZLE STAGNATION PRESSURE | 612.70 | PSIA |
| ACTION TIME AVERAGE NOZZLE STAGNATION PRESSURE | 585.90 | PSIA |
| WEB TIME AVERAGE THRUST CORRECTED TO VACUUM | 239050 | LB |
| ACTION TIME AVERAGE THRUST CORRECTED TO VACUUM | 233362 | LB |

E. IMPULSE DATA

| | | |
|--|---------|----------------|
| TOTAL IMPULSE CORRECTED TO VACUUM | 296.600 | MILLION LB-SEC |
| 20 SEC IMPULSE CORRECTED TO VACUUM | 62.657 | MILLION LB-SEC |
| 60 SEC IMPULSE CORRECTED TO VACUUM | 168.917 | MILLION LB-SEC |
| WEB TIME IMPULSE CORRECTED TO VACUUM | 289.010 | MILLION LB-SEC |
| ACTION TIME IMPULSE CORRECTED TO VACUUM | 298.481 | MILLION LB-SEC |
| SPECIFIC IMPULSE CORRECTED TO VACUUM | 266.180 | SEC |
| WEB TIME SPECIFIC IMPULSE CORRECTED TO VACUUM | 266.180 | SEC |
| ACTION TIME SPECIFIC IMPULSE CORRECTED TO VACUUM | 267.705 | SEC |
| PROPELLANT SPECIFIC IMPULSE CORRECTED TO VACUUM | | |

*** 02***

INIKOL CORPORATION SRM STATIC TEST TEN-10 27 APRIL 1993 60 DFG

MISSILE TEST/ID NUMBER 00000001 NUMBER OF CHANNELS 10 NUMBER OF TESTS/RECORD 10

SOURCE TCDD TYPE STATIC FIRING DATE

| NUMBER | CHANNEL | UNITS | NUMBER | CHANNEL | UNITS | NUMBER | CHANNEL | UNITS |
|--------|---------|---------|--------|---------|-------|--------|---------|-------|
| 1 | TIME | SECONDS | 2 | PHOTO | | 3 | PSI/SEC | |
| 4 | SPIN | RPM | 5 | SPIN | RPM | 6 | SPIN | RPM |
| 7 | SPIN | RPM | 8 | SPIN | RPM | 9 | SPIN | RPM |
| 10 | SPIN | RPM | 11 | SPIN | RPM | 12 | SPIN | RPM |

**** 02****

THIokol CORPORATION SRM STATIC TEST ITEM-10 27 APRIL 1993 5

CORRECTED TO 60 DEGREES

U. TIME AND BALLISTIC DATA

TIME AT FIRST INDICATION OF HEAD END PRESSURE 0.028 SEC
TIME WHEN HEAD END CHAMBER PRESSURE
ACHIEVES 50% PSIA DURING IGNITION 0.239 SEC
TIME AT LAST INDICATION OF HEAD END PRESSURE 124.566 SEC
TIME AT WEB BISECTION 111.541 SEC
WEB TIME 111.203 SEC
ACTION TIME 111.759 SEC
MAX MEASURED HEAD END PRESSURE 897.69 PSIA
TIME AT MAX HEAD END PRESSURE 1.483 SEC
MAXIMUM THRUST CORRECTED TO VACUUM 3113460 LB
MAXIMUM STAGNATION PRESSURE 845.6 PSIA
WEB TIME AVERAGE HEAD END CHAMBER PRESSURE 603.02 PSIA
ACTION TIME AVERAGE HEAD END CHAMBER PRESSURE 611.34 PSIA
WEB TIME AVERAGE NOZZLE STAGNATION PRESSURE 647.87 PSIA
ACTION TIME AVERAGE NOZZLE STAGNATION PRESSURE 597.64 PSIA
WEB TIME AVERAGE THRUST CORRECTED TO VACUUM 2399930 LB
ACTION TIME AVERAGE THRUST CORRECTED TO VACUUM 2398693 LB

E. IMPULSE DATA

TOTAL IMPULSE CORRECTED TO VACUUM 297.025 MILLION LB-SEC
20 SEC IMPULSE CORRECTED TO VACUUM 65.193 MILLION LB-SEC
60 SEC IMPULSE CORRECTED TO VACUUM 172.356 MILLION LB-SEC
WEB TIME IMPULSE CORRECTED TO VACUUM 298.379 MILLION LB-SEC
ACTION TIME IMPULSE CORRECTED TO VACUUM 298.379 MILLION LB-SEC
SPECIFIC IMPULSE CORRECTED TO VACUUM 268.509 SEC
WEB TIME SPECIFIC IMPULSE CORRECTED TO VACUUM 268.773 SEC
ACTION TIME SPECIFIC IMPULSE CORRECTED TO VACUUM 268.509 SEC
PROPELLANT SPECIFIC IMPULSE CORRECTED TO VACUUM 268.035 SEC

**** 02****

THIokol CORPORATION SRM STATIC TEST ITEM-10 27 APRIL 1993 90 DFG
MISSILE TEST/RUN NUMBER 00000000 NUMBER OF CHANNELS 10 NUMBER OF LOGS/RECORD 10
SOURCE (CCD) TYPE STATIC FIRING DATE

| TIME | THIOLON CORPORATION | SRM STATIC TEST | 10M-10 | 27 APRIL 1993 | 5 |
|--|---------------------|-----------------|--------|---------------|---|
| CORRECTED TO 90. DEGREES | | | | | |
| U. TIME AND BALLISTIC DATA | | | | | |
| TIME AT FIRST INDICATION OF HEAD END PRESSURE | | 0.026 | | SEC | |
| TIME WHEN HEAD END CHAMBER PRESSURE | | 0.276 | | SEC | |
| ACHIEVES 56.5 PSIA DURING IGNITION | | 120.533 | | SEC | |
| TIME AT LAST INDICATION OF HEAD END PRESSURE | | 107.775 | | SEC | |
| TIME AT WEB BISECTION | | 107.350 | | SEC | |
| WEB TIME | | 116.750 | | SEC | |
| MAX MEASURED HEAD END PRESSURE | | 930.02 | | PSIA | |
| TIME AT MAX HEAD END PRESSURE | | 1.436 | | SEC | |
| MAXIMUM STAGNATION PRESSURE TO VACUUM | | 34350.1 | | PSIA | |
| WEB TIME AVERAGE HEAD END CHAMBER PRESSURE | | 276.0 | | PSIA | |
| ACTION TIME AVERAGE HEAD END CHAMBER PRESSURE | | 287.0 | | PSIA | |
| WEB TIME AVERAGE NOZZLE STAGNATION PRESSURE | | 271.0 | | PSIA | |
| ACTION TIME AVERAGE NOZZLE STAGNATION PRESSURE | | 281.0 | | PSIA | |
| WEB TIME AVERAGE THRUST CORRECTED TO VACUUM | | 2694569 | | LBS | |
| ACTION TIME AVERAGE THRUST CORRECTED TO VACUUM | | 2433726 | | LBS | |

| DESCRIPTION | QUANTITY | UNIT | VALUE |
|--------------------------------------|----------|------|-------|
| TOTAL IMPULSE CORRECTED TO VACUUM | 297.5 | SEC | 297.5 |
| 20 SEC IMPULSE CORRECTED TO VACUUM | 20 | SEC | 20 |
| 40 SEC IMPULSE CORRECTED TO VACUUM | 40 | SEC | 40 |
| 60 SEC IMPULSE CORRECTED TO VACUUM | 60 | SEC | 60 |
| 80 SEC IMPULSE CORRECTED TO VACUUM | 80 | SEC | 80 |
| 100 SEC IMPULSE CORRECTED TO VACUUM | 100 | SEC | 100 |
| 120 SEC IMPULSE CORRECTED TO VACUUM | 120 | SEC | 120 |
| 140 SEC IMPULSE CORRECTED TO VACUUM | 140 | SEC | 140 |
| 160 SEC IMPULSE CORRECTED TO VACUUM | 160 | SEC | 160 |
| 180 SEC IMPULSE CORRECTED TO VACUUM | 180 | SEC | 180 |
| 200 SEC IMPULSE CORRECTED TO VACUUM | 200 | SEC | 200 |
| 220 SEC IMPULSE CORRECTED TO VACUUM | 220 | SEC | 220 |
| 240 SEC IMPULSE CORRECTED TO VACUUM | 240 | SEC | 240 |
| 260 SEC IMPULSE CORRECTED TO VACUUM | 260 | SEC | 260 |
| 280 SEC IMPULSE CORRECTED TO VACUUM | 280 | SEC | 280 |
| 300 SEC IMPULSE CORRECTED TO VACUUM | 300 | SEC | 300 |
| 320 SEC IMPULSE CORRECTED TO VACUUM | 320 | SEC | 320 |
| 340 SEC IMPULSE CORRECTED TO VACUUM | 340 | SEC | 340 |
| 360 SEC IMPULSE CORRECTED TO VACUUM | 360 | SEC | 360 |
| 380 SEC IMPULSE CORRECTED TO VACUUM | 380 | SEC | 380 |
| 400 SEC IMPULSE CORRECTED TO VACUUM | 400 | SEC | 400 |
| 420 SEC IMPULSE CORRECTED TO VACUUM | 420 | SEC | 420 |
| 440 SEC IMPULSE CORRECTED TO VACUUM | 440 | SEC | 440 |
| 460 SEC IMPULSE CORRECTED TO VACUUM | 460 | SEC | 460 |
| 480 SEC IMPULSE CORRECTED TO VACUUM | 480 | SEC | 480 |
| 500 SEC IMPULSE CORRECTED TO VACUUM | 500 | SEC | 500 |
| 520 SEC IMPULSE CORRECTED TO VACUUM | 520 | SEC | 520 |
| 540 SEC IMPULSE CORRECTED TO VACUUM | 540 | SEC | 540 |
| 560 SEC IMPULSE CORRECTED TO VACUUM | 560 | SEC | 560 |
| 580 SEC IMPULSE CORRECTED TO VACUUM | 580 | SEC | 580 |
| 600 SEC IMPULSE CORRECTED TO VACUUM | 600 | SEC | 600 |
| 620 SEC IMPULSE CORRECTED TO VACUUM | 620 | SEC | 620 |
| 640 SEC IMPULSE CORRECTED TO VACUUM | 640 | SEC | 640 |
| 660 SEC IMPULSE CORRECTED TO VACUUM | 660 | SEC | 660 |
| 680 SEC IMPULSE CORRECTED TO VACUUM | 680 | SEC | 680 |
| 700 SEC IMPULSE CORRECTED TO VACUUM | 700 | SEC | 700 |
| 720 SEC IMPULSE CORRECTED TO VACUUM | 720 | SEC | 720 |
| 740 SEC IMPULSE CORRECTED TO VACUUM | 740 | SEC | 740 |
| 760 SEC IMPULSE CORRECTED TO VACUUM | 760 | SEC | 760 |
| 780 SEC IMPULSE CORRECTED TO VACUUM | 780 | SEC | 780 |
| 800 SEC IMPULSE CORRECTED TO VACUUM | 800 | SEC | 800 |
| 820 SEC IMPULSE CORRECTED TO VACUUM | 820 | SEC | 820 |
| 840 SEC IMPULSE CORRECTED TO VACUUM | 840 | SEC | 840 |
| 860 SEC IMPULSE CORRECTED TO VACUUM | 860 | SEC | 860 |
| 880 SEC IMPULSE CORRECTED TO VACUUM | 880 | SEC | 880 |
| 900 SEC IMPULSE CORRECTED TO VACUUM | 900 | SEC | 900 |
| 920 SEC IMPULSE CORRECTED TO VACUUM | 920 | SEC | 920 |
| 940 SEC IMPULSE CORRECTED TO VACUUM | 940 | SEC | 940 |
| 960 SEC IMPULSE CORRECTED TO VACUUM | 960 | SEC | 960 |
| 980 SEC IMPULSE CORRECTED TO VACUUM | 980 | SEC | 980 |
| 1000 SEC IMPULSE CORRECTED TO VACUUM | 1000 | SEC | 1000 |
| 1020 SEC IMPULSE CORRECTED TO VACUUM | 1020 | SEC | 1020 |
| 1040 SEC IMPULSE CORRECTED TO VACUUM | 1040 | SEC | 1040 |
| 1060 SEC IMPULSE CORRECTED TO VACUUM | 1060 | SEC | 1060 |
| 1080 SEC IMPULSE CORRECTED TO VACUUM | 1080 | SEC | 1080 |
| 1100 SEC IMPULSE CORRECTED TO VACUUM | 1100 | SEC | 1100 |
| 1120 SEC IMPULSE CORRECTED TO VACUUM | 1120 | SEC | 1120 |
| 1140 SEC IMPULSE CORRECTED TO VACUUM | 1140 | SEC | 1140 |
| 1160 SEC IMPULSE CORRECTED TO VACUUM | 1160 | SEC | 1160 |
| 1180 SEC IMPULSE CORRECTED TO VACUUM | 1180 | SEC | 1180 |
| 1200 SEC IMPULSE CORRECTED TO VACUUM | 1200 | SEC | 1200 |
| 1220 SEC IMPULSE CORRECTED TO VACUUM | 1220 | SEC | 1220 |
| 1240 SEC IMPULSE CORRECTED TO VACUUM | 1240 | SEC | 1240 |
| 1260 SEC IMPULSE CORRECTED TO VACUUM | 1260 | SEC | 1260 |
| 1280 SEC IMPULSE CORRECTED TO VACUUM | 1280 | SEC | 1280 |
| 1300 SEC IMPULSE CORRECTED TO VACUUM | 1300 | SEC | 1300 |
| 1320 SEC IMPULSE CORRECTED TO VACUUM | 1320 | SEC | 1320 |
| 1340 SEC IMPULSE CORRECTED TO VACUUM | 1340 | SEC | 1340 |
| 1360 SEC IMPULSE CORRECTED TO VACUUM | 1360 | SEC | 1360 |
| 1380 SEC IMPULSE CORRECTED TO VACUUM | 1380 | SEC | 1380 |
| 1400 SEC IMPULSE CORRECTED TO VACUUM | 1400 | SEC | 1400 |
| 1420 SEC IMPULSE CORRECTED TO VACUUM | 1420 | SEC | 1420 |
| 1440 SEC IMPULSE CORRECTED TO VACUUM | 1440 | SEC | 1440 |
| 1460 SEC IMPULSE CORRECTED TO VACUUM | 1460 | SEC | 1460 |
| 1480 SEC IMPULSE CORRECTED TO VACUUM | 1480 | SEC | 1480 |
| 1500 SEC IMPULSE CORRECTED TO VACUUM | 1500 | SEC | 1500 |
| 1520 SEC IMPULSE CORRECTED TO VACUUM | | | |

| TITLE THOROL CORPORATION SRM STATIC TEST TEN-10 27 APRIL 1993 | | | | | | | | | | | |
|---|---------|--------------------|--------|-----------------------|-------|--------|---------|-------|--------|---------|----------|
| MISSILE TEST/RUN NUMBER | | NUMBER OF CHANNELS | | NUMBER OF LOIS/RECORD | | | | | | | |
| SOURCE TC00 | | TYPE STATIC | | FIRING DATE | | | | | | | |
| NUMBER | CHANNEL | UNITS | NUMBER | CHANNEL | UNITS | NUMBER | CHANNEL | UNITS | NUMBER | CHANNEL | UNITS |
| 1 | TIME | SECONDS | 2 | AVG-3-A | | 3 | AVGPI-1 | PSTA | 4 | AVGPI-4 | PST3-SEC |
| 2 | AVG1-3 | | 6 | AVG1-2-A | | | | | | | |

APPENDIX C

TEM-10 Timeline of Events

TEM-10 Time Line of Events

6/22/93

| <u>Time (sec.)</u> | <u>Event</u> |
|------------------------|--|
| 50.0 | |
| 50.1 | |
| 50.2 | |
| 50.3 | |
| 50.4 | |
| 50.5 | |
| 50.6 | |
| 50.7 | |
| 50.8 | |
| 50.9 | |
| 51.0 | |
| 51.1 | |
| 51.2 | |
| 51.3 | |
| 51.4 | |
| 51.5 | |
| 51.6 | |
| 51.7 | |
| 51.8 | |
| 51.9 | |
| 52.0 | Pressure event maximum Nozzle Accelerometer event (STA-1950, 0 deg) |
| 52.1 | |
| 52.2 | |
| 52.3 | |
| 52.4 | |
| 52.5 | |
| 52.6 | |
| 52.7 | |
| 52.8 | |
| 52.9 | |
| 53.0 | |
| 53.1 | |
| 53.2 | |
| 53.3 | |
| 53.4 | |
| 53.5 | |
| 53.6 | |
| 53.7 | Pressure event maximum Nozzle Accelerometer event (STA-1950, 0 deg) |
| 53.8 | |
| 53.9 | |
| 54.0 | |
| 54.1 | Pressure event maximum Nozzle Accelerometer event (STA-1950, 0 deg) |
| 54.2 | |
| 54.3 | |
| 54.4 | |
| 54.5 | |

| | |
|------|---|
| 54.6 | |
| 54.7 | |
| 54.8 | Pressure event maximum |
| | Nozzle Accelerometer event (STA-1950, 0 deg) |
| 54.9 | |
| 55.0 | |
| 55.1 | |
| 55.2 | |
| 55.3 | |
| 55.4 | |
| 55.5 | |
| 55.6 | |
| 55.7 | |
| 55.8 | |
| 55.9 | |
| 56.0 | |
| 56.1 | |
| 56.2 | |
| 56.3 | |
| 56.4 | |
| 56.5 | |
| 56.6 | |
| 56.7 | Nozzle Accelerometer event (STA-1950, 0 deg) |
| 56.8 | |
| 56.9 | |
| 57.0 | |
| 57.1 | |
| 57.2 | Nozzle Accelerometer event (STA-1950, 0 deg) |
| 57.3 | |
| 57.4 | |
| 57.5 | Pressure event maximum |
| | Nozzle Accelerometer event (STA-1950, 0 deg) |
| | Case hoop strain event (SHIAIO42 @ STA 1409.00) |
| 57.6 | |
| 57.7 | |
| 57.8 | |
| 57.9 | |
| 58.0 | |
| 58.1 | Nozzle Accelerometer event (STA-1950, 0 deg) |
| 58.2 | |
| 58.3 | Case hoop strain event (SHIAIO42 @ STA 1409.00) |
| 58.4 | |
| 58.5 | |
| 58.6 | |
| 58.7 | |
| 58.8 | |
| 58.9 | |
| 59.0 | |
| 59.1 | |
| 59.2 | |
| 59.3 | |
| 59.4 | |
| 59.5 | |
| 59.6 | Nozzle Accelerometer event (STA-1950, 0 deg) |

| | |
|----------------|---|
| 59.7 | Pressure event maximum |
| 59.8 | |
| 59.9 | |
| 60.0 | |
| 60.1 | Nozzle Accelerometer event (STA-1950, 0 deg) |
| 60.2 | |
| 60.3 | |
| 60.4 | |
| 60.5 | |
| 60.6 | Nozzle Accelerometer event (STA-1950, 0 deg) |
| 60.7 | Pressure event maximum |
| 60.8 | Case hoop strain event (SHIAIO42 @ STA 1409.00) |
| 60.9 | |
| 61.0 | |
| 61.1 | |
| 61.2 | |
| 61.3 | |
| 61.4 | |
| 61.5 | |
| 61.6 | |
| 61.7 | |
| 61.8 | |
| 61.9 | |
| 62.0 | Nozzle Accelerometer event (STA-1950, 0 deg) |
| 62.1 | |
| 62.2 | Nozzle Accelerometer event (STA-1950, 0 deg) |
| 62.3 | |
| 62.4 | |
| 62.5 | Nozzle Accelerometer event (STA-1950, 0 deg) |
| 62.6 | |
| 62.7 | Pressure event maximum Calorimeter/Radiometer event Case hoop strain event (SHIAIO42 @ STA 1409.00) |
| 62.8 | |
| 62.9 | |
| 63.0 | |
| 63.1 | |
| 63.2 (approx.) | Ejecta noted on video & high speed film-- |
| 63.3 | Nozzle Accelerometer event (STA-1950, 0 deg) |
| 63.4 | |
| 63.5 | |
| 63.6 | |
| 63.7 | |
| 63.8 | |
| 63.9 | |
| 64.0 | |
| 64.1 | |
| 64.2 | Pressure event maximum |
| 64.3 | |
| 64.4 | |
| 64.5 | Nozzle Accelerometer event (STA-1950, 0 deg) |
| 64.6 | |
| 64.7 | Pressure event maximum |
| 64.8 | |

| | |
|------|---|
| 64.9 | |
| 65.0 | Nozzle Accelerometer event (STA-1950, 0 deg) |
| 65.1 | |
| 65.2 | |
| 65.3 | |
| 65.4 | Pressure event maximum Case hoop strain event (SHIAIO42 @ STA 1409.00) |
| 65.5 | |
| 65.6 | |
| 65.7 | |
| 65.8 | |
| 65.9 | |
| 66.0 | |
| 66.1 | |
| 66.2 | |
| 66.3 | |
| 66.4 | Calorimeter/Radiometer event |
| 66.5 | |
| 66.6 | |
| 66.7 | |
| 66.8 | Nozzle Accelerometer event (STA-1950, 0 deg) |
| 66.9 | |
| 67.0 | |
| 67.1 | |
| 67.2 | Pressure event maximum Case hoop strain event (SHIAIO42 @ STA 1409.00) Nozzle fixed link strain event (nose down) |
| 67.3 | |
| 67.4 | |
| 67.5 | |
| 67.6 | |
| 67.7 | |
| 67.8 | |
| 67.9 | |
| 68.0 | |
| 68.1 | |
| 68.2 | |
| 68.3 | |
| 68.4 | Nozzle Accelerometer event (STA-1950, 0 deg) |
| 68.5 | Nozzle fixed link strain event (nose up) |
| 68.6 | Nozzle fixed link strain event (nose up) |
| 68.7 | White emissions @ 90 deg (high speed film) Nozzle fixed link strain event (nose left) |
| 68.8 | Case hoop strain event (SHIAIO42 @ STA 1409.00) Pressure event maximum Nozzle Accelerometer event (STA-1950, 0 deg) |
| 68.9 | Nozzle fixed link strain event (nose down) |
| 69.0 | RTR event (slag approaches inlet) Pressure event maximum Nozzle Accelerometer event (STA-1950, 0 deg) |
| 69.1 | |
| 69.2 | |
| 69.3 | |
| 69.4 | |
| 69.5 | |

| | |
|----------------|--|
| 69.6 | Bottom ejecta with ground impact (high speed film) |
| 69.7 | |
| 69.8 | Nozzle fixed link strain event (nose up) |
| 69.9 | Nozzle Accelerometer event (STA-1950, 0 deg) |
| 70.0 (approx.) | Ejecta noted on video |
| 70.1 | Case hoop strain event (SHIAIO42 @ STA 1409.00) |
| 70.2 | Nozzle Accelerometer event (STA-1950, 0 deg) |
| | Pressure event maximum |
| 70.3 | Nozzle fixed link strain event (nose down) |
| 70.4 | |
| 70.5 | Case hoop strain event (SHIAIO42 @ STA 1409.00) |
| 70.6 | Calorimeter/Radiometer event |
| 70.7 | |
| 70.8 | Pressure event maximum |
| | Case hoop strain event (SHIAIO42 @ STA 1409.00) |
| | Nozzle Accelerometer event (STA-1950, 0 deg) |
| 70.9 | Nozzle fixed link strain event (nose down) |
| 71.0 | |
| 71.1 | Nozzle Accelerometer event (STA-1950, 0 deg) |
| 71.2 | |
| 71.3 | |
| 71.4 | |
| 71.5 | |
| 71.6 | Nozzle fixed link strain event (nose down) |
| | Calorimeter/Radiometer event |
| 71.7 | |
| 71.8 | |
| 71.9 | |
| 72.0 | |
| 72.1 | |
| 72.2 | Nozzle fixed link strain event (nose up) |
| | Nozzle Accelerometer event (STA-1950, 0 deg) |
| 72.3 | |
| 72.4 | Nozzle Accelerometer event (STA-1950, 0 deg) |
| 72.5 | |
| 72.6 | Nozzle Accelerometer event (STA-1950, 0 deg) |
| | Pressure event maximum |
| | Case hoop strain event (SHIAIO42 @ STA 1409.00) |
| 72.7 | |
| 72.8 | |
| 72.9 | White emissions (High Speed Film) |
| | Nozzle Accelerometer event (STA-1950, 0 deg) |
| 73.0 | Nozzle fixed link strain event (nose down) |
| 73.1 | |
| 73.2 | |
| 73.3 | |
| 73.4 | |
| 73.5 | White emissions @ 90 deg. (High Speed Film) |
| 73.6 | Pressure event maximum |
| 73.7 | |
| 73.8 | |
| 73.9 | |
| 74.0 | |
| 74.1 | |
| 74.2 | |

| | |
|----------------|---|
| 74.3 | Nozzle fixed link strain event (nose right) |
| 74.4 | Pressure event minimum |
| 74.5 | Nozzle fixed link strain event (nose up) |
| | Bottom plume fluctuations (high speed film) |
| 74.6 | Nozzle Accelerometer event (STA-1950, 0 deg) |
| 74.7 | Case hoop strain event (SHIAIO42 @ STA 1409.00) |
| | Pressure event maximum |
| 74.8 | |
| 74.9 | |
| 75.0 | |
| 75.1 | Nozzle Accelerometer increase in activity (STA-1950, 0 deg) |
| 75.2 | |
| 75.3 | |
| 75.4 | |
| 75.6 | Nozzle Accelerometer event (STA-1950, 0 deg) |
| 75.7 (approx.) | Ejecta noted on high speed film |
| 75.8 | Nozzle fixed link strain event (nose up) |
| 75.9 | Nozzle Accelerometer event (STA-1950, 0 deg) |
| 76.0 | Pressure event maximum |
| 76.1 | Nozzle Accelerometer event (STA-1950, 0 deg) |
| | Case hoop strain event (SHIAIO42 @ STA 1409.00) |
| 76.2 | |
| 76.3 | |
| 76.4 | |
| 76.5 | |
| 76.6 | |
| 76.7 | |
| 76.8 | |
| 76.9 | |
| 77.0 | |
| 77.1 | |
| 77.2 | |
| 77.3 (approx.) | Ejecta (multiple objects) noted on video & high speed film |
| 77.4 | |
| 77.5 | |
| 77.6 | |
| 77.7 | |
| 77.8 | |
| 77.9 | Nozzle Accelerometer event (STA-1950, 0 deg) |
| 78.0 | Pressure event maximum |
| 78.1 | |
| 78.2 | |
| 78.3 | |
| 78.4 | |
| 78.5 | Calorimeter/Radiometer event |
| | Case hoop strain event (SHIAIO42 @ STA 1409.00) |
| 78.6 | |
| 78.7 | |
| 78.8 | |
| 78.9 | Nozzle fixed link strain event (nose up) |
| 79.0 | |
| 79.1 | |
| 79.2 | |
| 79.3 | |

| | |
|------|---|
| 79.4 | Nozzle fixed link strain event (nose down) |
| 79.5 | Nozzle Accelerometer event (STA-1950, 0 deg) |
| 79.6 | |
| 79.7 | |
| 79.8 | |
| 79.9 | |
| 80.0 | |
| 80.1 | |
| 80.2 | |
| 80.3 | |
| 80.4 | |
| 80.5 | |
| 80.6 | |
| 80.7 | |
| 80.8 | Calorimeter/Radiometer event |
| 80.9 | |
| 81.0 | |
| 81.1 | |
| 81.2 | |
| 81.3 | |
| 81.4 | |
| 81.5 | |
| 81.6 | |
| 81.7 | |
| 81.8 | |
| 81.9 | |
| 82.0 | |
| 82.1 | |
| 82.2 | Case hoop strain event (SHIAIO42 @ STA 1409.00) |
| 82.3 | |
| 82.4 | |
| 82.5 | |
| 82.6 | |
| 82.7 | |
| 82.8 | |
| 82.9 | |
| 83.0 | Nozzle Accelerometer event (STA-1950, 0 deg) |
| 83.1 | |
| 83.2 | |
| 83.3 | |
| 83.4 | |
| 83.5 | |
| 83.6 | |
| 83.7 | |
| 83.8 | |
| 83.9 | Calorimeter/Radiometer event |
| 84.0 | |
| 84.1 | |
| 84.2 | |
| 84.3 | |
| 84.4 | |
| 84.5 | |
| 84.6 | |
| 84.7 | |

| | |
|----------------|---|
| 84.8 | |
| 84.9 | Calorimeter/Radiometer event |
| 85.0 (approx.) | Ejecta noted (?) on video |
| 85.1 | |
| 85.2 | |
| 85.3 | |
| 85.4 | |
| 85.5 | |
| 85.6 | |
| 85.7 | Calorimeter/Radiometer event |
| 85.8 | |
| 85.9 | |
| 86.0 | |
| 86.1 | |
| 86.2 | |
| 86.3 | |
| 86.4 | |
| 86.5 | |
| 86.6 | |
| 86.7 | Nozzle Accelerometer event (STA-1950, 0 deg) |
| 86.8 | |
| 86.9 | Case hoop strain event (SHIAIO42 @ STA 1409.00) |
| | Nozzle Accelerometer event (STA-1950, 0 deg) |
| | Pressure event maximum |
| 87.0 | Nozzle Accelerometer event (STA-1950, 0 deg) |
| 87.1 | |
| | Nozzle Accelerometer event (STA-1950, 0 deg) |
| 87.2 | |
| 87.3 | |
| 87.4 | |
| 87.5 | |
| 87.6 | |
| 87.7 | Calorimeter/Radiometer event |
| 87.8 | |
| 87.9 | |
| 88.0 | |
| 88.1 | |
| 88.2 | |
| 88.3 | |
| 88.4 | Nozzle Accelerometer event (STA-1950, 0 deg) |
| 88.5 | |
| 88.6 | |
| 88.7 | |
| 88.8 | |
| 88.9 | |
| 89.0 | |
| 89.1 | |
| 89.2 | |
| 89.3 | |
| 89.4 | |
| 89.5 | |
| 89.6 | |
| 89.7 | |
| 89.8 | |

| | |
|------|---|
| 89.9 | |
| 90.0 | Calorimeter/Radiometer event |
| | Nozzle Accelerometer event (STA-1950, 0 deg) |
| 90.1 | |
| 90.2 | |
| 90.3 | |
| 90.4 | |
| 90.5 | Case hoop strain event (SHIAIO42 @ STA 1409.00) |
| 90.6 | |
| 90.7 | |
| 90.8 | |
| 90.9 | |
| 91.0 | |
| 91.1 | |
| 91.2 | |
| 91.3 | |
| 91.4 | |
| 91.5 | |
| 91.6 | |
| 91.7 | |
| 91.8 | Nozzle Accelerometer event (STA-1950, 0 deg) |
| 91.9 | |
| 92.0 | |
| 92.1 | |
| 92.2 | |
| 92.3 | |
| 92.4 | |
| 92.5 | Nozzle Accelerometer event (STA-1950, 0 deg) |
| 92.6 | Pressure event maximum |
| 92.7 | |
| 92.8 | |
| 92.9 | |
| 93.0 | |
| 93.1 | |
| 93.2 | |
| 93.3 | Calorimeter/Radiometer event |
| 93.4 | |
| 93.5 | |
| 93.6 | |
| 93.7 | |
| 93.8 | |
| 93.9 | |
| 94.0 | |
| 94.1 | |
| 94.2 | |
| 94.3 | |
| 94.4 | |
| 94.5 | |
| 94.6 | |
| 94.7 | |
| 94.8 | |
| 94.9 | |
| 95.0 | RTR event (slag approaches left) |
| 95.1 | |

| | |
|-------|---|
| 95.2 | |
| 95.3 | |
| 95.4 | Calorimeter/Radiometer event |
| 95.5 | Case hoop strain event (SHIAIO42 @ STA 1409.00) |
| | Nozzle Accelerometer event (STA-1950, 0 deg) |
| 95.6 | |
| 95.7 | |
| 95.8 | |
| 95.9 | |
| 96.0 | |
| 96.1 | |
| 96.2 | |
| 96.3 | |
| 96.4 | Pressure event maximum |
| 96.5 | |
| 96.6 | |
| 96.7 | |
| 96.8 | |
| 96.9 | |
| 97.0 | |
| 97.1 | |
| 97.2 | |
| 97.3 | |
| 97.4 | |
| 97.5 | |
| 97.6 | |
| 97.7 | |
| 97.8 | |
| 97.9 | |
| 98.0 | Calorimeter/Radiometer event |
| 98.1 | |
| 98.2 | |
| 98.3 | |
| 98.4 | |
| 98.5 | |
| 98.6 | |
| 98.7 | |
| 98.8 | |
| 98.9 | |
| 99.0 | |
| 99.1 | |
| 99.2 | |
| 99.3 | Calorimeter/Radiometer event |
| 99.4 | |
| 99.5 | |
| 99.6 | |
| 99.7 | |
| 99.8 | |
| 99.9 | Case hoop strain event (SHIAIO42 @ STA 1409.00) |
| | Pressure event maximum |
| 100.0 | |
| 100.1 | |
| 100.2 | |
| 100.3 | |

| | |
|-------|---|
| 100.4 | |
| 100.5 | |
| 100.6 | |
| 100.7 | |
| 100.8 | |
| 100.9 | |
| 101.0 | |
| 101.1 | |
| 101.2 | |
| 101.3 | |
| 101.4 | |
| 101.5 | |
| 101.6 | |
| 101.7 | Nozzle Accelerometer event (STA-1950, 0 deg) |
| 101.8 | |
| 101.9 | |
| 102.0 | |
| 102.1 | |
| 102.2 | |
| 102.3 | |
| 102.4 | |
| 102.5 | |
| 102.6 | |
| 102.7 | |
| 102.8 | |
| 102.9 | |
| 103.0 | |
| 103.1 | |
| 103.2 | |
| 103.3 | |
| 103.4 | |
| 103.5 | |
| 103.6 | |
| 103.7 | |
| 103.8 | Nozzle Accelerometer event (STA-1950, 0 deg) |
| 103.9 | Calorimeter/Radiometer event |
| | Case hoop strain event (SHIAIO42 @ STA 1409.00) |
| 104.0 | |
| 104.1 | |
| 104.2 | |
| 104.3 | |
| 104.4 | |
| 104.5 | |
| 104.6 | |
| 104.7 | |
| 104.8 | |
| 104.9 | |
| 105.0 | |
| 105.1 | |
| 105.2 | |
| 105.3 | |
| 105.4 | |
| 105.5 | Calorimeter/Radiometer event |
| 105.6 | |

| | |
|-------|--|
| 105.7 | |
| 105.8 | |
| 105.9 | Nozzle Accelerometer event (STA-1950, 0 deg) |
| 106.0 | |
| 106.1 | |
| 106.2 | |
| 106.3 | |
| 106.4 | |
| 106.5 | Calorimeter/Radiometer event Nozzle Accelerometer event (STA-1950, 0 deg) |
| 106.6 | |
| 106.7 | |
| 106.8 | |
| 106.9 | |
| 107.0 | |
| 107.1 | |
| 107.2 | Nozzle Accelerometer event (STA-1950, 0 deg) |
| 107.3 | |
| 107.4 | |
| 107.5 | |
| 107.6 | |
| 107.7 | Nozzle Accelerometer start of an event (STA-1950, 0 deg) |
| 107.8 | |
| 107.9 | |
| 108.0 | |
| 108.1 | |
| 108.2 | |
| 108.3 | |
| 108.4 | Case hoop strain event (SHIAIO42 @ STA 1409.00) Nozzle Accelerometer maximum of the event (STA-1950, 0 deg) Pressure event maximum Calorimeter/Radiometer event |
| 108.5 | |
| 108.6 | |
| 108.7 | |
| 108.8 | Nozzle Accelerometer end of the event (STA-1950, 0 deg) |
| 108.9 | |
| 109.0 | |
| 109.1 | |
| 109.2 | |
| 109.3 | Nozzle Accelerometer event (STA-1950, 0 deg) |
| 109.4 | Case hoop strain event (SHIAIO42 @ STA 1409.00) Pressure event maximum |
| 109.5 | |
| 109.6 | |
| 109.7 | |
| 109.8 | |
| 109.9 | |
| 110.0 | |
| 110.1 | |
| 110.2 | |
| 110.3 | Nozzle Accelerometer event (STA-1950, 0 deg) |
| 110.4 | |
| 110.5 | |
| 110.6 | |

110.7
110.8 Nozzle Accelerometer start of an event (STA-1950, 0 deg)
110.9 Nozzle Accelerometer maximum of the event (STA-1950, 0 deg)
111.0
111.1
111.2
111.3
111.4
111.5 Calorimeter/Radiometer event
111.6 Nozzle Accelerometer end of the event (STA-1950, 0 deg)
111.7
111.8 Nozzle Accelerometer event (STA-1950, 0 deg)
111.9
112.0
112.1
112.2
112.3
112.4
112.5
112.6
112.7
112.8
112.9
113.0
113.1
113.2
113.3
113.4
113.5
113.6
113.7
113.8
113.9
114.0
114.1
114.2
114.3
114.4
114.5
114.6
114.7
114.8
114.9
115.0
115.1
115.2
115.3
115.4
115.5
115.6
115.7
115.8
115.9
116.0

116.1
116.2
116.3
116.4
116.5
116.6
116.7
116.8
116.9
117.0
117.1
117.2
117.3
117.4
117.5
117.6
117.7
117.8
117.9
118.0
118.1
118.2
118.3
118.4
118.5
118.6
118.7
118.8
118.9
119.0
119.1
119.2
119.3
119.4
119.5
119.6
119.7
119.8
119.9
120.0

DISTRIBUTION

| <u>Name</u> | <u>M/S</u> | <u>Copies</u> |
|-----------------|------------|---------------|
| R. Papasian | E62A | 31 |
| S. Vigil | E62 | 1 |
| T. Johnson | E62 | 1 |
| E. Bott | E63 | 1 |
| B. Russell | E64 | 1 |
| C. Vogt | E65 | 1 |
| J. Oosteyn | E66 | 1 |
| J. Vulgan | J61 | 1 |
| A. Carlisle | L61 | 1 |
| D. South | L62 | 1 |
| B. Lesko | L62 | 1 |
| M. Clark | L62 | 1 |
| M. Tobias | L62 | 1 |
| A. Drendel | L63 | 1 |
| E. Mathias | L63 | 1 |
| P. Simpson | L61 | 1 |
| J. Furgeson | L87 | 1 |
| A. Schilling | K68 | 1 |
| L. Bailey | L80 | 1 |
| S. Pottorff | L87 | 1 |
| F. Duersch | 851 | 1 |
| Print Crib | LO1A | 3 |
| Data Management | MICRO | 5 |

